การขนส่งฟอสเฟตและการถ่ายโอนสัญญาณในไซยาโนแบคทีเรีย *Synechocystis* sp. PCC 6803

นาย สุรเชษฐ์ บุรุษอาชาไนย

วิทยานิพนธ์นี้เป็นส่วนหนึ่งของการศึกษาตามหลักสูตรปริญญาวิทยาศาสตรดุษฎีบัณฑิต
สาขาวิชาชีวเคมี ภาควิชาชีวเคมี
คณะวิทยาศาสตร์ จุฬาลงกรณ์มหาวิทยาลัย
ปีการศึกษา 2552

PHOSPHATE TRANSPORT AND SIGNAL TRANSDUCTION IN A CYANOBACTERIUM *Synechocystis* sp. PCC 6803

Mr. Surachet Burut-Archanai

A Dissertation Submitted in Partial Fulfillment of the Requirements

for the Degree of Doctor of Philosophy Program in Biochemistry

Department of Biochemistry

Faculty of Science

Chulalongkorn University

Academic Year 2009

Thesis Title	PHOSPHATE TRANSPORT AND SIGNAL TRANSDUCTION IN A CYANOBACTERIUM *Synechocystis* sp. PCC 6803
By	Mr. Surachet Burut-Archanai
Field of Study	Biochemistry
Thesis Advisor	Professor Aran Incharoensakdi, Ph.D.
Thesis Co-Advisor	Associate Professor Julian Eaton-Rye, Ph.D.

Accepted by the Faculty of Science, Chulalongkorn University in Partial Fulfillment of the Requirements for the Doctoral Degree

S. Hannongbua ..... Dean of the Faculty of Science
(Professor Supot Hannongbua, Dr.rer.nat.)

THESIS COMMITTEE

P. Pongsawasdi ..... Chairman
(Associate Professor Piamsook Pongsawasdi)

Aran Incharoensakdi ..... Thesis Advisor
(Professor Aran Incharoensakdi, Ph.D.)

J. Eaton-Rye ..... Thesis Co-Advisor
(Associate Professor Julian Eaton-Rye, Ph.D.)

Teerapong Buaboocha ..... Examiner
(Assistant Professor Teerapong Buaboocha, Ph.D.)

W. Chungjatupornchai ..... External Examiner
(Associate Professor Wipa Chungjatupornchai, Ph.D.)

Waraporn Juntarajumnong ..... External Examiner
(Waraporn Juntarajumnong, Ph.D.)

สุรเชษฐ์ บุรุษอาชาไนย : การขนส่งฟอสเฟตและการถ่ายโอนสัญญาณในไซยาโนแบคทีเรีย *Synechocystis* sp. PCC 6803. (PHOSPHATE TRANSPORT AND SIGNAL TRANSDUCTION IN A CYANOBACTERIUM *Synechocystis* sp. PCC 6803) อ. ที่ปรึกษาวิทยานิพนธ์หลัก : ศ.ดร. อรัญ อินเจริญศักดิ์, อ. ที่ปรึกษาวิทยานิพนธ์ร่วม : Assoc. Prof. Julian Eaton-Rye, Ph.D., 116 หน้า.

ระบบการเหนี่ยวนำสัญญาณแบบสององค์ประกอบประกอบด้วย ฮิสทิดีนไคเนสและโปรตีนควบคุมการตอบสนอง การถ่ายโอนสัญญาณฟอสเฟตในไซยาโนแบคทีเรีย *Synechocystis* sp. PCC 6803 ใช้ฮิสทิดีนไคเนส SphS และ โปรตีนควบคุมการตอบสนอง SphR ได้มีการรายงานถึงรหัสเริ่มต้นในการแปลรหัสกรดอะมิโนของยีน *sphS* และอันตรกิริยาที่เป็นไปได้ของ SphS และ โปรตีนควบคุมการตอบสนองแง่ลบ SphU ในปีพ.ศ. 2550 ในงานวิจัยนี้ได้รายงานถึงความต้องการกรดอะมิโนที่ปลายด้านกรดอะมิโน (N-terminal) ของ SphS และระบบขนส่งฟอสเฟตอย่างจำเพาะในการควบคุมการทำงานของระบบ SphS-SphR โดยบริเวณกรดอะมิโนไอโซลิวซีนที่ 4 ถึงกรดอะมิโนไอโซลิวซีนที่ 19 ซึ่งน่าจะเป็นบริเวณที่แทรกอยู่ที่เยื่อหุ้มเซลล์ มีความสำคัญในการกระตุ้นการทำงานของระบบ SphS-SphR ในการตอบสนองต่อสภาวะขาดฟอสเฟต ในสายพันธุ์กลายที่ขาดบริเวณนี้ไม่สามารถตอบสนองสภาวะขาดฟอสเฟตแม้ว่าจะเลี้ยงในสภาวะขาดฟอสเฟต หรือทำการกลายพันธุ์โปรตีนควบคุมการตอบสนองแง่ลบ SphU โดยวัดจากกิจกรรมของอัลคาไลน์ฟอสฟาเทส อย่างไรก็ตามการตัดให้กรดอะมิโนไอโซลิวซีนที่ 8 ถึงกรดอะมิโนไกลซีนที่ 15 (Δ (I8-G15)) หายไปพบว่าในสายพันธุ์กลายนี้มีกิจกรรมของอัลคาไลน์ฟอสฟาเทสตลอดเวลา ผลนี้ไม่เกี่ยวเนื่องกับความยาวของสายโปรตีนที่หายไป เนื่องจากการตัดกรดอะมิโนไป 4, 6 และ 9 กรดอะมิโนในบริเวณอื่นไม่ได้ส่งผลใดต่อการทำงานของระบบ SphS-SphR นอกจากนี้ในไซยาโนแบคทีเรีย *Synechocystis* sp. PCC 6803 มีระบบขนส่งฟอสเฟตอย่างจำเพาะ 2 ระบบ ซึ่งได้ทำการตัดให้หายไป ได้เป็นสายพันธุ์กลาย ΔPst1 และ ΔPst2 การทดลองนี้แสดงให้ทราบว่าเฉพาะระบบขนส่งฟอสเฟตอย่างจำเพาะที่ 1 (Pst1 system) เท่านั้นที่เซลล์ต้องการในการกดการแสดงออกของยีนในในโฟ-เรคตูลอนในสภาวะที่มีฟอสเฟตพอเพียง และการกลายพันธุ์จุดเดียวที่บริเวณที่แทรกอยู่ที่เยื่อหุ้มเซลล์ของ SphS (Δ (I8-G15)) และ ระบบขนส่งฟอสเฟตอย่างจำเพาะที่ 1 (ΔPst1) หรือการกลายพันธุ์ทั้งสองจุดทำให้มีกิจกรรมของอัลคาไลน์ฟอสฟาเทสในปริมาณใกล้เคียงกัน จึงเป็นไปได้ที่บริเวณทั้งสองจะควบคุมกลไกการถ่ายโอนสัญญาณฟอสเฟต ณ จุดเดียวกัน นอกจากนี้ระบบขนส่งฟอสเฟตอย่างจำเพาะทั้งสองทำงานได้อย่างมีประสิทธิภาพซึ่งขนส่งฟอสเฟตในระดับที่พอเพียงต่อการเจริญเติบโตรวมถึงการสังเคราะห์รงควัตถุเมื่อเทียบกับสายพันธุ์ดั้งเดิม

การศึกษาจลนพลศาสตร์ของการนำเข้าฟอสเฟตพบว่า มีค่า K_m เท่ากับ 0.13, 5.16 และ 80.67 ไมโครโมลาร์ในสายพันธุ์ ΔPst1, ΔPst2 และ สายพันธุ์ดั้งเดิม ตามลำดับ และมีค่า V_{max} กับ 0.18, 2.17 และ 3.12 ไมโครโมลต่อนาทีต่อมิลลิกรัมคลอโรฟิลล์ เอ ในสายพันธุ์ ΔPst1, ΔPst2 และ สายพันธุ์ดั้งเดิม ตามลำดับ การนำเข้าฟอสเฟตนี้แปรตามระดับพลังงานและ ขึ้นกับค่าพีเอช ซึ่งสามารถทำงานได้ในช่วงกว้างคือระหว่างค่าพีเอช 7 ถึง 10 และออสโมแลลิตีซึ่งเกิดจากเกลือ NaCl กระตุ้นการนำเข้าฟอสเฟตแต่ออสโมแลลิตีที่เกิดจากซอร์บิทอล ไปลดกิจกรรมการขนส่งฟอสเฟต จึงอาจบอกได้ว่าการนำเข้าฟอสเฟตนี้ขึ้นกับระดับไอออนิก

ภาควิชา.....ชีวเคมี.....ลายมือชื่อนิสิต.....สุรเชษฐ์ บุรุษอาชาไนย.....

สาขาวิชา.....ชีวเคมี.....ลายมือชื่อ อ.ที่ปรึกษาวิทยานิพนธ์หลัก.....

ปีการศึกษา.....2552.....ลายมือชื่อ อ.ที่ปรึกษาวิทยานิพนธ์ร่วม.....

4873863123 : MAJOR BIOCHEMISTRY
KEYWORDS : HISTIDINE KINASE / PHOSPHATE-SPECIFIC TRANSPORT SYSTEM / MEMBRANE-SPANNING DOMAIN

SURACHET BURUT-ARCHANAI : PHOSPHATE TRANSPORT AND SIGNAL TRANSDUCTION IN A CYANOBACTERIUM *Synechocystis* sp. PCC 6803. THESIS ADVISOR : Prof. Aran Incharoensakdi, Ph.D., THESIS CO-ADVISOR : Assoc. Prof. Julian Eaton-Rye, Ph.D., 116 pp.

A two-component signal transduction system involved in phosphate-sensing system, SphS-SphR system, was reported for an actual start codon of *sphS* and a possible interaction between a SphS kinase protein and a negative regulator SphU in 2007. In this study the requirement of the N-terminus of SphS and the phosphate-specific transport (Pst) system for regulation of the SphS-SphR system has been shown. A putative membrane-spanning region between amino acids Ile-4 and Ile-19 of SphS is required for activation of the SphS–SphR phosphate-sensing two-component system under phosphate-limiting conditions as mutants lacking this region are unable to express alkaline phosphatase, the Pho regulon expression indicator, even grown under phosphate-limiting conditions or the negative regulator SphU is inactivated. Internal deletion of 8 amino acids of the putative membrane-spanning region between amino acids Ile-8 and Gly-15, however, leads to constitutive alkaline phosphatase expression. This constitutive expression is not related to protein length as deletions of 4, 6 and 9 amino acids in other region do not affect the regulation of the SphS–SphR phosphate-sensing system. Furthermore, it seems regulation of SphS-SphR system does not need specific amino acids around Ile-8 and Gly-15, alanine substitutions in some amino acids do not alter SphS-SphR system activity. In addition, two Pst systems in *Synechocystis* sp. PCC 6803 have been deleted, designated ΔPst1 and ΔPst2 strains. Our results show that the Pst1 system, but not the Pst2 system, is required for suppression of the Pho regulon under phosphate-sufficient conditions. Deletion of the *pst1* operon and disruption of the membrane-spanning domain may both target the same control mechanism since constitutive alkaline phosphatase activity is similar in the double and single mutants. Both Pst1 and Pst2 systems are active and can transport phosphate in the amount that is sufficient for cell growth and pigment biosynthesis, compared to wild type.

The study of kinetics of phosphate uptake showed a K_m of 0.13, 5.16 and 80.67 μM in ΔPst1, ΔPst2 and wild type, respectively. In addition, V_{max} values of 0.18, 2.17 and 3.12μmol/ min/ mg of chlorophyll *a* were obtained for the ΔPst1, ΔPst2 and wild-type strains, respectively. The uptake of phosphate was energy and pH-dependent with a broad pH optimum between pH 7-10. Osmolality imposed by NaCl stimulated phosphate uptake whereas that imposed by sorbitol decreased uptake, suggesting stimulation of uptake was dependent upon ionic effects.

Department :..... Biochemistry..... Student's Signature Surachet Burut-Archanai

Field of Study :..... Biochemistry..... Advisor's Signature

Academic Year :.....2009..... Co-Advisor's Signature

ACKNOWLEDGEMENTS

I would like to express my deepest gratitude to my advisor, Professor Dr. Aran Incharoensakdi and my co-advisor, Associate Professor Dr. Julian Eaton-Rye, for their brilliant instruction, guidance, encouragement and support throughout this thesis. Without their kindness this work could not be accomplished.

My gratitude is also extended to Associate Professor Dr. Piamsook Pongsawasdi, Associate Professor Dr. Wipa Chungjatupornchai, Assistant Professor Dr. Teerapong Buaboocha and Dr. Waraporn Juntarajumnong for serving as thesis committee, for their available comments and also useful suggestions.

I am very grateful to my family for their support with love and care.

My appreciation is also expressed to all friends and staffs in Biochemistry Department, Chulalongkorn University especially the members in lab 617, as well as, members in JER's lab room 308, Biochemistry Department, University of Otago, New Zealand for their friendship to make me have a very nice time either in Thailand or New Zealand.

This work was supported by the Royal Golden Jubilee Ph.D. program (PHD/0037/2548) and the 90th Anniversary of Chulalongkorn University Fund (Ratchadaphiseksomphot Endowment Fund).

CONTENTS

Page

Page

Page

Page

LIST OF TABLES

Page

LIST OF FIGURES

Page

Page

Page

LIST OF ABBREVIATIONS

A	Alanine
Ala	Alanine
a.u.	Arbitrary units
bp	Base pair
CCCP	carbonyl cyanide *m*-chlorophenylhydrazone
Chl a	chlorophyll *a*
D	Aspartic acid
DCCD	N.N-dicyclohexylcarbodiimide
DCMU	3-(3,4-dichlorophenyl)-1,1-dimethylurea
DTT	Dithiothreitol
EDTA	Ethylenediamine tetraacetic acid
G	Glycine
g	Gram
µg	Microgram
Gly	Glycine
H	Histidine
h	hour
HEPES	Hydroxyethyl piperazineethanesulfonic acid
I	Isoleucine
Ile	Isoleucine
kb	Kilo base
kDa	Kilo Dalton

L	Leucine
l	Liter
µl	Microliter
Leu	Leucine
M	Molar
min	Minute
ml	Milliliter
mM	Milliampere
mM	Millimolar
nm	nanometer
^{o}C	Degree Celsius
OD	Optical density
PCR	Polymerase Chain Reaction
Pi	inorganic phosphate
R	Arginine
RT-PCR	Reverse transcription PCR
S	Serine
Ser	Serine
UV	Ultraviolet
V	Valine
Val	Valine

CHAPTER I

INTRODUCTION

1.1 Phosphate

Phosphorus is the third most abundant element after carbon and nitrogen in terms of cellular content. A fully oxidized form of phosphorus, phosphate, is a water-soluble, inorganic salt, rendering the second least available nutrient, after nitrogen, in natural ecosystems (Schahtman et al., 1998). Phosphate is an essential element nutrient for all organisms for a building block for most biomolecules; such as, membrane lipids, complex carbohydrates, nucleotides, and nucleic acids. Furthermore, it is used to control the function of protein by phosphorylation. Despite abundance of phosphorus in nature, only inorganic phosphate is an available form of phosphorus. There are many reports that the concentrations of inorganic phosphate (Pi) in natural water are very low at nanomolar or extremely at picomolar ranges (Schindler, 1977; Hudson, 2000; Wu et al., 2000; Sundareshwar et al., 2003).

There are three chemical forms of inorganic phosphates that are of biological importance; free phosphate, pyrophosphate, and polyphosphate. Only free phosphate appears to be taken up from the environment (Wanner, 1996). The organisms have evolved the response strategy via enhanced expression of phosphate transport system and enzymes involved in phosphate availability, for example, phosphatase, to cope with phosphate insufficient conditions (Aiba et al., 1993; Hirani et al., 2001; Wanner, 1996; Schahtman et al., 1998; Wu et al., 2003). In prokaryotic cells, the genes involved in phosphate metabolism are called Pho regulon genes which are under the

control of a two-component phosphate sensing system (Wanner, 1996; Aiba et al., 1993; Hirani et al., 2001; Suzuki et al., 2004).

1.2 Two-component signal transduction systems

The two-component signal transduction system typically consists of a histidine kinase and a response regulator, which is used to monitor environmental parameters, including osmotic and ionic strength, pH, temperature, and the concentrations of nutrients and harmful compounds. The histidine kinase is a sensor protein kinase comprising an N-terminal input domain that senses specific stimulus, and a C-terminal transmitter domain that activates its cognate response regulator at the N-terminal regulatory (receiver) domain. The response regulator also contains the C-terminal effector (output) domain for protein-protein or protein-DNA interactions to control gene expression to specific stimulus (Stock et al., 2000; Mascher et al., 2006). Typically, histidine kinases are membrane-bound proteins with two transmembrane helices and highly varied periplasmic sensing domain between transmembrane helices at the N-terminal input domain. The C-terminal transmitter domains are more conserved which can be identified by a set of conserved primary sequence motifs designated the H, N, G1, F and G2 boxes as shown in Figure 1 (West & Stock, 2001). The H motif and residues around it are involved in the autophosphorylation activity forming dimerization (sub)domain, while, the N, G1, F and G2 motifs are involved in ATP binding (sub)domain. Histidine kinases can be grouped into two major classes on the basis of their domain organization (Dutta et al., 1999). In class I histidine kinases, the H box containing region is directly linked the region that contains the other four conserved boxes. However, in class II histidine kinases, the H box

containing region is distant from the others. Alternatively, on the basis of sensing mechanism and domain architecture, histidine kinases fall into three major groups (Mascher et al., 2006). The first group, the periplasmic-sensing histidine kinases, is the largest group containing an extracellular sensory domain which lies between (at least) two transmembrane helices. The second group contains histidine kinases with sensing mechanisms associated with the membrane-spanning helices. The third group, the cytoplasmic-sensing histidine kinases, includes either membrane-anchored or soluble proteins with their input domains inside the cytoplasm.

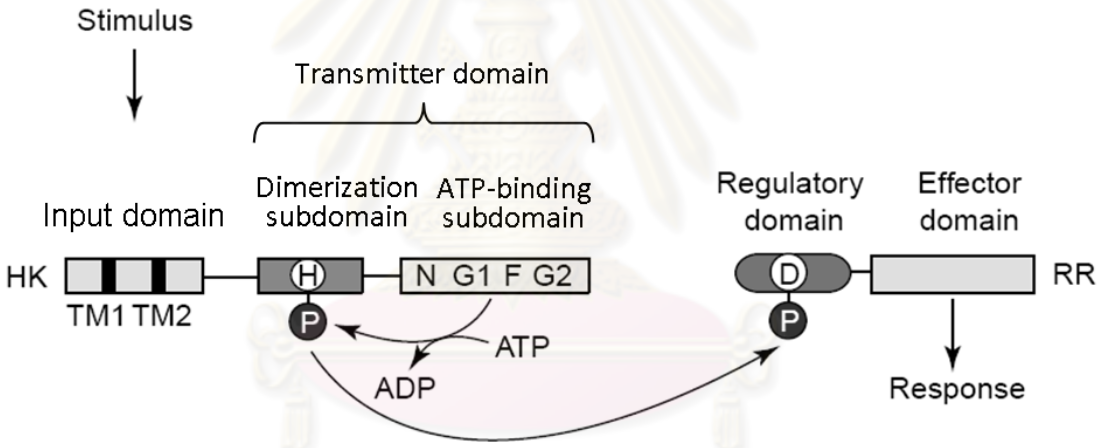

Figure 1 Typical domain organization and phosphotransfer schemes of proteins involved in two-component signal transduction systems. The conserved His and Asp residues, indicated using the single letter amino acid code, are phosphorylated in H box and regulatory (receiver) domain, respectively. The highly conserved H motif is located in the dimerization subdomain and the other four motifs are located in ATP-binding subdomain (modified from West & Stock 2001).

The signal transduction pathway involves three phosphotransfer reactions and two phosphoprotein intermediates: (i) the autophosphorylation of a conserved histidine in the transmitter domain of the sensor kinase, (ii) the phosphotransfer

reaction, transferring of the phosphoryl group from transmitter domain to a conserved aspartate in the receiver domain of the response regulator, and (iii) dephosphorylation of the response regulator (Stock et al., 2000). Autophosphorylation of histidine kinases is a bimolecular reaction between homodimers, in which one histidine kinase monomer catalyzes the phosphorylation of the conserved His residue in the second monomer, called trans-autophosphorylation. The structures of dimerization and histidine phosphotransfer (DHp) or histidine kinase A (sub)domains have been reported that they form antiparallel four-helix bundles with the active site of His residue located in the middle of the exposed face of helix (Fig. 2A). The catalytic ATP-binding or histidine kinase-like ATPase (HATPase_c) (sub)domain has an α/β-sandwich fold with five antiparallel β strands and three α helices (Fig. 2B). The dimeric histidine kinase cores containing both dimerization and catalytic domains have also been solved (Fig. 2C) (Stock et al., 2000; Cai et al., 2003).

In 2006, it was revealed that signaling through the membrane of EnvZ needs the linker region, HAMP domain, found in over 7500 proteins (Hulko et al., 2006). The HAMP domain is named by occurrence of this domain in histidine kinases, adenylyl cyclases, methyl-accepting chemotaxis proteins, and phosphatases, forming a homodimeric, four-helical, parallel coiled coil structure. Signal is transduced by a rotation of four-helix coiled coil in HAMP domains (Fig. 3).

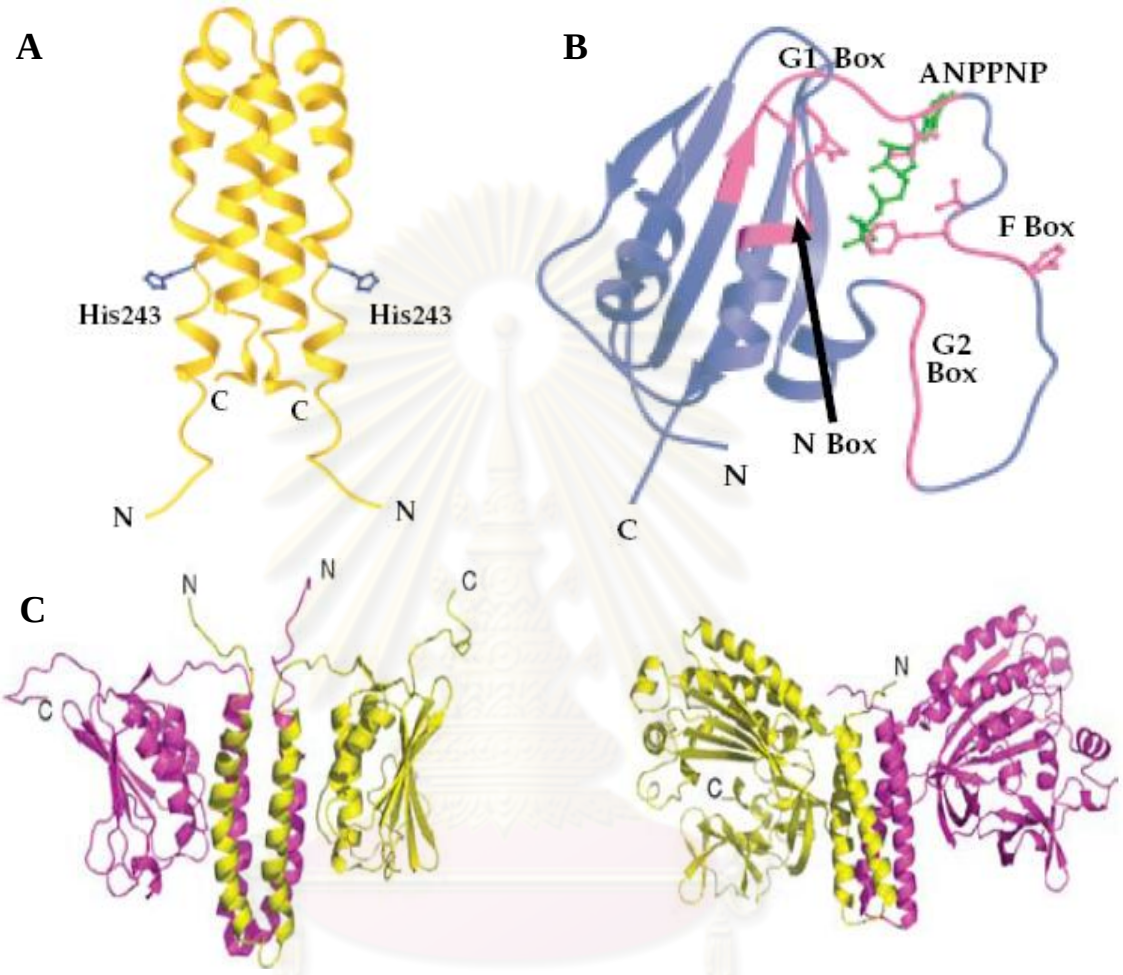

EnvZ CheA

Figure 2 The histidine kinase core. (A) The dimerization domain (gold ribbon) of *E. coli* EnvZ contains a conserved His (blue ball-stick) that is the phosphorylation site. (B) The catalytic ATP-binding domain (blue ribbon) of *E. coli* EnvZ contains four highly conserved sequence motifs (magenta) that form a binding site of ATP (ANPPNP, ATP analog shown in green ball-stick) (modified from Stock et al., 2000). (C) The dimeric kinase core domains of *E. coli* EnvZ and CheA, individual monomers are yellow and magenta (modified from Khorchid and Ikura, 2006).

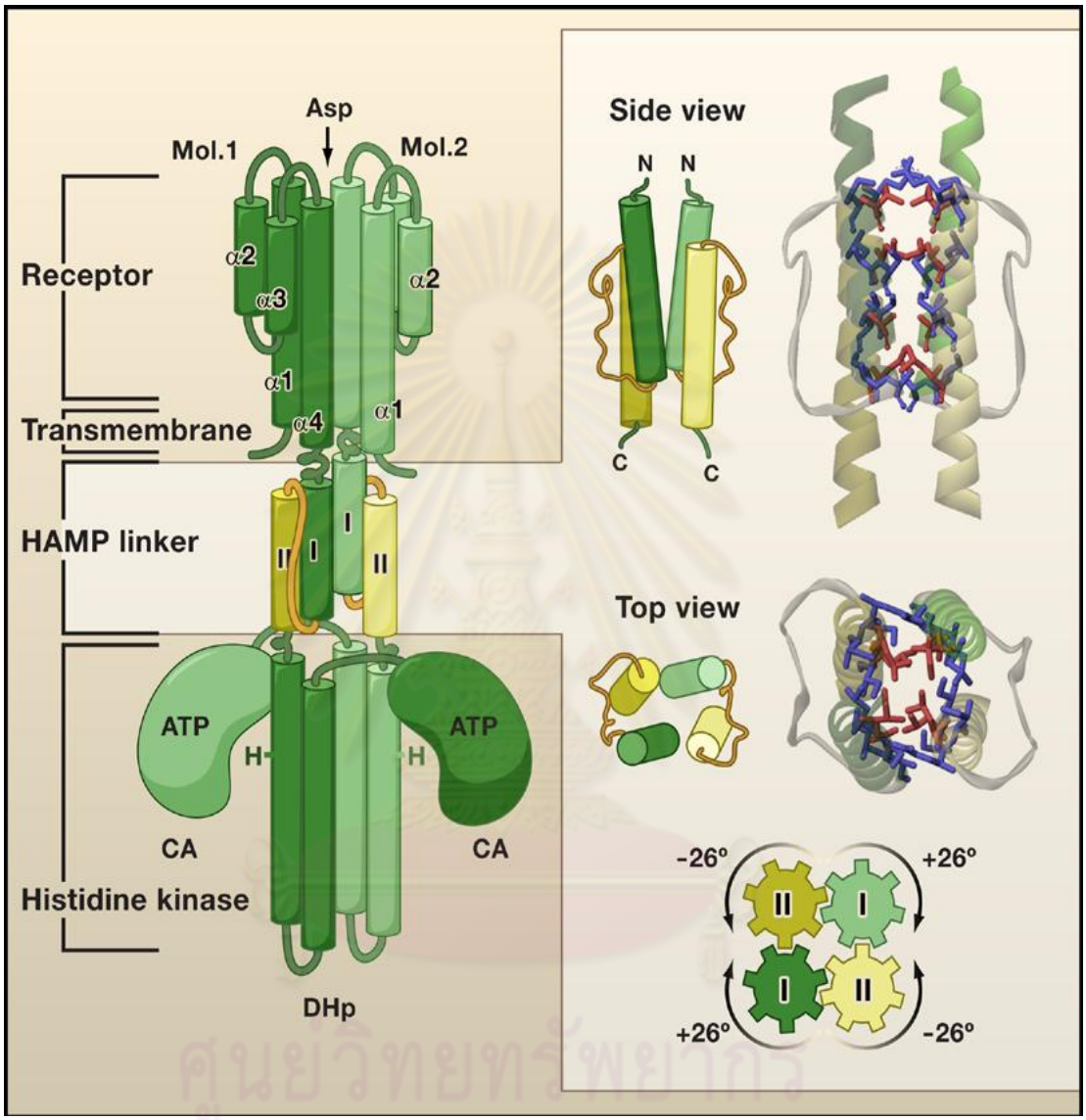

Figure 3 Structure of HAMP domain. A histidine kinase is depicted based on Taz1 chimeric protein (Left). A HAMP dimer is shown in side and top views (Right). The helix I (green) and the helix II (yellow) form a four-helical, parallel coiled coil, monomers distinguished by bold and faint colors. Side chains of residues involved in packing interactions within the core of the domain are shown in wireframe. A cogwheel diagram corresponding to the top view is shown in which two packing modes are interconvertible by rotating adjacent helices by 26° in opposite directions (Inouye 2006).

The overall activity of the kinase is modulated by sensing domain which controls the phosphorylation state of the downstream response regulator. Many response regulators have autophosphatase activity and many histidine kinases also possess a phosphatase activity, enabling them to dephosphorylate their response regulators, in phosphotransfer pathways that can be shut down quickly (Stock et al., 2000). Some two-component systems need auxiliary proteins to regulate downstream gene expression properly as found in NtrB-NtrC nitrogen regulation system (Kamberov et al., 1994), PhoR-PhoB phosphate regulation system (Wanner, 1996) and YycG-YycF cell wall regulation system (Szumant et al., 2008).

Abundance of histidine kinase-response regulator pairs has been reported in a number of bacteria. *E. coli* contains 29 histidine kinases and 34 response regulators, *Bacillus subtilis* contains 36 histidine kinases and 34 response regulators, *Anabaena* sp. PCC 7120 contains 131 histidine kinases and 80 response regulators, *Prochlorococcus* MED4 contains 5 histidine kinases and 6 response regulators and *Synechocystis* sp. PCC 6803 contains 42 histidine kinases and 38 response regulators (Wang et al., 2002; Mary & Vaulot, 2003). Cells must maintain the specificity of distinct pathways and avoid unwanted crosstalk, using variety of mechanisms (Ubersax & Ferrell, 2007). The specificity of phosphotransfer of histidine kinases to their cognate response regulators has been revealed recently, to be controlled by a cluster of residues within dimerization subdomain (Skerker et al., 2008). The two-component systems can be reprogrammed, for example, the high osmolarity signal can activate the phosphorylation of CheY in the case that the dimerization subdomain of EnvZ has been replaced with dimerization subdomain of CheA, the so-called rewiring system (Fig. 4).

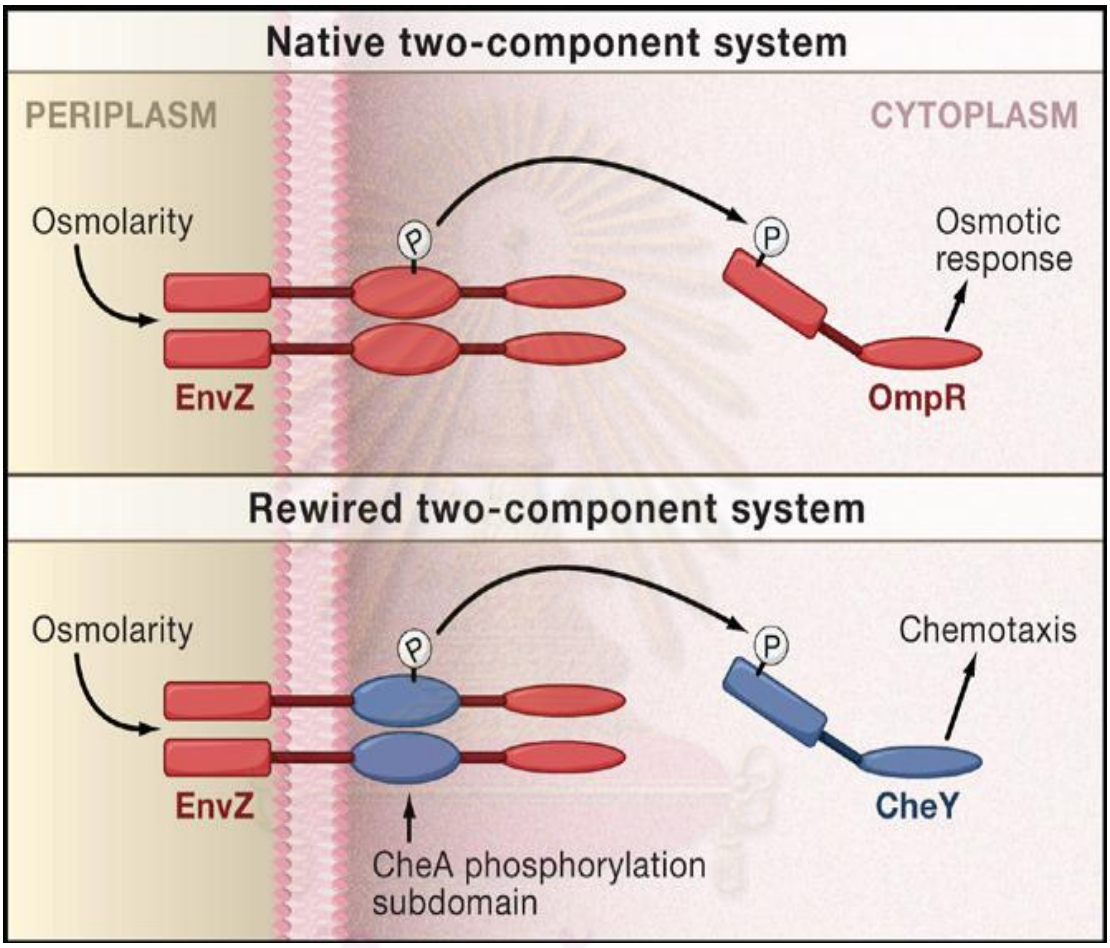

Figure 4 Rewiring a bacterial two-component system. (Top) The native EnvZ-OmpR two-component system (red) of *E. coli* for sensing and responding to osmolarity changes, the EnvZ activates the phosphorylation of OmpR in response to high osmolarity. (Bottom) A rewired EnvZ for chemotaxis pathway (CheA-CheY system; blue), the rewired EnvZ activates the phosphorylation of CheY in response to high osmolarity (Kohanski & Collins, 2008).

Two-component systems are widely found in organisms of all domains, but quite rare in eukaryotes. So far, the absence of two-component systems in animals and the requirement of two-component systems for bacterial regulations and infectivity by pathogenic bacteria make two-component systems very attractive for antimicrobial therapy (Stock et al., 2000). Mutations at two-component systems resulted in less virulence, more sensitive pathogenicity (Daigle et al., 1995; Haralalka et al., 2003; Lamarche et al., 2005). Moreover, the Pho regulon influences the virulence of several bacteria (Lamarche et al., 2008).

1.3 phosphate-sensing system

Most organisms respond to phosphate-limiting signal similarly by increasing the phosphate availability, such as, (alkaline or acid) phosphatase and phosphate transport efficiency, in which prokaryotic cells use the two-component signal transduction system for their perception and response (Aiba et al., 1993; Wanner, 1996; Sun et al., 1996; Hirani et al., 2001; Suzuki et al., 2004; Wu et al., 2003).The two-component system involved in phosphate assimilation has been extensively studied so far, especially in *E. coli*. The PhoR-PhoB phosphate-sensing system regulates at least 31 genes in 8 operons for phosphate metabolism, for example, *phoA* for alkaline phosphatase, *pstSCAB* for high-affinity phosphate transport system, *phoE* for polyanionic porin, *phnCDEFGHIJKLMNOP* for carbon-phosphorus (phosphonate) lyase pathway and *ugpBAECQ* for glycerol phosphate transport system (Wanner, 1993; Baek & Lee, 2006). The alkaline phosphatase, a member of Pho regulon, is an indicator for Pho regulon expression where activity can be detected spectrophotometrically (Yamada et al., 1990; Aiba et al., 1993; Scholten &

Tommassen, 1993; Hirani et al., 2001; Carmany et al., 2003). In contrast to a typical two-component system, PhoR-PhoB system requires auxiliary proteins including PstSCAB, the high-affinity phosphate transport ABC system, and PhoU whose function is still unclear. In addition, the N-terminus of PhoR histidine kinase lacks a periplasmic sensing domain, only 3-5 residues are exposed to periplasm (Scholtan & Tomassen 1993) and the linker region of PhoR contains a PAS domain, not HAMP domain as EnvZ. The *pstSCAB* and *phoU* are in the same operon and both are members of Pho regulon. They are required to form an inhibition complex with PhoR (Fig. 5), since mutations at either this operon or *phoR* results in constitutive expression of Pho regulon (Wanner, 1996). The Pst system is thought to be a phosphate sensor and somehow transduces the signal through to PhoR. The requirement of Pst system for regulation of Pho regulon, however, it is not required phosphate uptake activity as an R220E mutation in PstA demolishes phosphate transport without affecting inhibition of Pho regulon expression (Cox et al., 1988). In addition, despite the specificity of phosphor transfer reaction between histidine kinase and its cognate response regulator, the response regulator PhoB can be phosphorylated by the histidine kinase CreC of CreC-CreB system involved in carbon catabolism. This cross-talk occurs only in the absence of PhoR, not found in wild-type strains (Laub & Goulian, 2007).

PhoR kinase is a member of the class I of histidine kinases in which H box is adjacent to catalytic region and in the third group “the cytoplasmic-sensing histidine kinase” based on sensing mechanism (Mascher et al., 2006). The essential role of each region of PhoR has been studied so far by deletions of various regions (Yamada et al.,

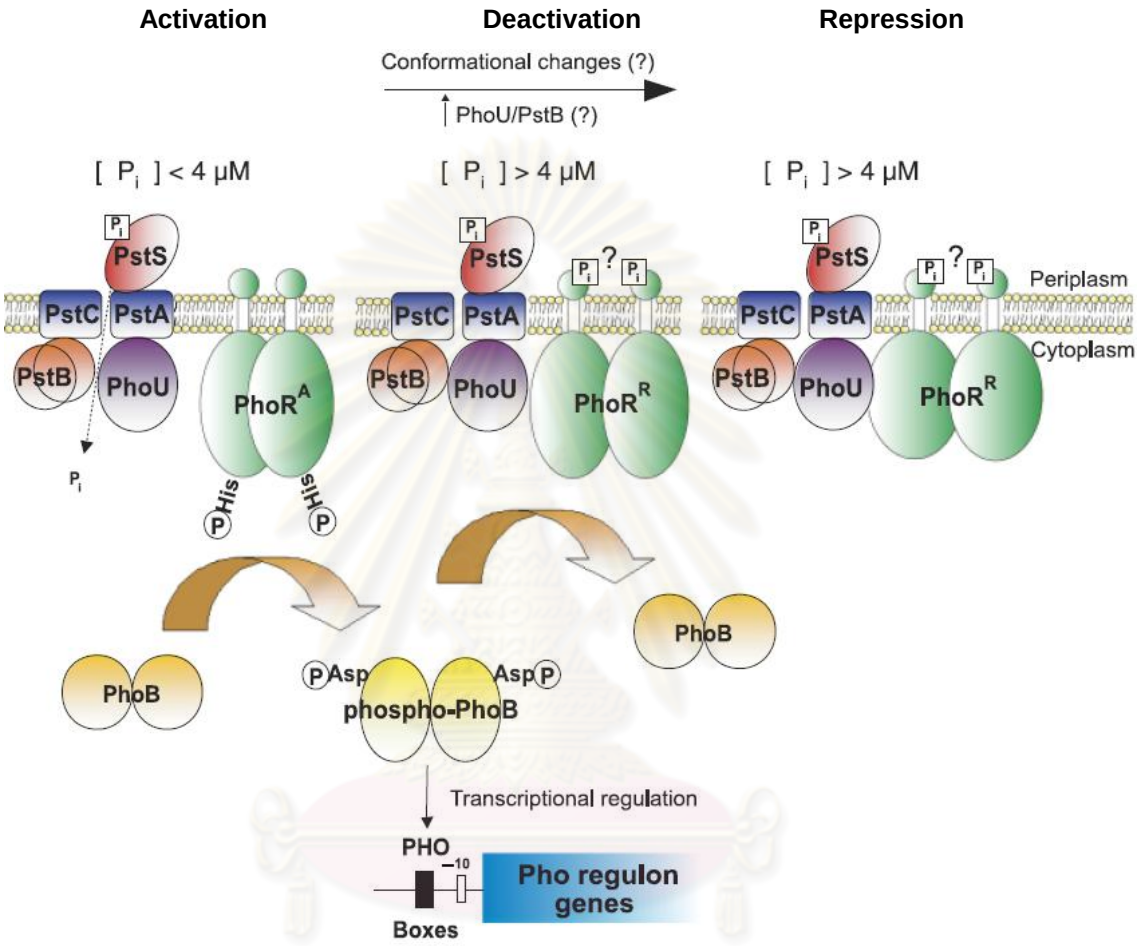

Figure 5 Control of the Pho regulon transmembrane signal transduction by environmental inorganic phosphate. $PhoR^A$ and $PhoR^R$ represent state of PhoR at activation and repression, respectively. PstS, PstC, PstA, and PstB altogether form high-affinity phosphate transport system. PhoU, Pst system and PhoR form inhibition complex. Small squares mark a phosphate-binding site on PstS and a hypothetical site on PhoR. Phosphorylated PhoB binds at Pho boxes to regulate Pho regulon gene expression (modified from Lamarche et al., 2008).

1990; Scholten & Tommassen, 1993; Carmany et al., 2003). The PhoR contains 5 main regions, a membrane-spanning region, a charged region, a PAS domain, a dimerization region (subdomain) and a catalytic region (subdomain) (Fig. 6) and a small periplasmic region between amino acids 29 and 33 (Scholten & Tommassen, 1993).

Figure 6 Domain topology of PhoR. The diagram indicates the predicted protein domains of PhoR, including the membrane-spanning region, the charged region (CR), the PAS domain, the dimerization and histinide phosphotransfer (DHp), and catalytic ATP (CA) subdomains (modified from Carmany et al., 2003).

Deletions at the N-terminal membrane-spanning region of PhoR cause constitutive expression of alkaline phosphatase even under phosphate-sufficient conditions (Yamada et al., 1990). The internal deletions of PAS domain result similarly in constitutive expression of alkaline phosphatase (Scholten & Tommassen, 1993). These results suggest that the membrane-spanning region and PAS domain are required for negative regulation of the Pho regulon expression. By contrast, deletions at dimerization (DHp) or ATP-binding (CA) subdomains (histidine kinase core) result in loss of induction of alkaline phosphatase. In addition, PhoR possesses phosphatase activity using DHp domain but is not a substrate for a reverse phosphotransfer reaction (Carmany et al., 2003).

In contrast to *E. coli*, a gram-positive bacterium, *Bacillus subtilis* contains the Pho regulon which is controlled by three two-component systems (Sun et al., 1996). Moreover, a large periplasmic region is present, the PhoU is absent, neither the Pst system nor the N-terminal membrane-spanning and periplasmic loop region is involved in Pho regulon regulation (Qi et al., 1997; Shi & Hullet, 1999). These indicate the different mechanisms in Pho regulon regulation between organisms.

1.4 Phosphate transport

The phosphate transport systems are widely studied in either prokaryotic or eukaryotic organisms. It has been reported that the high-affinity phosphate transport system is induced in that organisms when they are grown under phosphate-limiting conditions, while the low-affinity phosphate transport system functions constitutively (Wanner, 1996; van Veen, 1997; Schachtman et al., 1998; Wu et al., 2003; Dyhrman & Haley, 2006; Martiny et al., 2006). In a well characterized prokaryote, *E. coli*, there are 4 phosphate transport systems, two inorganic phosphate transport systems and two organic phosphate transport systems (Fig. 7) (van Veen, 1997). The inorganic phosphate transport systems are classified 2 types based on the kinetic differences, a low-affinity phosphate transport (phosphate inorganic transport; Pit) system and a high-affinity phosphate transport (phosphate specific transport; Pst) system. The organic phosphate transport systems consist of a glycerol-3-phosphate transport (GlpT) system and a glucose-6-phosphate transport (UhpT) system, which do not function for inorganic phosphate movement. Both Pit and Pst system are designed for net inorganic phosphate transport in which the Pst system is activated more than 100-fold when external phosphate is restricted (<4 μM), while the Pit system is

constitutetive (Wanner, 1996; van Veen, 1997). Kinetic studies revealed that the Pst is a high-affinity, low-velocity system, having a K_m of 0.4 µM and a V_{max} of 15.9 nmol Pi/min/mg protein. In contrast, Pit is a low-affinity, high velocity system, having a K_m of 38 µM and a V_{max} of 55 nmol Pi/min/mg protein. In wild-type strain containing both Pit and Pst system, however, both of them do not operate at full capacity as the apparent K_m is 25 µM and V_{max} is 43 nmol Pi/min/mg protein, in which V_{max} is lower than Pit system alone (Willsky & Malamy, 1980).

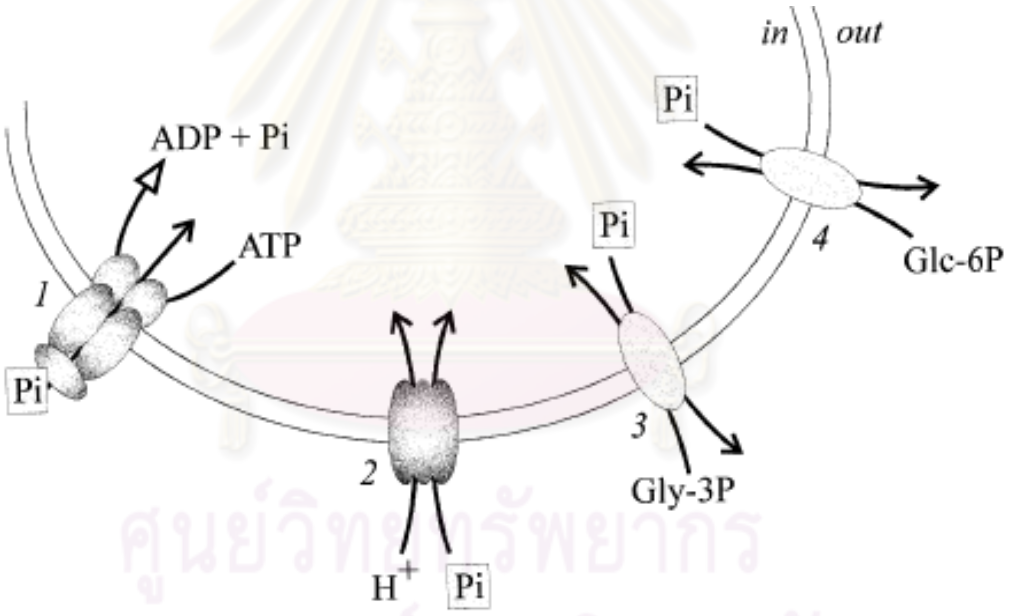

Figure 7 Phosphate transport systems in *Escherichia coli*. 1. phosphate specific transport (Pst) system 2. phosphate inorganic transport (Pit) system 3. phosphate/ glycerol-3-phosphate (GlpT) antiport system 4. phosphate/glucose-6-phosphate (UhpT) antiport system (van Veen, 1997).

1.5 *Synechocystis* sp. PCC 6803

Synechocystis sp. PCC 6803 is a unicellular non-nitrogen-fixing cyanobacterium, which could be classified in Kingdom of Bacteria, Phylum of Cyanobacteria, Order of Chroococcales, and Genus of *Synechocystis*. It is the first cyanobacterium whose genome has been completely sequenced since 1996 (Kaneko et al., 1996). It is a very good model to study molecular biology since it is naturally transformable (William, 1988; Ikeuchi & Tabata, 2001). Two-component involved in phosphate-sensing system has been studied in 2001. The *sll0337* encodes a SphS histidine kinase protein whereas the *slr0081* codes for a SphR response regulator (Hirani et al., 2001). The SphS-SphR system controls the Pho regulon expression by binding of phosphorylated SphR at Pho boxes as found in *E. coli* (Suzuki et al., 2004). Twelve genes in three operons, namely, *pst1*, *pst2* and *phoA-nucH* operon, were reported to be induced but *urtA* gene was repressed in response to phosphate-limiting conditions based on DNA microarray analysis (Suzuki et al., 2004). Together with 13 genes, *ack* and *pta* genes encoding acetate kinase and phosphotransacetylase also were up-regulated when *Synechocystis* sp. PCC 6803 cells were exposed to phosphate-limiting conditions (Juntarajumnong et al., 2007a). These genes were assigned to the Pho regulon in *Synechocystis* sp. PCC 6803. *Synechocystis* sp. PCC 6803 also possesses a regulator SphU, encoded by *slr0741*, which functions as a negative regulator for Pho regulon, PhoU homolog (Juntarajumnong et al., 2007b). The *sphU* shows no increased expression under phosphate-limiting conditions and is not in the same operon with either *pst1* or *pst2*. The presence of two Pst systems and extended N-terminus of SphS made them very attractive models to study the mechanism of signal transduction in *Synechocystis* sp. PCC 6803.

Objectives of this research

1. To study the function of the extended N-terminal region of SphS and identify the important region in the Pho regulon control.
2. To identify the requirement of Pst1 system in regulation of the SphS-SphR two-component signal transduction system and show the possible interaction between Pst system and SphS sensor.
3. To characterize the phosphate transport in *Synechocystis* sp. PCC 6803 wild-type, ΔPst1 and ΔPst2 strains.

CHAPTER II

MATERIALS AND METHODS

2.1 Materials

2.1.1 Chemicals

Reagents used in this study were of analytical grade and obtained from either Ajax Finechem Limited, Australia; BDH Chemical Limited, England, Invitrogen Corporation, USA, Merck, Germany, or Sigma Chemical Company, USA.

2.1.2 Equipments

Autoclave: Sanyo, Japan

Centrifuge: Model J-21C, Beckman Instrument Inc, USA

Laminar flow:International Scientific Supply, Thailand

Micropipette: Pipetman, Gilson, France

PCR machine: Mastercycler Gradient, Eppendorf, Germany

Power supply: Bio-Rad POWER PAC 1000

Spectrophotometer: Model DU-650 and Model Jasco V-550, Beckman Instrument Inc, USA

2.1.3 Enzymes

Klenow polymerase: Invitrogen, USA

Lysosyme: Sigma, USA

Platinum *Taq* DNA polymerase: Invitrogen, USA

Restriction enzymes: Fermentas, Canada

Reverse transcriptase, SuperScript® II, Invitrogen, USA

2.1.4 Antibiotics

Ampicillin: Sigma, USA

Chloramphenicol: Sigma, USA

Kanamycin: Sigma, USA

Spectinomycin: Sigma, USA

2.1.5 Supplies

Hybond-N membrane: Amersham Biosciences, USA

X-ray film: X-Omat XK-1, Eastman Kodak, USA

Minisart membrane: Sartorious, Geramany

2.1.6 Kit

1 kb Plus DNA Ladder: Invitrogen, USA

NucleoSpin® Extract II, PCR purification kit, Machery-Nagel, USA

2.1.7 Organisms and plasmids

The two organisms *Escherichia coli* and *Synechocystis* sp. PCC 6803 were used in this study. All strains and plasmids were kindly provided by Assoc. Prof. Dr. Julian Eaton-Rye, Department of Biochemistry, University of Otago, New Zealand.

E. coli strain CJ236 carrying pTZsll0337 (Juntarajumnong et al., 2007c)

E. coli strain DH5α

Synechocystis sp. PCC 6803 wild-type strain, glucose sensitive

Synechocystis sp. PCC 6803 SphS control strain, a kanamycin-resistance cassette was inserted at nine nucleotides downstream of the stop codon of the *sll0337* (*sphS*) gene, indistinguishable from wild type with the exception that it was resistant to kanamycin (Juntarajumnong et al., 2007c).

Synechocystis sp. PCC 6803 ΔSphS strain, the *sll0337* (*sphS*) gene was replaced with a chloramphenicol-resistance cassette (Hirani et al., 2001)

Synechocystis sp. PCC 6803 ΔSphU strain, the *slr0741* (*sphU*) gene was replaced with a chloramphenicol-resistance cassette (Juntarajumnong et al., 2007b).

pΔslr0741-cam^{R}, pGEM T-easy derivative carrying a *slr0741* (*sphU*) interrupted with a chloramphenicol-resistance cassette (Juntarajumnong et al., 2007b).

pGEM® T-easy, cloning vector, Promega, USA

2.1.8 Oligonucleotides

Oligonucleotides were purchased form Sigma-Aldrich, Australia.

2.1.8.1 Mutagenic primers for internal deletions and alanine substitutions of SphS

The mutagenesis primers were used to construct mutagenic strands of *sphS* gene in pTZsll0337 shown in Table 1.

Table 1 Oligonucletide sequences used to introduce deletions and alanine substitutions into SphS of *Synechocystis* sp. PCC 6803.

Amino acid deletion	Oligonucleotides[a]	Introduced restriction site
Δ(I3-R23)	AATTTTATTATTGAG/*C*TCCATGTTCTAGCA	*Sac I*
Δ(I3-L31)	CGGCAGCCCAGTGAG/*C*TCCATGTTCTAGCA	*Sac I*
Δ(I3-S44)	GGACACAAGGGA*G*AG/*C*TCCATGTTCTAGCA	*Sac I*
Δ(I3-S49)	TTCTCGCCGCAC*G*AG/*C*TCCATGTTCTAGCA	*Sac I*
Δ(I8-G15)	TTCGATCGCCCCGAT/*G*GCCAATGTAATTAT	*Bgl I*
Δ(V41-S44)	GGACACAAGGGA*G*AG/*C*TCCTGGGTATCCGG	*Sac I*
Δ(V41-S46)	CACCAGGGACAC*G*AG/*C*TCCTGGGTATCCGG	*Sac I*
Δ(V41-S49)	TTCTCGCCGCAC*G*AG/*C*TCCTGGGTATCCGG	*Sac I*
I8A,G9A,G10A	AACCAATTGCC<u>G</u>C<u>TG</u>C<u>AGC</u>CGCCAATGTAA	-
G15A,I16A	TTCGATCGCCCC<u>TGCAG</u>CAAAACCAATTGC	-

[a]The oligonucleotides are designed for the complimentary strand. The site of deletion is indicated by a backslash. Italics represent base substitutions to introduce restriction sites used for initial screening. Underlines demonstrate base substitutions to change amino acids to be alanine.

2.1.8.2 Sequencing primers

The forward primer used for sequencing, to verify the deletions of *sphS* was 5'-GGAAAAAATGCTGCTCCGGA-3'. This primer was located between nucleotides -38 and -19 upstream of the ATG start codon of *sphS*. Similarly, the reverse primer used for sequencing was 5'-GCTAAAGTTTGGCGATTTTCCA-3', located between nucleotides 554 and 575 of *sphS*.

2.1.8.3 PCR primers

The Polymerase Chain Reaction (PCR) was used to amplify upstream and downstream fragments of both *pst1* and *pst2* operons, as well as, full length of *sphS* gene. The sequences of all primers are shown in Table 2.

2.1.8.4 RT-PCR primers

The Reverse Transcription Polymerase Chain Reaction (RT-PCR) was used to detect the expression of the deleted *sphS* transcript, as well as, the *psbB* transcript as a control. The primers for both genes are shown in Table 3.

2.1.8.5 Oligonucleotide probes

The probe for *pst1* was established from 2.1 kb PCR product of upstream fragment of *pst1* operon. This fragment was digested with *Ban* II produced 262, 630, and 1257 bp fragments. The 630 bp fragment was subsequently used as a template for *pst1* probe, which was located between -649 and -20 nucleotides upstream of the ATG start codon of *sphX* (*sll0679*).

The probe for *pst2* was done similarly from 2.1 kb PCR product of upstream fragment of *pst2* operon. *EcoR* I and *Hpa* I were used to double digest this fragment produced 400, 695, and 1030 bp fragments. The 695 bp fragment was subsequently

used as a template for *pst2* probe, which was located between -1127 and -433 nucleotides upstream of the ATG start codon of *pstS2* (*slr1247*).

Table 2 PCR primers for genomic PCR.

DNA region	Oligonucleotides
upstream of *pst1* operon (upstream of *sll0679*)	forward primer: CCAGGAATTGGACGACCTAC reverse primer: GGGTGGTCGATTGTGATTAG
downstream of *pst1* operon (downstream of *sll0684*)	forward primer: TTAAATAAATCCAAAAGCCGGG reverse primer: TCCCTTACCAGGACTGGATTTT
upstream of *pst2* operon (upstream of *slr1247*)	forward primer: AAAACTGTTGGGTGGGAGTGC reverse primer : AAACAGTCAGCCCTTGTTCG
downstream of *pst2* operon (downstream of *slr1250*)	forward primer: ATGTATTGCCAGGGCGTTAG reverse primer : CCACTTTTCAACGGGTAGGA
sphS (*sll0337*)	forward primer: CCCCCTCAATGCTGACTCCA reverse primer : CCAGTTTAAGGGCTGTCCCG
sphU (*slr0741*)	forward primer: CGCCAAGGAATTCTTGTTGCCATAACCCTG reverse primer : CTGCCTCTCCATGTCGACCTTGTAAACTCC

Table 3 PCR primers for RT-PCR.

Gene	Oligonucleotides
sphS (*sll0337*)	forward primer: ATTCTTCTCAGGGGATCGGGATTT reverse primer : GGTGATATTTTTTACCACGG
psbB (*slr0906*)	forward primer: ACCGGTGCTATGAACAGTGG reverse primer : CTTCTTTCCGGGTGGAAAGG

2.2 Methods

2.2.1 Culture conditions

2.2.1.1 Growth conditions for *Escherichia coli*

The different strains of *E. coli* were maintained on LB agar with the addition of suitable antibiotics at 4°C. Liquid cultures were grown in LB media at 37°C for overnight, shaking 200 rpm on a GIO GYROTORY® shaker. For long-term storage, the strains were stored at -80°C in 80% glycerol.

2.2.1.2 Growth conditions for *Synechocystis* sp. PCC 6803

The *Synechocystis* sp. PCC 6803 strains were maintained on BG-11 agar, containing suitable antibiotics, at 30°C under constant illumination of 25 μE/m^2/s. Liquid cultures were grown photoautotrophically in BG-11, containing suitable antibiotics, at 30 °C with constant illumination, aerating with filtered air by an aquarium pump or shaking 160 rpm on an INNOVA™ 4340 shaker. For long-term storage, the strains were stored at -80°C in BG-11liquid medium containing 15% glycerol.

For phosphate -limiting experiments, 175 µM K_2HPO_4, in BG-11 was replaced with 175 µM KCl (Aiba et al., 1993; Hirani et al., 2001).

2.2.2 General molecular biology methods

2.2.2.1 PCR

10X PCR Buffer: 200 mM Tris-HCl (pH 8.4), and 500 mM KCl.

2X PCR Mix: 2X PCR buffer, 0.4 mM dNTPs mixture, and 20 ng/µl of each primer.

The PCR was performed in a 1X PCR mix using 0.1-1 µg of template DNA (or picked colony for colony PCR), 0.5 U of Platinum *Taq* polymerase, and 1.5–2 mM of $MgCl_2$, making to 20 µl of reaction mixture with sterile H_2O. The PCR was carried out in a Mastercycler Gradient, Eppendorf. The reaction involved an initial denaturing step of 5 min at 94°C followed by 30 cycles of 1 min annealing at 45-65°C, depending on the oligonucleotides used, 1-3 min extension at 72°C, depending on length of expected PCR product, and 30 s denaturing at 94°C. The reaction ended with a final extension at 72°C for 5 min. the PCR product was analyzed by electrophoresis.

2.2.2.2 Restriction digestion

Single or double restriction digestion was incubated at the optimum temperature of restriction enzymes for 60 min. The total volume of the reaction was 10 µl containing 1X proper restriction buffer, 1-2 U of restriction enzyme, and the DNA sample.

2.2.2.3 Gel electrophoresis

DNA samples were analyzed by electrophoresis in 0.8% agarose gels. The gels were run in either 1X TBE buffer or 1X SB buffer. DNA samples were mixed

with 1 µl of DNA loading buffer before samples were loaded and electrophoresesd at 80-100 V (for TBE buffer) or 100-200 V (for SB buffer) until blue dye had run three-quarters the length of the gel. After that, gels were stained in ethidium bromide solution of 1 ng/µl for 10 min.

RNA samples were analyzed by electrophoresis in 1% MOPS agarose gels containing 2% formaldehyde. The gels were run in 1X MOPS buffer. RNA samples were mixed with 3 µl of RNA loading buffer before samples were loaded and electrophoresesd at 80V until blue dye had run three-quarters the length of the gel.

DNA and RNA were visualized under UV light on a gel document Stratrgene Eagle Eye II or Syngene.

2.2.3 Molecular biology methods for *Escherichia coli*

2.2.3.1 Preparation of competent cells

A single well isolated colony of DH5α on LB agar was inoculated in 10 ml of LB and grown at 37°C for overnight with shaking at 200 rpm on a GIO GYROTORY® shaker. Two ml of overnight culture was transferred to 100 ml of pre-warmed ψB media, and grown at 37°C with shaking at 250 rpm on a GIO GYROTORY® shaker until an optic density at 600 nm reached 0.3-0.4 (~2 h). Cells were collected in pre-chilled 50 ml Falcon tubes by centrifugation at 2760 g at 4°C for 10 min. The supernatant was decanted and the cells were resuspended gently in 15 ml of chilled TfBI. The cells were again centrifuged immediately and the pellets resuspended gently in 2 ml of chilled TfBII. Resuspended cells were aliqouted 200 µl volumes, snap frozen in liquid nitrogen or dry ice and ethanol, and stored at -80 °C.

2.2.3.2 Heat-shock transformation

An aliquot of competent cells was first thawed on ice, mixed gently with DNA, and incubated on ice for 30 min. The cell/DNA mix was heat shocked at 37 °C for 2 min, and placed on ice for 3 min. After that, a 1 ml of LB was added and incubated at 37 °C for 60-90 min, shaking at 200 rpm on a GIO GYROTORY® shaker. The cells were collected and resuspended in 200 µl of LB before spreading on LB agar containing suitable antibiotics and incubated at 37°C for 16 h.

2.2.3.3 Alkaline lysis minipreparation

A single colony of DH5α strain was inoculated in 2 ml of LB, containing suitable antibiotics, and grown at 37°C for overnight with shaking at 200 rpm on a GIO GYROTORY® shaker. A 1.5 ml of the overnight culture was transferred to a 1.5 ml tube and centrifuged for 30 s. The pellet was resuspended in 100 µl of Solution 1 and incubated at room temperature for 5 min. The sample was placed on ice for 5 min before adding 200µl of Solution 2. The sample was again incubated on ice for 5 min before adding 200 µl of Solution 3. The sample was mixed gently, incubated on ice for 5 min, and centrifuged for 5 min. The 350 µl of supernatant was transferred to a new 1.5 ml tube and extracted with 100 µl of 1:1 solution of chloroform: phenol. The sample was centrifuged for 5 min, 300 µl of aqueous phase transferred to a tube and mixed thoroughly with 180 µl of 100% isopropanol. The sample was incubated at room temperature for 10 min and the nucleic acid pellet collected by centrifuging for 10 min. The pellet was washed with chilled 70% ethanol and dried at 37 °C for 10 min. The pellet was resuspended in 40 µl of TE. All centrifugations were carried out at 13400 g in a microfuge.

2.2.3.4 Sequencing minipreparation

All centrifugations were carried out at 13400 g in a microfuge. A single colony of DH5α strain was inoculated in 5 ml of LB, containing suitable antibiotics, and grown at 37°C for overnight with shaking at 200 rpm on a GIO GYROTORY® shaker. A 1.5 ml of the overnight culture was transferred to a 1.5 ml tube and centrifuged for 30 s. This step was repeated twice, each time adding 1.5 ml of the culture to the tube. The pellet was resuspended in 200 µl of Solution 1 and incubated at room temperature for 5 min. A 300 µl of Solution 2 was added and the sample placed on ice for 5 min before adding 300 µl of chilled Solution 3. The sample was first incubated on ice for 5 min and then centrifuged for 5 min. The supernatant (~700 µl) was transferred to a 1.5 ml tube and 2µl of 10 mg/ml RNase A added. The sample was incubated at 37 °C for 20 min. It was extracted twice with an equal volume of 1/25 isoamyl alcohol/ chloroform. The aqueous phase was transferred to a new tube and the DNA precipitated with 700 µl of isopropanol. After an incubation of 10 min, the sample was centrifuged for 10 min, washed with chilled 70% ethanol, dried at37 °C for 10 min, and resuspended in 32 µl of sterile water. An 8 µl of 4 M NaCl and 40 µl of 13% polyethylene glycol (PEG) 8000 were added and the sample incubated on ice for 60 min. The sample was centrifuged for 20 min, washed with chilled 70% ethanol, dried and resuspended in 20 µl TE. The DNA was sent to sequence at the Allan Wilson Centre for Molecular Ecology and Evolution, Massey University, New Zealand.

2.2.3.5 Oligonucleotide-directed mutagenesis

2.2.3.5.1 Single-stranded DNA

Growth of Uracil-containing Phagemids

The CJ236 strain carrying pTZsll0337 was obtained from 80% glycerol stock solution and streaked on LB agar containing 50 µg/ml of ampicillin, 50 µg/ml of kanamycin, and 15 µg/ml of chloramphenicol, and incubated at37 °C for 16 h. A single colony was inoculated in 20 ml of LB containing suitable antibiotics for overnight with shaking at 200 rpm on a GIO GYROTORY® shaker. One ml of the overnight culture was transferred to 50 ml of pre-warmed 2x YT media containing suitable antibiotics and grown at37 °C with shaking at 260 rpm on a GIO GYROTORY® shaker until an optical density at 600 nm reaches 0.3. The culture was added M13K07 helper phage to obtain a multiplicity of infection of around 20 and further grown for 1 h. The culture was added kanamycin to a final concentration of 70 µg/ml and grown for 5-6 h. The culture was then transferred to two round-bottomed centrifuge tubes and centrifuged at 17000g 4 °C for 15 min. The supernatant containing phagemid particles was transferred to a new round-bottomed centrifuge tube and centrifuged at 17000g 4 °C for 15 min. The supernatant was collected, added 150 µg of RNase A, and incubated at room temperature for 30 min. The sample was added 1/4 volume 3.5 M ammonium acetate/20% PEG-6000 and incubated on ice for 30 min. The phagemids were collected by centrifugation at 17000g 4 °C for 15 min and the pellet was resuspended in 200 µl of high salt buffer. The resuspended solution was transferred to a 1.5 ml tube, chilled on ice for 30 min and centrifuged at 12000g for 5 min to remove insoluble substances. The supernatant was transferred to a new tube.

Extraction of Phagemid DNA

The phagemid solution was extracted twice with an equal volume of neutralized phenol and once with 1:1 solution of chloroform: phenol. The aqueous

phase was extracted further with an equal volume of 1:25 isoamyl alcohol: chloroform 3-4 times. The aqueous phase was added 1/10 volume of 7.8 M ammonium acetate and 2.5x volume of 100% ethanol and incubated at –80ºC for 30 min. The sample was centrifuged at 12000g 4 °C for 15 min and the pellet was washed with 70% ethanol, dried and resuspended in 20 µl of TE. One µl of single-stranded DNA was checked by gel electrophoresis.

2.2.3.5.2 Synthesis of the mutagenic strands

Phosphorylation of the oligonucleotide

The total volume of the reaction was 30 µl containing 200 pmol of oligonucleotide, 100 mM of Tris/HCl buffer pH 8.0, 10 mM of $MgCl_2$, 5 mM of DTT, and 0.4 mM of ATP. The reaction mixture was added with 4.5 U of T_4 polynucleotide kinase and incubated at37°C for 45 min. The reaction was stopped by heating at 65 °C for 10 min.

Annealing of the mutagenic oligonucleotide

The total volume of the reaction was 10 µl containing 200 ng of single-stranded DNA (phagemid), 6-9 pmol of phosphorylated mutagenic oligonucleotide, and 1x annealing buffer. A control was performed similarly without the mutagenic oligonucleotide. The mixture was heated to 95°C then allowed to cool at room temperature and placed on ice.

Synthesis of the complementary strand

After annealing, the mixture was added 1 µl of 10x synthesis buffer, 1µl of T_4 DNA ligase, and 1 µl of T_7 polymerase and incubated further on ice for 5 min. The reaction mixture was incubated at 25°C for 5 min and incubated at 37°C for 60 min.

The reaction was stopped by adding of 90µl of TE stop buffer. Ten µl of the sample was transformed into competent cells.

2.2.4 Molecular biology methods for *Synechocystis* sp. PCC 6803 strains

2.2.4.1 DNA extraction

Total DNA extraction of *Synechocystis* sp. PCC 6803 strains was performed according to the method of Williams (1988). The *Synechocystis* sp. PCC 6803 strains were grown in 200 ml of BG-11 containing suitable antibiotics for 3-4 days. The cells were harvested by centrifuging at 2760 g for 10 min, resuspended in 2 ml of saturated NaI and incubated at 37°C for 20 min. The cell suspension was diluted with 1 ml of sterile water and centrifuged at 2760 g for 10 min. The cell pellet was resuspended in 8 ml of TES solution, added 1.25 ml of 50 mg/ml lysozyme per gram of cells and incubated at 37°C for 20 min. The lysate was mixed gently with 1 ml of 10% N-lauryl sarcosine per gram of cells and incubated at 37°C for 20 min. The sample was extracted with an equal volume of equilibrated phenol and rotated on a wheel for 1 h. The sample was centrifuged at 2760 g for 10 min and the upper phase was transferred to a new tube. The sample was extracted with an equal volume of 1/25 isoamyl alcohol/ chloroform and rotated on wheel for 30 min. The upper phase was separated by centrifugation at 2760 g for 10 min and transferred to a new tube. The sample was added 1/10 volume of 3 M Na-acetate (pH 5) and 2.5 volumes of 100% ethanol and incubated at -20°C for overnight. The DNA pellet was collected by centrifuging at 2760 g for 15 min and washed with chilled 70% ethanol. The pellet was dried at room temperature, resuspended in 200 µl of TE, and transferred to a sterile 1.5 ml tube.

2.2.4.2 Transformation

Transformation of *Synechocystis* sp. PCC 6803 strains with the various plasmids was carried out according to the method of Williams (1988). Liquid cultures of *Synechocystis* sp. PCC 6803 strains were grown for 2-3 days and harvested by centrifuging at 2760 g for 10 min in 50 ml Falcon tubes. The cells were resuspended in BG-11 to an optical density at 730 nm of 2.5, transferred to sterile glass tubes and mixed with 2-8 µg of DNA. The total volume was made up to 0.5 ml with sterile water. A mixture of cells without DNA was used as a negative control. The cells were placed at 30 °C under constant illumination of 25 µE/m^2/s for 6 h. A 200 µl of the cells were plated on sterile filter membranes on BG-11 agar plates, and the plates incubated at 30 °C under constant illumination of 25 µE/m^2/s for 24 h. The following day, the filter membranes were transferred to BG-11 agar containing suitable antibiotics. Isolated colonies were re-streaked three times to obtain a homozygous strain. To verify its homozygosity, genomic DNA was extracted, and either amplified by PCR followed by sequencing of the appropriate region, or digested with restriction enzymes followed by Southern analysis.

2.2.4.3 Southern analysis

Blotting

Capillary transfer of DNA from 0.8% agarose gel to GENE-Screen® hybridization transfer membrane was carried out according to method of Sambrook et al. (2001) with following changes. The gel was washed in 0.25 M HCl for 10 min, rinsed in sterile water and incubated in transfer buffer for 30 min. After transfer, the membrane was soaked in 2x SSC for 2 min and partially dried under a lamp at room temperature.

Labeling of probes

Twenty-five ng of DNA was denatured by boiling for 10 min and rapidly cooled on ice for 5 min. The denatured DNA solution was added 10 µl of OLB solution, 2 µl of 10 mg/ml BSA, 5 U of Klenow, and 2µl of 10 µCi/µl[α-^{32}P]dCTP, and made up to 50 µl with sterile water. The mixture was incubated at room temperature for 2-3 h and added 120 µl of Stop solution. To remove the unincorporated [α-^{32}P]dCTP, the mixture was centrifuged through a Sephadex G-50 column at 2700 g for 2 min. A 1 µl of 10 mg/ml salmon sperm DNA was added to the probe before boiling for 10 min followed by rapid cooling on ice for 5 min to denature the probe.

Pre-hybridization, hybridization and washing

The membrane was placed in a hybridization bottle with a 5-10 ml of pre-hybridization solution. The hybridization bottle was put in a hybridization oven at 37°C for 6 h, added the probe and incubated overnight at 37°C. The solution was decanted and the membrane was washed twice in 2x SSC for 5 min at room temperature in the hybridization bottle. The blot was washed twice in 2x SSC with 0.2% SDS for 30 min at 65°C. The blot was again washed twice in 0.1x SSC for 10 min at room temperature. The membrane was dried and exposed at -80°C with a Kodak Imaging Film in a Kodak X-Omatic cassette.

2.2.4.4 RNA extraction

Synechocystis sp. PCC 6803 strains were grown in 200 ml of BG-11 containing suitable antibiotics for 3 days. The cells were collected by centrifuging at 2760 g 4°C for 10 min and resuspended in 2 ml hot phenol (65°C).All following steps were done on ice. A 2 ml of NAES solution was added and aliquoted to 4 tubes

containing glass beads. The tubes were agitated three times in a bead beater for 20s at 5000 rpm. The samples were centrifuged at 14000g 4°C for 10 min to separate phase. All following centrifugations were carried out at 14000 g 4°C for 10 min in a microfuge. The upper phase was transferred to a new tube and extracted twice with phenol: chloroform. The sample was extracted again with chloroform and the upper phase was transferred to a new tube. The RNA was precipitated by adding 2 volumes of chilled 100% ethanol and kept at -20°C for 20 min. The pellet was collected by centrifuging and dried at 37°C for 10 min. The pellet was resuspended in 250 µl of DEPC-treated water. The sample was added 62.5 µl of 10 M LiCl and incubated at 4°C overnight to remove DNA. The following day, the pellet was collected by centrifuging and rinsed with 0.5 ml of 2 M LiCl. The RNA sample was resuspended in 400 µl of DEPC-treated water and precipitated with 2 volumes of 100% ethanol and 1/10 volume of sodium acetate. The sample was frozen at -20°C for 20 min, thawed at room temperature and centrifuged. The RNA pellet was dried and resuspended in 50 µl of DEPC-treated water. The RNA samples were analyzed in 1% MOPS agarose gel electrophoresis.

2.2.4.5 RT-PCR

The reverse transcription (RT) PCR was performed according to SuperScript® II protocol with following changes.

cDNA systhesis

The RNA samples were first treated with DNase. Five-hundreded ng of RNA was mixed with 2 µl of random hexamers, 2 µl of 10 mM dNTPs and made up to 13 µl with DEPC-treated water. The sample was incubated at 65°C for 5 min and placed on ice for 1 min. The sample was further added 4 µl of 5x first-strand buffer, 1 µl of

0.1 M DTT, 1 µl of RNaseOUT, and 1 µl of SuperScript II reverse transcriptase and incubated room temperature for 5 min. The reaction mixture was subsequently incubated at 55°C for 30 min and heated at 85°C for 10 min. The same reaction was also performed without enzyme used as a negative control.

PCR

The *sphS* and *psbB* cDNA were amplified by PCR with forward and reverse primers (Table 3).

2.2.5 Characterization of *Synechocystis* sp. PCC 6803 strains

2.2.5.1 Photoautotrophic growth curve measurements

Starter cultures were grown in 150 ml BG-11 containing suitable antibiotics for 3 days. Each culture was split into two 50 ml Falcon tubes and centrifuged at 2760 g for 10 min. The cells were washed twice and resuspended in 2 ml of phosphate-limiting BG-11 and an optical density at 730 nm was measured. The cultures were set up in a volume of 150 ml in BG-11 and phosphate-limiting BG-11 to a starting $OD_{730\ nm}$ of 0.05. Measurements of the $OD_{730\ nm}$ were taken every 12 h or 24 h and the cells were diluted to an $OD_{730\ nm}$ of less than 0.4 for each measurement.

2.2.5.2 Absorption spectra

Spectra were collected on a Jasco V550 UV/Vis spectrophotometer. Whole cells were used at an $OD_{800\ nm}$ of 0.4 and scanned from 800 to 400 nm. To correct for scattering, a piece of cellotape was put on either side of the sample cuvette holder and the reference cuvette holder such that the cellotape covered the light path. The cuvette holder was covered before setting up the reference with BG-11 (Hirani et al., 2001)

2.2.5.3 Alkaline phosphatase assay

Solution 1: 0.2 M Tris-HCl pH 8.5 and 2 mM $MgCl_2$.

A culture of 50 ml was harvested by centrifuging at 2760g for 10 min and resuspended in 1 ml of Solution 1. The $OD_{730\ nm}$ was measured for each resuspended pellet. A 60 µl of cell suspension was mixed with 910 µl of Solution 1. The substrate *p*-nitrophenyl phosphate was added to a final concentration of 3.6 mM in a total volume of 1 ml reaction mixture. The sample was incubated at 37°C for 20 min. The reaction was stopped by the addition of 150 µl of 4 M NaOH. Sample was centrifuged at 13400g for 5 min and the $OD_{400\ nm}$ of the *p*-nitrophenol in the supernatant was measured (Hirani et al, 2001).

2.2.5.4 Phosphate uptake

A 100 ml culture was harvested and washed twice with phosphate-free buffer by centrifugation at 2760 g for 10 min. Cells pellet was resuspended with phosphate-free buffer to an $OD_{730\ nm}$ of 0.3. The cell suspension was placed at room temperature under constant illumination for 30 min. The phosphate uptake was initiated by addition of K_2HPO_4 to cell suspension. At different time intervals, aliquots were withdrawn, filtered through 0.45 µm cellulose acetate filters to remove cells. The filtrates were collected to determine the phosphate concentrations.

2.2.5.5 Chlorophyll extraction

Chlorophyll was extracted from cells with methanol according to MacKinney (1941). One ml of culture was collected by centrifugation and resuspended in 1 ml of 100% methanol. The sample was mixed thoroughly and the pellet was removed by centrifugation at 14400 g for 5 min.

2.2.6 Phosphate concentration measurements

Ammonium molybdate solution: 2.5% (w/v) ammonium molybdate in 3 N H_2SO_4

Reducing agent solution: 2% (w/v) ascorbic acid

Phosphate concentrations were measured spectrophotometrically using coloring method modified by Katewa and Katyare, (2003). Five-hundreded µl sample was mixed with 400 µl of ammonium molybdate solution, forming phosphomolybdic acid, and 100 µl of reducing agent solution was finally added to develop blue color of molybdenum blue with an absorption maximum at 820 nm.

2.2.7 Calculations

Estimation of DNA concentration:

50 µg/ml = $A_{260\ nm}$ of 1 for dsDNA

33 µg/ml = $A_{260\ nm}$ of 1 for ssDNA

Estimation of RNA concentration:

40 µg/ml = $A_{260\ nm}$ of 1 for ssRNA

Estimation of alkaline phosphatase activity:

Arbitrary units (a.u.) = $1000 \times A_{400\ nm}/t \times v \times OD_{730\ nm}$

where: t = incubation time (min)

v = cell volume (ml)

Estimation of cell count:

$OD_{730\ nm}$ of 0.25 = 1×10^8 cells (Mayes et al., 1991)

Estimation of chlorophyll concentration:

1 mg/ml = $OD_{663\ nm}$ of 82 (MacKinney, 1941)

CHAPTER III

RESULTS

3.1 Characterization of the SphS deletion and alanine replacement strains

3.1.1 Bioinformatics analysis of SphS

A SphS contains 430 amino acids with a highly conserved C-terminal region to PhoR of *E. coli* but not at the N-terminal region (Fig. 8). The PhoR of either *E. coli* or *B. subtilis* contains at least a transmembrane region at the N-terminus with high hydrophobicity. By contrast, the primary structure of SphS shows a very low hydrophobicity at the N-ternimus as analyzed by TMHMM (http://www.cbs.dtu.dk/services/TMHMM/) (Fig. 9). The different databases and programs were also used to analyze the SphS mainly for transmembrane domain, such as, PredictProtein (Rost et al., 1996), SMART (Letunic et al., 2006), TOPDOM (Tusnady et al., 2008), SOSUI (Gomi et al., 2004), InterProScan (http://www.ebi.ac.uk/Tools/InterProScan/), Pfam (http://pfam.sanger.ac.uk/). The presence of a transmembrane region was rarely reported, only PHD program from PredictProtein and TOPDOM indicated a putative membrane-spanning domain between amino acids Ile-4 and Ile-19 while the cytoplasmic portion was strongly revealed a PAS domain (residues 70-137), a Histidine Kinase A (HisKA) domain or Dimerization Histidine phosphotransfer (DHp) domain (residues 197–261), and a Histidine kinase-like ATPase (HATPase_c) or Catalytic ATP-binding (CA) domain (residues 307-424) (Fig. 10). This might be a result of almost programs calculate transmembrane domain on the basis of hydrophaty. In addition, the result of either SMART or PredictProtein also suggested

A

```
S6803   MEIITLAIGGAIGFGIGAIERFRLNNKIKKLLTGLPDTQEVSHSLSLVSLVRREINHLND 60
S7942   MAAWEFALGLLTASLWRWARKWRSPVKVKPMLA--------------------AVSSLEP 40
Ecoli   MLERLSWKRLVLELLLCCLPAFILGAFFGYLPWFLLASVTGLLIWHFWNLLRLSWWLWVD 60
        *                    :     .  :

S6803   LCAEYLDTIAHWRGVMSLSPLGYLLIDQE-----NNLEWCNPAAESLLHIRYWQPGERRL 115
S7942   QLEQITTDLRDRDRLLEDLPVSFLLLDAD-----NLVLEANRSARVLLALP--PEDYCRP 93
Ecoli   RSMTPPPGRGSWEPLLYGLHQMQLRNKKRRRELGNLIKRFRSGAESLPDAVVLTTEEGG- 119
                     ::       *  .       * :   . .*. *

S6803   FLEFIRSYELDQLIECTRQTQTNQTREWSFFPPLTAAMEGWGNHRPLTPES---ILLRGS 172
S7942   LLEVVRSYELDRLVARCRAANAPQTDRWTLTPVNPDPLQ----VVPQTPR-----PVQGQ 144
Ecoli   -IFWCNGLAQQILGLRWPEDNGQNILNLLRYPEFTQYLKTRDFSRPLNLVLNTGRHLEIR 178
         :   ..   : *       :  :  .    *  .  ::       * .         :.

S6803   GFPLKEGKVAVFVENRQTLAALRQGRDQAFSDLAHELRTPLTAVALIAERLQARLPA--E 230
S7942   AIPLSNGQIGVLIEDRQELVDLAQQRNRWVSDVAHELKTPLTSIRLLAEALRDRLQD--E 202
Ecoli   VMPYTHKQLLMVARDVTQMHQLEGARRNFFANVSHELRTPLTVLQGYLEMMNEQPLEGAV 238
         :* .. :: :. .:   :  *   * . .::::***:**** :    * :. :

S6803   DGDWAERLLKEISRLQNLVESWLHLTQITANPNLYLEPEPINLRHLLAITWERLTPIAVV 290
S7942   PQVWVDRLLGETQRLGQLVQDLLELSRLEQGPSGLQKLEAVDLVALLTSVRNSLEPLAEP 262
Ecoli   REKALHTMREQTQRMEGLVKQLLTLSKIEAAPTHLLN-EKVDVPMMLRVVEREAQTLSQK 297
             . :  : .*:  **:. * *:::   *.   : * :::  :*  . .   .::

S6803   KNITLDYQGPTKLNLEGDGDRLMQVLMNILDNTLKYSPPEGTIFVQGHQGTEGITMIIRD 350
S7942   LRLGWAYQGPEQGFVRGDRQRLFRLWLNLVDNAIRHSPSGGCLYVELRQRGDTWICDLYD 322
Ecoli   K-QTFTFEIDNGLKVSGNEDQLRSAISNLVYNAVNHTPEGTHITVRWQRVPHGAEFSVED 356
              ::       : *: ::*     *:: *::.::*    : *. ::  .     : *

S6803   QGLGFQPRDLPYIFERLYRGDSSRAR-LHPDSQRHGSGLGLAIAKEIVLAHRGNLTAANH 409
S7942   DGPGFADADLPYLFERFYRGDPSRVRPAAASSSSPGSGLGLAIARQVVEAHQGRISARNH 382
Ecoli   NGPGIAPEHIPRLTERFYRVDKARSR------QTGGSGLGLAIVKHAVNHHESRLNIEST 410
        :* *:   .:* : **:** * :* *      .  ********.:. *  *...:.  .

S6803   ETGG---------AMFTIELPYEPNMDENP--- 430
S7942   PSPAGLGCGYNCPKNHPSPLRLRSELDVAAAEP 415
Ecoli   VGKG---------TRFSFVIPERLIAKNSD--- 431
           .           ..  :  .  .
```

B

```
S6803    -MEIITLAIGGAIGFGIGAIERFRLNNKIKKLLTGLPDTQEVSHSLSLVSLVRREINHLN 59
Ecoli    MLERLSWKR-LVLELLLCCLPAFILGAFFGYLPWFLLASVTGLLIWHFWNLLRLSWWLWV 59
          :* ::     .: : : .:  * *.  :  *   *  :        : .*:* .

S6803    DLCAEYLDTIAHWRGVMS-LSPLGYLLIDQE----NNLEWCNPAAESLLHIRYWQPGERR 114
Ecoli    DRSMTPPPGRGSWEPLLYGLHQMQLRNKKRRRELGNLIKRFRSGAESLPDAVVLTTEEGG 119
         * .       . *. ::  *  :     .:.    * ::  ...**** .     . *

S6803    LFLEFIRSYELDQLIECTRQTQTNQTREWSFFPPLTAAMEGWGNHRPLTPES---ILLRG 171
Ecoli    IFWCNGLAQQILGLRWPEDNGQN--ILNLLRYPEFTQYLKTRDFSRPLNLVLNTGRHLEI 177
         :*     : ::  *     : *.    :   :* :*  ::  .  ***.        *.

S6803    SGFPLKEGKVAVFVENRQTLAALRQGRDQAFSDLAHELRTPLTAVALIAERLQAR--LPA 229
Ecoli    RVMPYTHKQLLMVARDVTQMHQLEGARRNFFANVSHELRTPLTVLQGYLEMMNEQPLEGA 237
           :* .. :: :...:   :  *. .* : *::::********.:    * :: :    *

S6803    EDGDWAERLLKEISRLQNLVESWLHLTQITANPNLYLEPEPINLRHLLAITWERLTPIAV 289
Ecoli    VREKALHTMREQTQRMEGLVKQLLTLSKIEAAPTHLLN-EKVDVPMMLRVVEREAQTLSQ 296
            .  . : :: .*::.**:. * *::* * *.  *: * :::  :* :. ..  .::

S6803    VKNITLDYQGPTKLNLEGDGDRLMQVLMNILDNTLKYSPPEGTIFVQGHQGTEGITMIIR 349
Ecoli    KK-QTFTFEIDNGLKVSGNEDQLRSAISNLVYNAVNHTPEGTHITVRWQRVPHGAEFSVE 355
          *  *: ::  . *::.*: *:* ..: *:: *::::*    * *: :: ..*  : :.

S6803    DQGLGFQPRDLPYIFERLYRGDSSRARLHPDSQRHGSGLGLAIAKEIVLAHRGNLTAANH 409
Ecoli    DNGPGIAPEHIPRLTERFYRVDKARSRQTG-----GSGLGLAIVKHAVNHHESRLNIEST 410
         *:* *: *..:* : **:** *.:*:*        ********.*. *  *...*.  .

S6803    ETGGAMFTIELPYEPNMDENP 430
Ecoli    VGKGTRFSFVIPERLIAKNSD 431
            *: *:: :* .   .:.
```

Figure 8 Alignment of protein sequences encoding histidine kinases involved in phosphate regulation. (A) Alignment of SphS phosphate sensor of *Synechocystis* sp. PCC 6083 (S6803), SphS phosphate sensor of *Synechococcus* sp. PCC 7942 (S7942) (Genbank accession number BAA02454.1) and PhoR phosphate sensor of *E. coli* K-12 (Ecoli) (Genbank accession number AAC73503.1). (B) Pairwise alignment of SphS phosphate sensor of *Synechocystis* sp. PCC 6083 (S6803) and PhoR phosphate sensor of *E. coli* (Ecoli). Alignment was done with CLUSTAL W 2.0.12 using default parameters. The conserved His residue that is phosphorylated site in histidine kinases are indicated in underline.

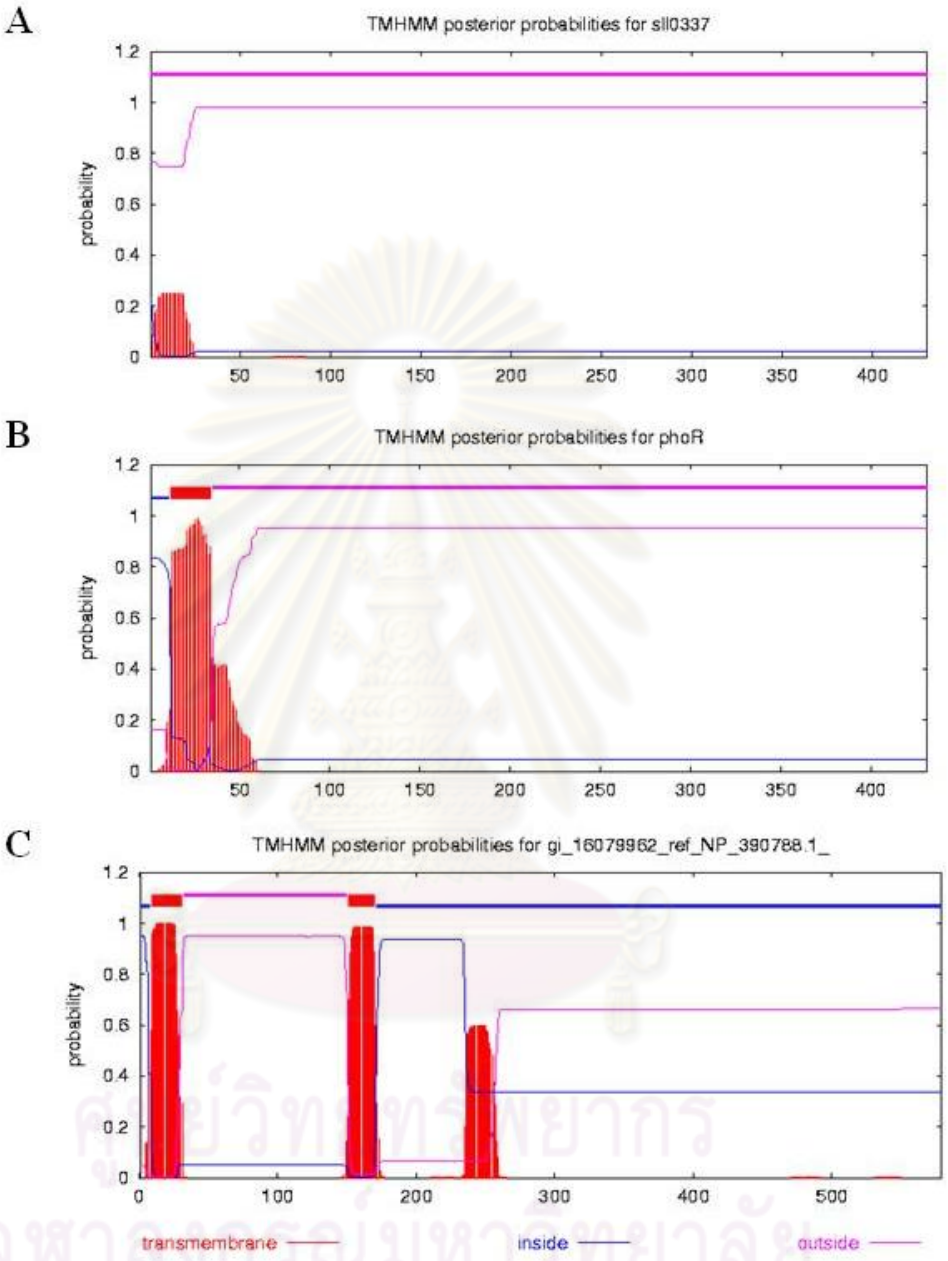

Figure 9 The transmembrane helix prediction in phosphate-sensing proteins. The histidine kinases for phosphate-sensing systems of *Synechocystis* sp. PCC 6803, (A) SphS, (B) *E. coli*, PhoR and (C) *B. subtilis*, PhoR. The vertical axis is the probability of transmembrane helix formation and the horizontal bar is amino acid length. The amino acid sequences were analyzed by TMHMM V 2.0 at http://www.cbs.dtu.dk/services/TMHMM/.

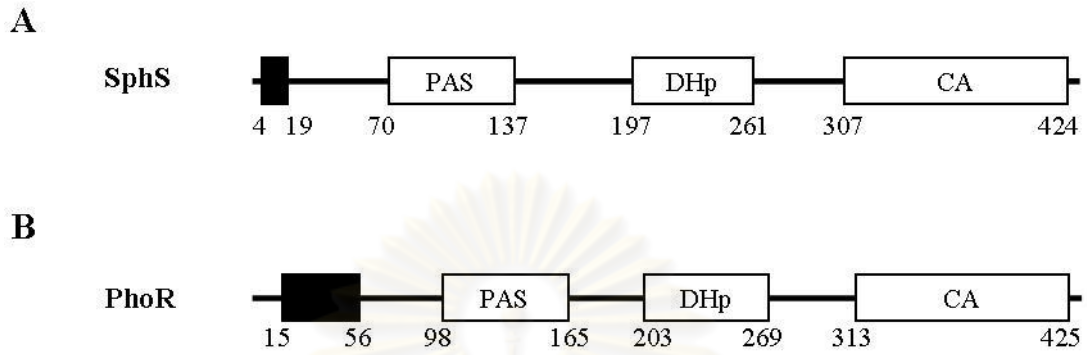

Figure 10 Domain architectures of phosphate-sensing histidine kinases. (A) SphS phosphate sensor of *Synechocystis* sp. PCC 6803. (B) *E. coli* phosphate sensor PhoR. The domain assignment based on the output of the SMART (Letunic et al., 2006) except that the transmembrane domain assigned by PredictProtein (Rost et al., 1996). The black boxes represent transmembrane domain, the boxes labeled PAS represent PAS domain, the boxes labeled DHp represent Dimerization Histidine phosphotransfer domain , and the boxes labeled CA represent Catalytic ATP-binding domain.

two low-complexity regions between amino acids Ile-3 and Ile-19 and between Val-41and Val-51 (data not shown). Deletions at either transmembrane or PAS domain, or both domains of PhoR lead to constitutive expression of Pho regulon in *E. coli* (Yamada et al., 1990; Scholten et al., 1993). In contrast, the removal of transmembrane domains of PhoR does not alter the expression pattern of alkaline phosphatase in *B. subtilis* (Shi & Hulett., 1999). To test whether *Synechocystis* sp. PCC 6803 cells need the N-terminal region or not, the deletions and Ala substitutions at the N-terminus were performed using oligonucleotide-directed mutagenesis.

3.1.2 Construction of the SphS deletion and alanine substitution strains

An *E. coli* strain CJ236 carrying pTZsll0337 has been created previously, which was used to introduce base substitutions into start codon of *sphS* (Juntarajumnong, 2007c). The oligonucleotide-directed mutagenesis was also done to introduce deletions and Ala substitutions into the extended N-terminal region of the SphS, the oligonucleotide sequences were shown in Table 1. The mutated pTZsll0337 was transformed into *Synechocystis* sp. PCC 6803 ΔSphS strain. The transformed cells were then plated onto BG-11 agar containing 25 µg/ml of kanamycin, resulting of eight deletion and two Ala substitution strains (Fig. 11). All ten strains were done colony PCR using the *sphS* primer pair (Table 2) to verify complete segregation of the mutated *sphS* with an expected band of 2.8 kb comparing to ΔSphS strain with an expected band of 2.36 kb (Fig. 12). The PCR product of each mutant was further sequenced to confirm the correctly mutated strain (data not shown).

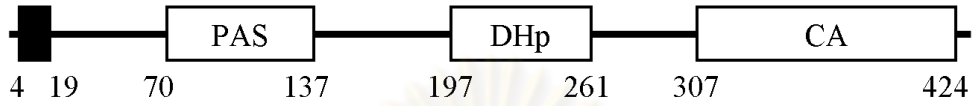


```
1 MEIITLAIGG AIGFGIGAIE RFRLNNKIKK LLTGLPDTQE VSHSLSLVSL 50 wild type
  MEIITLA--- -----IGAIE RFRLNNKIKK LLTGLPDTQE VSHSLSLVSL    Δ(I8-G15)
  ME-------- ---------- ---LNNKIKK LLTGLPDTQE VSHSLSLVSL    Δ(I3-R23)
  ME-------- ---------- ---------- -LTGLPDTQE VSHSLSLVSL    Δ(I3-L31)
  ME-------- ---------- ---------- ---------- ----LSLVSL    Δ(I3-S44)
  ME-------- ---------- ---------- ---------- ---------L    Δ(I3-S49)
  MEIITLAIGG AIGFGIGAIE RFRLNNKIKK LLTGLPDTQE ----LSLVSL    Δ(V41-S44)
  MEIITLAIGG AIGFGIGAIE RFRLNNKIKK LLTGLPDTQE ------LVSL    Δ(V41-S46)
  MEIITLAIGG AIGFGIGAIE RFRLNNKIKK LLTGLPDTQE ---------L    Δ(V41-S49)
  MEIITLAAAA AIGFGIGAIE RFRLNNKIKK LLTGLPDTQE VSHSLSLVSL    I8A,G9A,G10A
  MEIITLAIGG AIGFAAGAIE RFRLNNKIKK LLTGLPDTQE VSHSLSLVSL    G15A,I16A
```

Figure 11 Amino acid deletions and substitutions in the N-terminus of the SphS. The amino acid sequences are shown within 1-50 amino acids with dash represents deleted amino acid and underline letter indicates substituted amino acid.

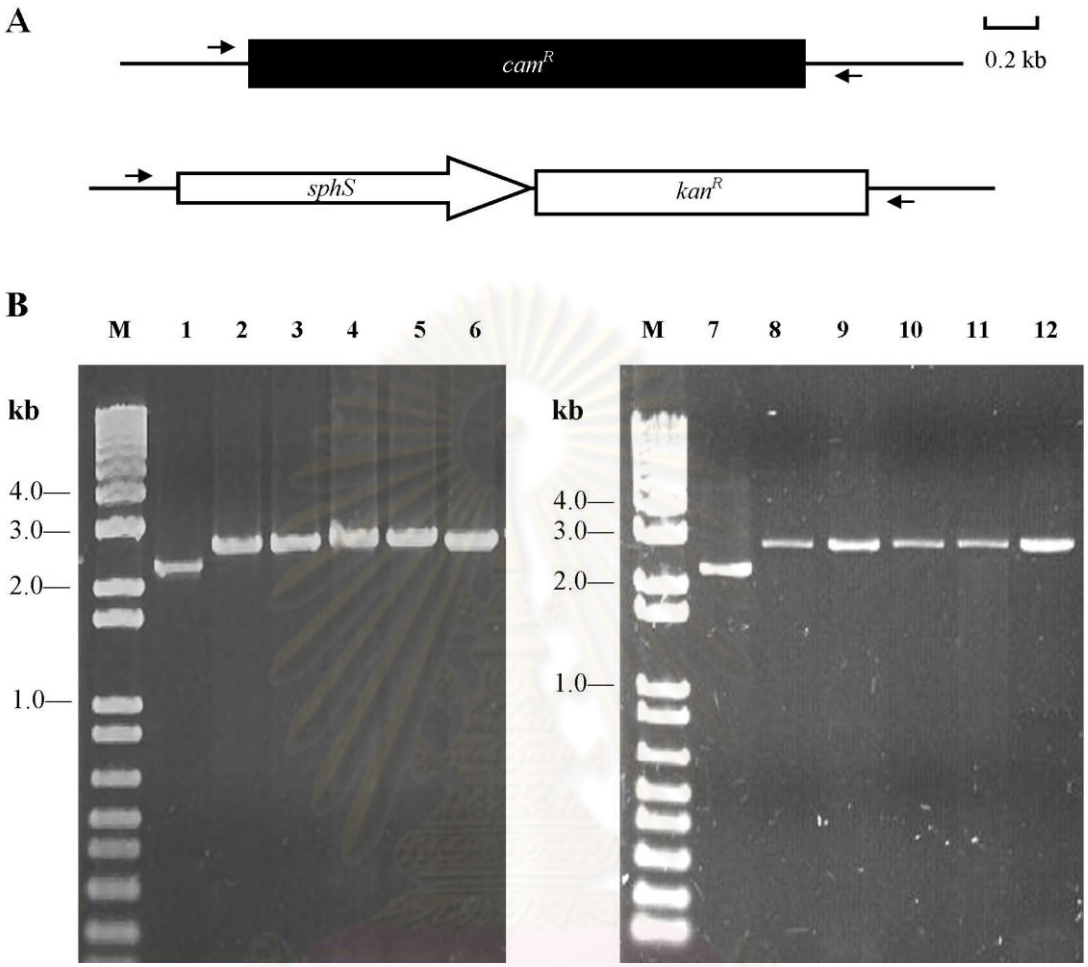

Figure 12 PCR demonstrating complete segregation of introduced mutated *sphS* genes. (A) Genomic DNA map showing the region of the *sphS* (*sll0337*) gene with the kanamycin-resistance cassette used as selectable marker. Diagram shows *sphS*, the kanamycin-resistance cassette and the chloramphenicol-resistance cassette of the *sphS* deletion (ΔSphS) mutant as a white arrow, white box, and black box, respectively. Short arrows indicate the position of the PCR primers. (B) Agarose gel electrophoresis with 1 kb Plus DNA marker (lane M), ΔSphS (lane 1 and 7), Δ(I8-G15) (lane 2), Δ(I3-R23) (lane 3), Δ(I3-L31) (lane 4), Δ(I3-S44) (lane 5), Δ(I3-S49) (lane 6), Δ(v41-S44) (lane 8), Δ(V41-S46) (lane 9), Δ(V41-S49) (lane 10), I8A,G9A,G10A(lane 11) and G15A,I16A (lane 12).

3.1.3 Measurement of growth and alkaline phosphatase activity

It has been shown that mutations at *sphS*, *sphR* or *sphU*, do not alter photoautotrophic growth rate of *Synechocystis* sp. PCC 6803 under either phosphate-sufficient or-limiting conditions, as well as the SphS control strain (Hirani et al., 2001; Juntarajumnong et al., 2007b, c). All ten constructed mutants also showed similar growth rate measured by the optical density at 730 nm, as wild-type and SphS control strains (Fig. 13, not showed all mutants). The alkaline phosphatase activity of each strain was measured spectrophotometrically at 400 nm, which showed no up-regulation of alkaline phosphatase in Δ(I3-R23), Δ(I3-L31), Δ(I3-S44) and Δ(I3-S49) mutants (Fig. 14A). All of those mutants lacked a region between amino acids 3-19 which could be a membrane-spanning domain or low-complexity region, indicating that this region was important for regulation of the Pho regulon. Internal deletions of the two low-complexity regions were performed, resulting in Δ(I8-G15) at the first low-complexity region (residues 3-19) and Δ(V41-S44), Δ(V41-S46) and Δ(V41-S49) at the second low-complexity region (residues 41-51). The results revealed no significant effect of alkaline phosphatase expression in the mutations at the second low-complexity region, while alkaline phosphatase was constitutively expressed in Δ(I8-G15) strain even when grown under phosphate-sufficient conditions (Fig. 14B). However, the Δ(I8-G15) strain still responded to phosphate limitations as well as under phosphate-sufficient conditions. The exhibited alkaline phosphatase activity was 66% under phosphate-sufficient conditions whereas the alkaline phosphatase activity was increased equally to that observed in control cells under phosphate-limiting conditions. These might point out that the regulation of the Pho regulon of SphS need the function of membrane-spanning domain rather than low-complexity

region. The essential function of amino acids between Ile-8 and Gly-15 was further studied by alanine-scanning mutagenesis, however, only alanine replacement at amino acids 8-10 (I8A,G9A,G10A) and 15-16 (G15A,I16A) were obtained. The results of alanine-scanning showed that alkaline phosphatase of both replaced strains were similar to SphS control strain (Fig. 14C). The ΔSphS and ΔSphU strains were used as negative and positive controls for alkaline phosphatase expression, respectively. These results suggested that the internal deletions at second low-complexity region of SphS, Δ(v41-S44), Δ(V41-S46) and Δ(V41-S49), and alanine substitutions at first low-complexity region of SphS, I8A,G9A,G10A and G15A,I16A, did not affect the regulation of Pho regulon.

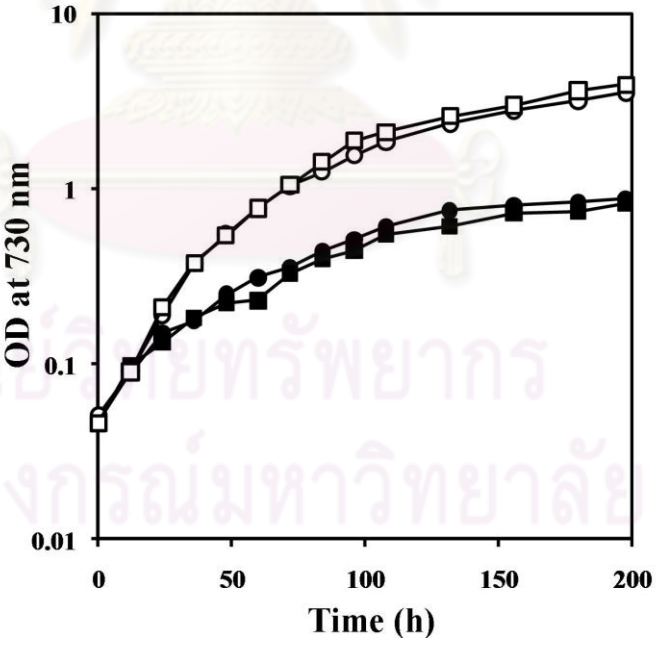

Figure 13 Photoautotrophic growth of the Δ(I8-G15) and control strains. Photoautotrophic growth measured by the optical density at 730 nm of Δ(I8-G15) mutant (squares) and SphS control strain (circles). Cells were grown in BG-11 (white symbols) and phosphate-limiting BG-11 (black symbols). Note, the other mutants had photoautotrophic growth similar to Δ(I8-G15).

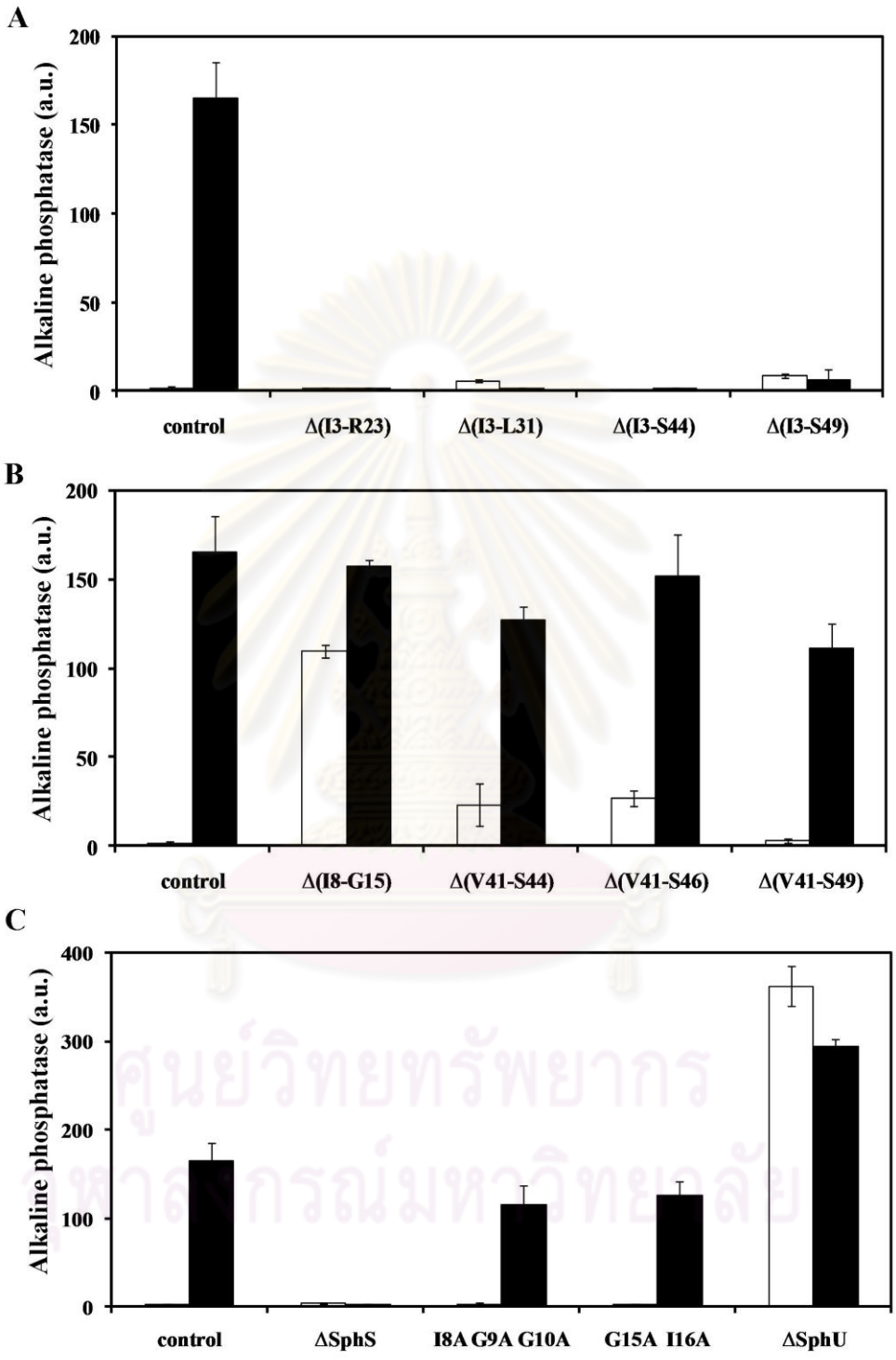

Figure 14 Alkaline phosphatase activity in SphS mutants. Cells were grown in BG-11 (white bars) and in phosphate-limiting BG-11 (black bars). Data are the average ± the standard error of three independent experiments. Note the difference in the scale on Y-axis for Fig. 14C.

3.1.4 Verification of the *sphS* expression in each mutant by RT-PCR

The RT-PCR was also performed to verify that the mutations did not affect the expression of *sphS* in which some mutated strains lacked alkaline phosphatase induction. The total cDNA synthesis was carried out with random hexamers and specific amplification of *sphS* was done subsequently by PCR with RT-PCR primers (Table 3). These experiments included the co-expression of *psbB*, constitutively expressed gene for chlorophyll-binding protein (Eaton-Rye & Vermaas, 1991), used as a positive control. A negative control for each strain was also included, demonstrating that there was no DNA contamination in the RNA samples. The expected PCR products of *sphS* and *psbB* are 0.35 kb and 0.66 kb, respectively (Fig. 15). The ΔSphS strain, however, showed only *psbB* PCR product at 0.66 kb (Fig. 15B, lane 1 & 10). Transcription of *sphS* in each mutant was similar to that of the control strain.

3.1.5 Construction of the SphS deletion: ΔSphU double mutation strains

The *sphU* (*slr0741*) encoding a negative regulator has been cloned and interrupted by insertion of chloramphenicol-resistance cassette previously, pΔslr0741-cam^R . In addition, it also has been transformed into *Synechocystis* sp. PCC 6803, resulting in ΔSphU strain (Juntarajumnong et al., 2007b). Both of them were obtained from laboratory stocks and pΔslr0741-cam^R was checked by restriction enzyme digestion. The *Not* I digest yielded fragments of 3.8 kb and 2.9 kb, while *Nco* I digest yielded fragments of 3.2 kb, 1.6 kb, 1.1 kb and 0.85 kb (Fig. 16).

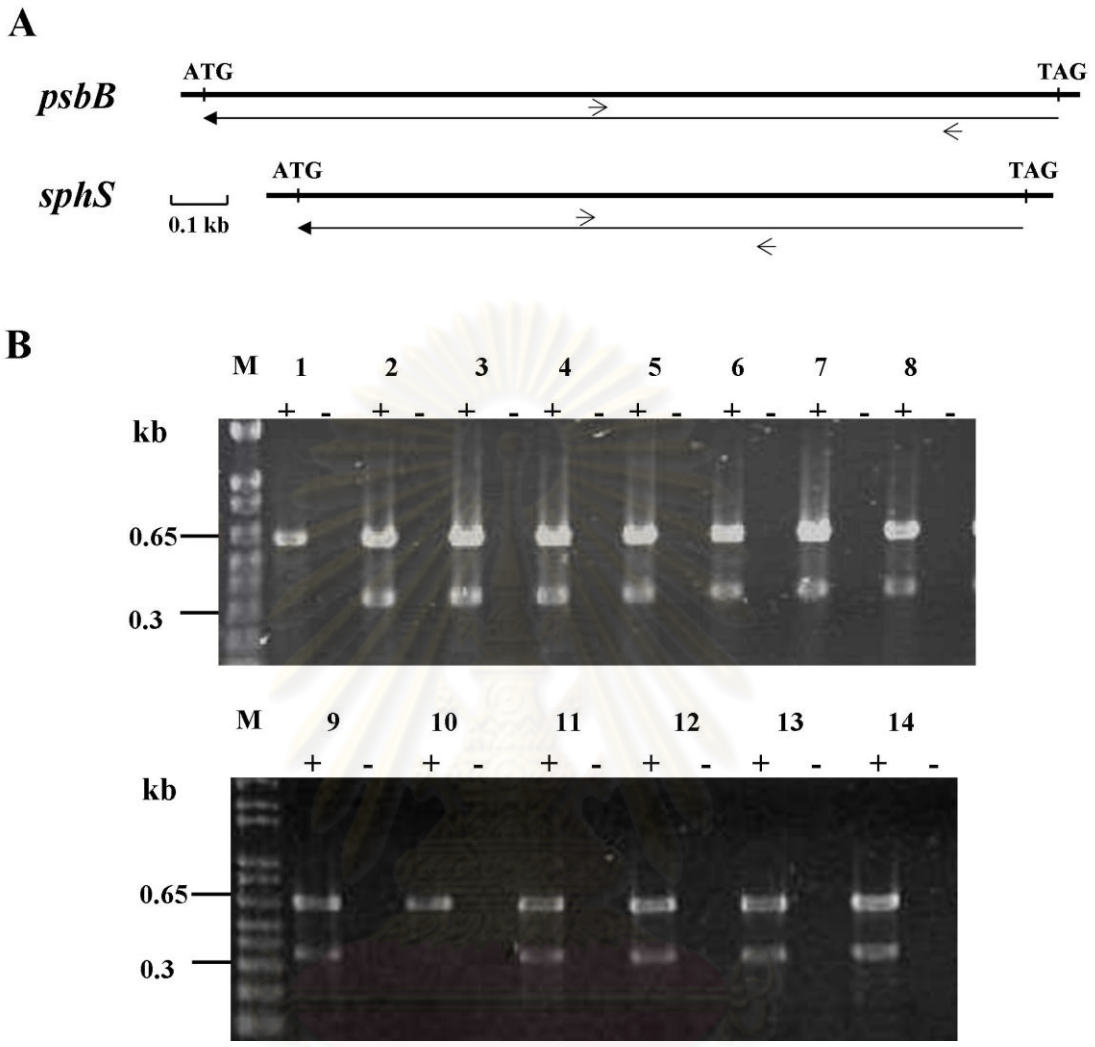

Figure 15 RT-PCR analysis of sphS expression. (A) Diagram shows open reading frames (bold lines) and cDNA (thin long arrows) for *psbB* and *sphS*. Short arrows indicate primers used for PCR. (B) Gel shows PCR products indicating *psbB* and *sphS* expression; ‘‘+”and “-” indicate the presence and absence of reverse transcriptase, respectively, with 1kb plus DNA marker (lane M). The strains are ΔSphS (lane 1 & 10), SphS control (lane 2 & 9), Δ(I8-G15) (lane 3), Δ(I3-R23) (lane 4), Δ(I3-L31) (lane 5), Δ(I3-S44) (lane 6), Δ(I3-S49) (lane 7), Δ(V41-S46) (lane 8), Δ(V41-S44) (lane 11), Δ(V41-S49) (lane 12), I8A,G9A,G10A (lane 13) and G15A,I16A (lane 14).

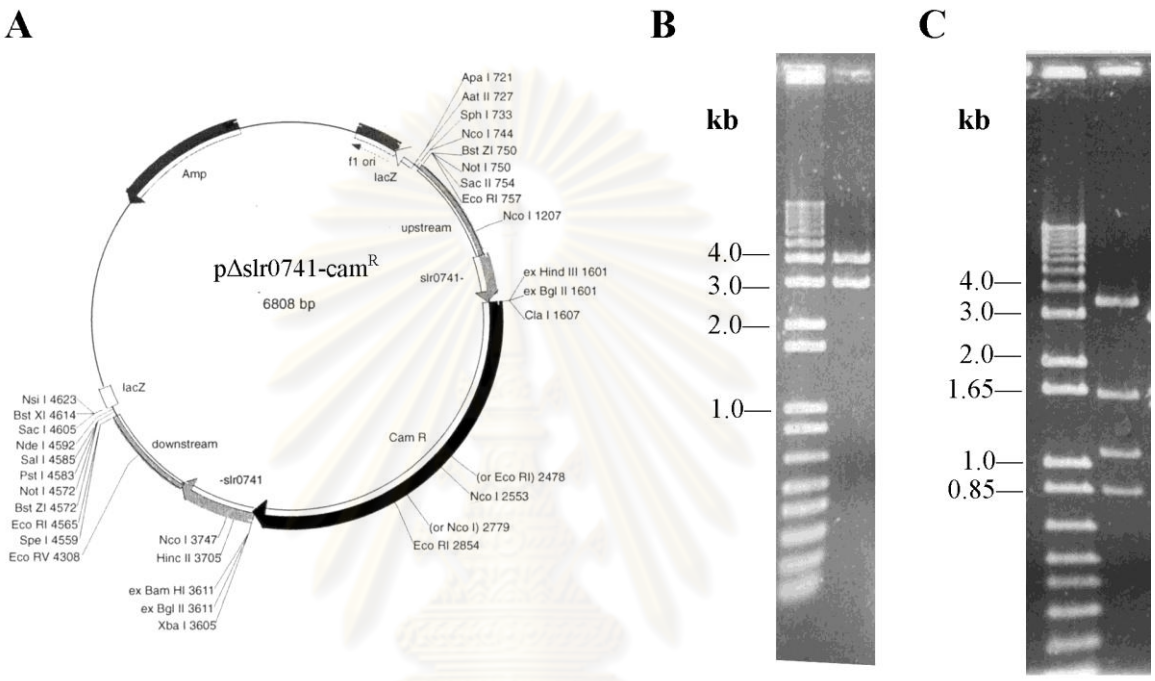

Figure 16 The pΔslr0741-cam^R plasmid. (A) The pΔslr0741-cam^R map which the open reading frames are indicated in arrows, the *slr0741* gene and chloramphenicol-resistance cassette are shown in gray and black arrows, respectively (modified from Juntarajumnong, 2004). (B) *Not* I digest of pΔslr0741-cam^R. (C) *Nco* I digest of pΔslr0741-cam^R.

.

One mutant lacking negative regulation, Δ(I8-G15), and four mutants lacking positive regulation, Δ(I3-R23), Δ(I3-L31), Δ(I3-S44) and Δ(I3-S49), were transformed with pΔslr0741-cam^R plasmid, resulting in Δ(I8-G15): ΔSphU, Δ(I3-R23): ΔSphU, Δ(I3-L31): ΔSphU, Δ(I3-S44): ΔSphU and Δ(I3-S49): ΔSphU. The mutants were grown on BG-11 plates containing 25 µg/ml of kanamycin and 15 µg/ml of chloramphenicol. In order to confirm the homozygosity of these strains, colony PCR was done using *slr0741* forward and reverse primers (Table 2). Figure 17 shows that *sphU* gene in each mutant was completely segregated showing a 3.9 kb band while a 1.8 kb band was obtained from SphS control strain.

3.1.6 Measurement of alkaline phosphatase activity

The ΔSphU strain constitutively expresses Pho regulon, indicated by alkaline phosphatase activity in which acitivity under phosphate-sufficient conditions is higher than that under conditions of phosphate limitation (Fig. 14C; Juntarajumnong et al., 2007b). Therefore, this strain was used as a positive control. The Δ(I8-G15): ΔSphU mutant exhibited constitutive alkaline phosphatase activity which was higher than Δ(I8-G15) ~2-fold either under phosphate-sufficient or phosphate-limiting conditions (Fig. 14B, Fig. 18) while the other four double mutation strains, Δ(I3-R23): ΔSphU, Δ(I3-L31): ΔSphU, Δ(I3-S44): ΔSphU and Δ(I3-S49): ΔSphU, still lost the positive function to up-regulate the Pho regulon in response to phosphate-limiting conditions (Fig. 18).

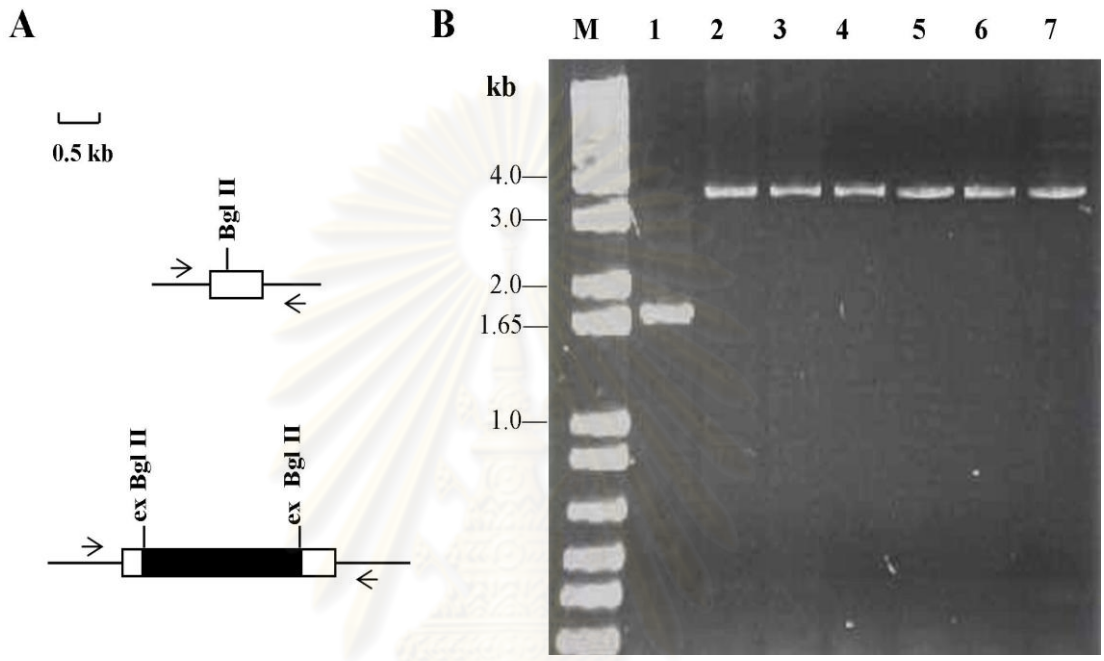

Figure 17 PCR demonstrating complete segregation of the gene encoding chloramphenicol-resistance cassette in the ΔSphU and SphS deletion: ΔSphU strains. (A) Diagram showing genomic map indicates *sphU* (white box) interrupted by chloramphenicol-resistance cassette (black box) at *Bgl* II site. Short arrows indicate the position of the PCR primers. (B) Agarose gel electrophoresis with 1 kb Plus DNA marker (lane M), SphS control (lane 1), ΔSphU (lane 2), Δ(I8-G15): ΔSphU (lane 3), Δ(I3-R23): ΔSphU (lane 4), Δ(I3-L31): ΔSphU (lane 5), Δ(I3-S44): ΔSphU (lane 6) and Δ(I3-S49) : ΔSphU (lane 7).

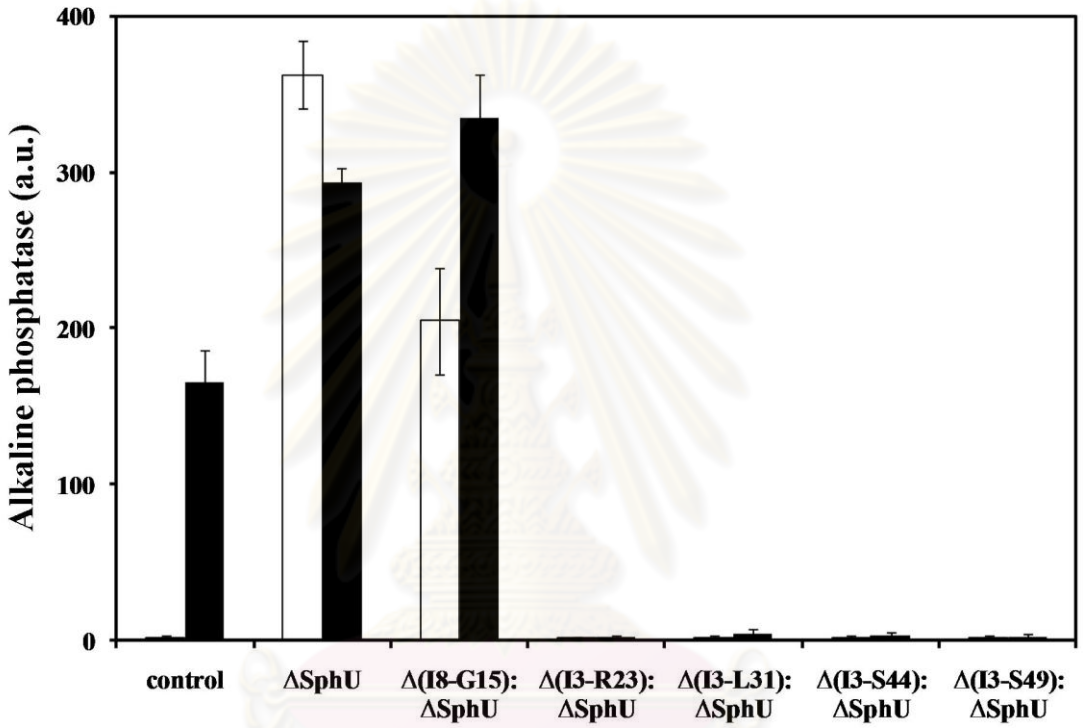

Figure 18 Alkaline phosphatase activity in SphS deletion: ΔSphU double mutation strains. Cells were grown in BG-11 (white bars) and in phosphate-limiting BG-11 (black bars). Data are the average ± the standard error of three independent experiments.

3.2 Characterization of the ΔPst1 and ΔPst2 strains

The Pst system is required for Pho regulon control in *E. coli*, while *Synechocystis* sp. PCC 6803 possesses 2 Pst systems. The *pst1* operon consists of *sphX, pstS1, pstC1, pstA1, pstB1* and *pstB1'*, and the *pst2* operon consists of *pstS2, pstC2, pstA2*, and *pstB2* (Fig. 19). Both operons are up-regulated in *Synechocystis* sp. PCC 6803 after phosphate limitation exposure in which the *pst1* is rapidly increased expression levels while the *pst2* takes a longer time (Suzuki et al., 2004). In contrast to other cyanobacteria which their genome sequences have been reported, all other cyanobacteria posses only one *pst* system. Whether Pst1 or Pst2 system is required as in *E. coli*, deletion of each operon was created.

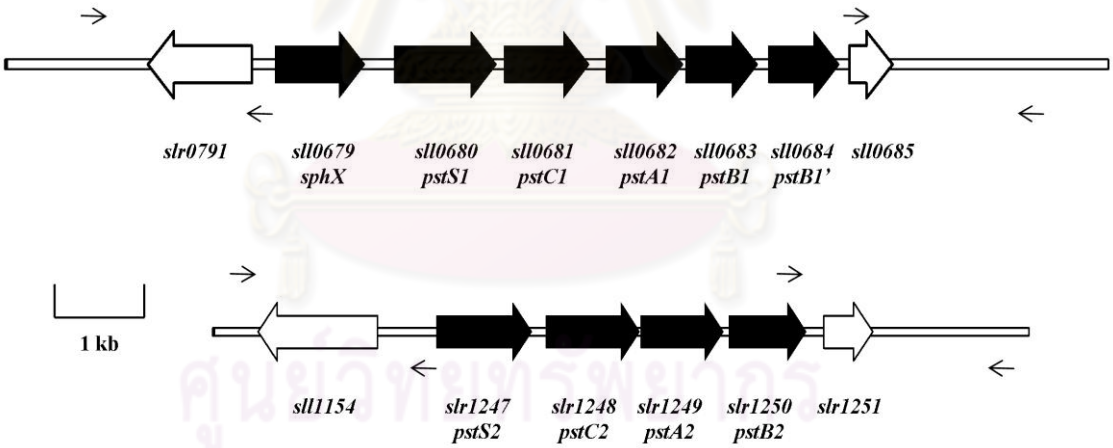

Figure 19 Diagram showing genomic map indicates *pst1* and *pst2* operons. (Top) The *pst1* operon contains six open reading frames. (Bottom) The pst2 operon contains four open reading frames. The open reading frames of genes in *pst* operons are demonstrated in black arrows and the genes located upstream and downstream of *pst* operons are indicated in white arrows. Short arrows indicate the position of the PCR primers.

3.2.1 Construction of the ΔPst1 and ΔPst2 strains

The 6.3 kb fragment containing six genes of *pst1* was replaced with a 1.8 kb spectinomycin-resistance cassette, yielding ΔPst1 strain. Similarly, the 3.9 kb fragment containing four genes of *pst2* was replaced with a 1.2 kb kanamycin-resistance cassette, resulting in ΔPst2 strain.

A 2.1 kb upstream fragment and a 2.3 kb downstream fragment of *pst1* operon were amplified by PCR and ligated to pGEM® T-easy, producing pUpst1 and pDpst1, respectively (Fig. 20A, 20B). A 2.0 kb spectinomycin-resistance cassette form pTrunc-spec^R was inserted into *Nde* I site of pDpst1, resulting in pDpst1-spec^R (Fig. 20C). A 4.1 kb downstream of *pst1*-spectinomycin-resistance cassette fragment of pDpst1-spec^R, obtained from *Sph* I digest, was introduced into pUpst1 at *Sac* I site, yielding a 9.3 kb pΔpst1-spec^R plasmid (Fig. 20D). On the pΔpst1-spec^R construct, spectinomycin-resistance cassette was replaced between -19 bp upstream of the ATG start codon of *sphX* and 38 bp downstream of the TAA stop codon of *pstB1'* in the same orientation as the pst1 operon.

In the same manner, a 2.1 kb upstream fragment and a 2.5 kb downstream fragment of *pst2* operon were amplified by PCR and ligated to pGEM® T-easy, producing pUpst2 and pDpst2, respectively (Fig. 21A, 21B). A 1.2 kb kanamycin-resistance cassette was inserted into *Nsi* I site of pUpst2, creating pUpst2-kan^R (Fig. 21C). A 3.2 kb upstream of *pst2*-kanamycin-resistance cassette fragment of pUpst2-kan^R, obtained from *Apa* I-*Stu* I double digest, was introduced into pDpst2 at *Bsm* I site, yielding an 8.6 kb pΔpst2-kan^R plasmid (Fig. 21D). On the pΔpst2-kan^R construct, kanamycin-resistance cassette was inserted between -220 bp upstream of the ATG start codon of *pstS2* and 86 bp downstream of TAG stop codon of *pstB2*. All

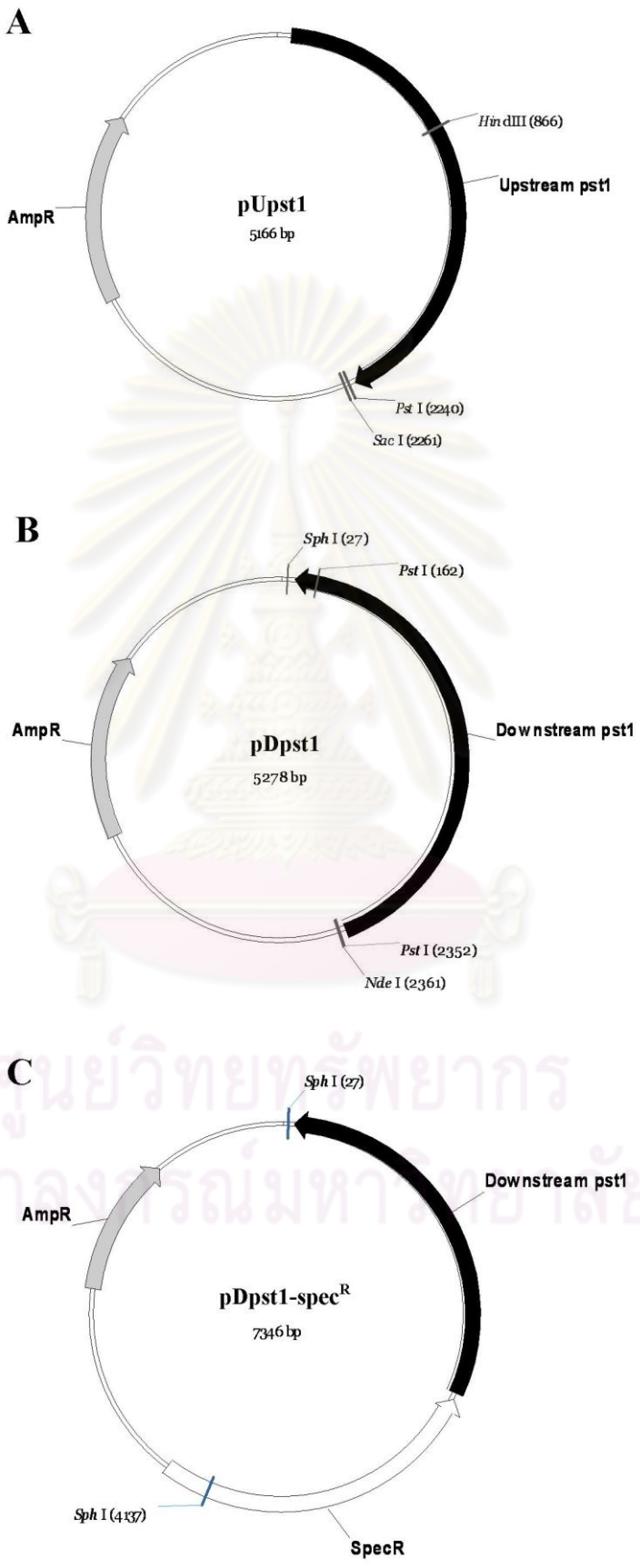

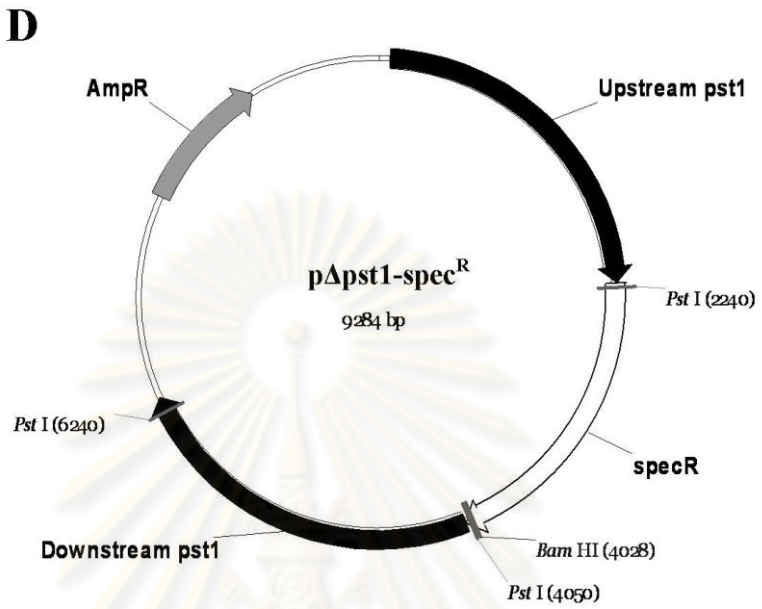

Figure 20 Plasmid maps of pUpst1, pDpst1, pDpst1-spec^R and pΔpst1- spec^R. (A) The pUpst1 plasmid, the upstream fragment of *pst1* was ligated into pGEM® T-easy vector. (B) The pDpst1 plasmid, the downstream fragment of *pst1* was ligated into pGEM® T-easy vector. (C) The pDpst1-spec^R plasmid, the spectinomycin-resistance cassette was inserted in the pDpst1 at *Nde* I site. (D) The pΔpst1- spec^R plasmid, the *Sph* I digested product containing downstream of *pst1* and spectinomycin-resistance cassette fragment was inserted in pUpst1 at *Sac* I site. The gray arrows indicate open reading frame of ampicillin-resistance cassette. The upstream and downstream fragments of *pst1* are shown in black arrows with indicated text. The white arrows represent spectinomycin-resistance cassette. The numbers in parentheses indicate the positions of the restriction enzyme sites in the plasmids.

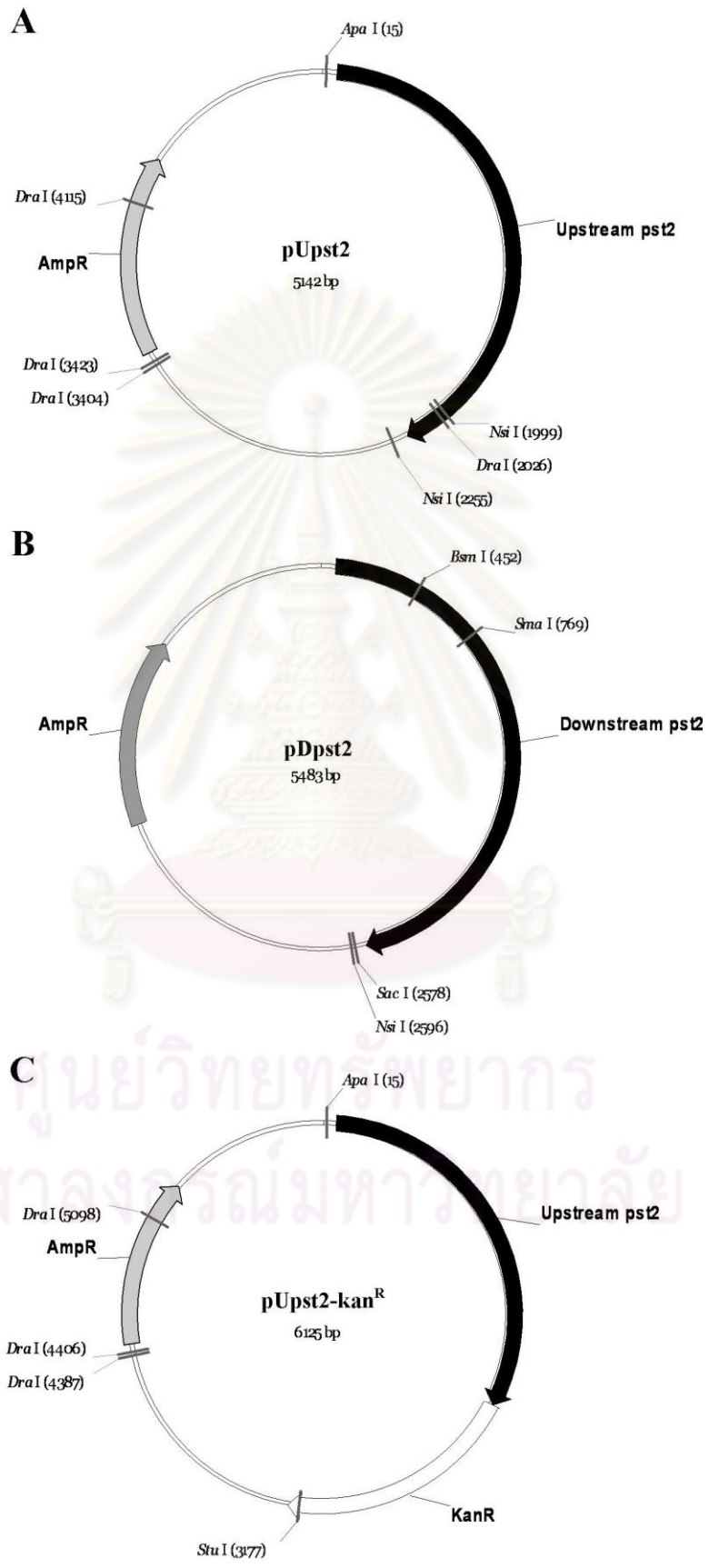

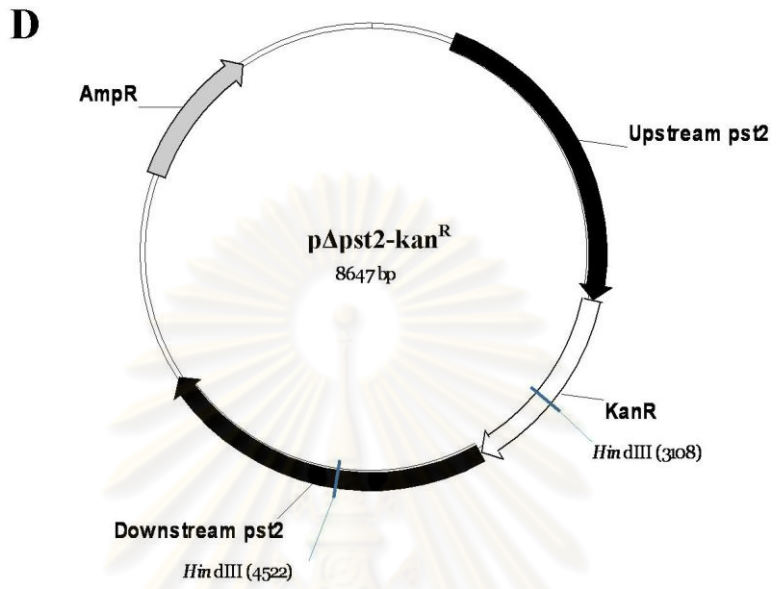

Figure 21 Plasmid maps of pUpst2, pDpst2, pUpst2-kan^R and pΔpst2-kan^R. (A) The pUpst2 plasmid, the upstream fragment of *pst2* was ligated into pGEM® T-easy vector. (B) The pDpst2 plasmid, the downstream fragment of *pst2* was ligated into pGEM® T-easy vector. (C) The pUpst2-kan^R plasmid, the kanamycin-resistance cassette was inserted in the pUpst2 at *Nsi* I site. (D) The pΔpst2-kan^R plasmid, the *Apa* I-*Stu* I double digest product containing upstream of *pst2* and kanamycin-resistance cassette fragment was inserted in pDpst2 at *Bsm* I site. The gray arrows indicate open reading frame of ampicillin-resistance cassette. The upstream and downstream fragments of *pst2* are shown in black arrows with indicated text. The white arrows represent kanamycin-resistance cassette. The numbers in parentheses indicate the positions of the restriction enzyme sites in the plasmids.

plasmids were confirmed by digesting them with restriction enzymes (data not shown).

Both pΔpst1-spec^R and pΔpst2-kan^R plasmids were transformed into *Synechocystis* sp. PCC 6803 wild-type strain and transformants were plated on BG-11 containing 25 µg/ml of spectinomycin and 25 µg/ml of kanamycin, respectively. In order to verify the homozygosity of both transformed strains, a Southern analysis was carried out.

The 2.1 kb upstream *pst1* product from PCR was digested with *Ban* II, resulted in two bands of 1.5 kb and 630 bp fragments. The 630 bp fragment located between nucleotides -649 and -20 bp upstream of the ATG start codon of *sphX* was chosen as a probe for Southern analysis to identify the homozygosity of ΔPst1 strain. Similarly, the 2.1 kb upstream of *pst2* product from PCR was double digested with *Eco*R I and *Hpa* I, resulted in three bands of 1 kb, 695 bp and 400 bp fragments. The 695 bp fragment located between nucleotides -1127 and -433 bp upstream of the ATG start codon of *pstS2* was used as a probe for Southern analysis to identify the homozygosity of ΔPst2 strain.

To perform a Southern analysis, genomic DNA of both wild-type and ΔPst1 strains were extracted and incubated with *Hin*d III. The expected 4.1 kb of wild type and 3.1 kb of ΔPst1 were obtained in Figure 22. For ΔPst2 identification, genomic DNA of both wild-type and ΔPst1 strains were extracted and digested with *Ban* II. Figure 23 shows a 4.1 kb band in wild type and a 2.2 kb band in ΔPst2 as expected.

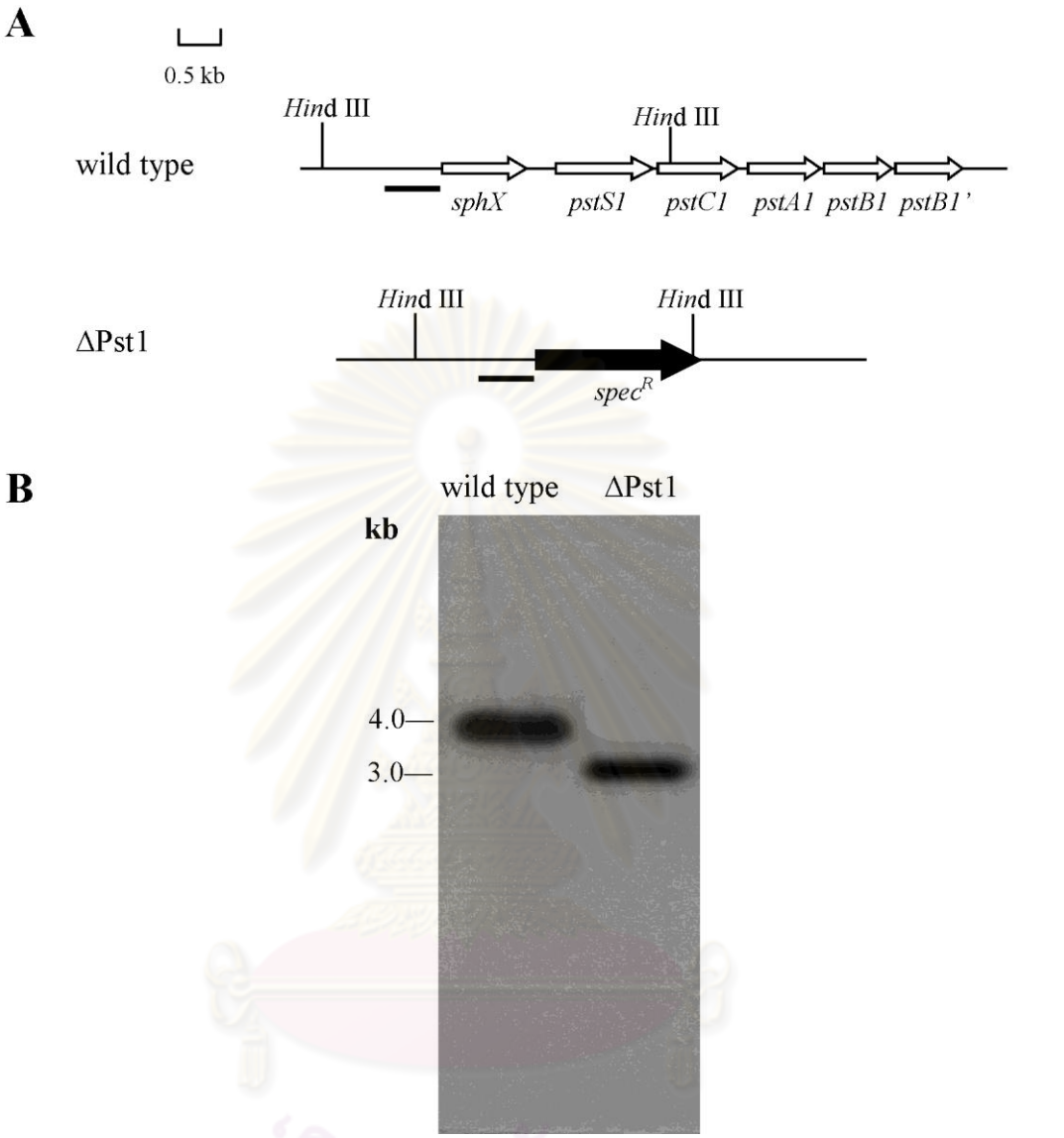

Figure 22 Southern blot showing full segregation of ΔPst1 strain. (A) Restriction map of the *pst1* region in wild-type and the ΔPst1 strains. The six genes belonging to *pst1* are shown in white arrows. The black arrow indicates the spectinomycin-resistance cassette. The position of the probe used in the Southern blot is shown in bold line. (B) Southern blot of wild type and ΔPst1. Genomic DNA was digested with *Hin*d III and probed with a 630 bp fragment.

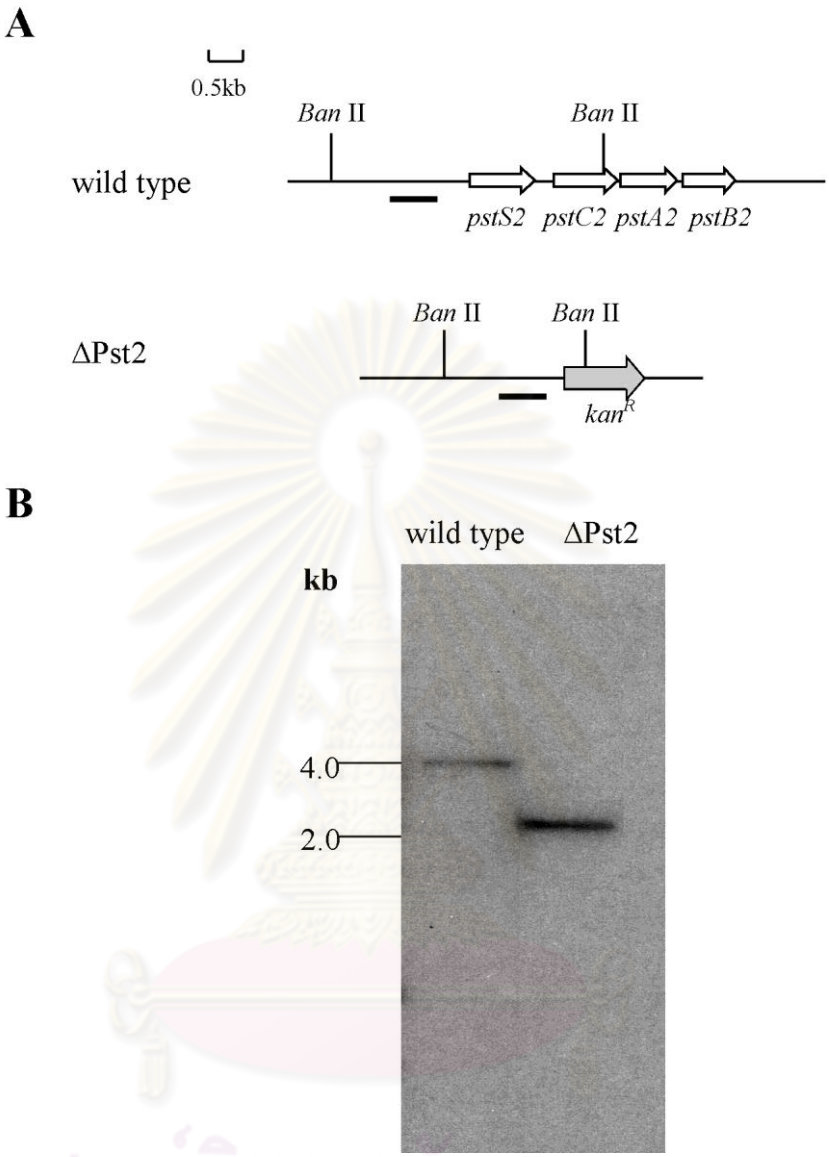

Figure 23 Southern blot showing full segregation of ΔPst2 strain. (A) Restriction map of the *pst2* region in wild-type and the ΔPst2 strains. The four genes belonging to *pst2* are shown in white arrows. The gray arrow indicates the kanamycin-resistance cassette. The position of the probe used in the Southern blot is shown in bold line. (B) Southern blot of wild type and ΔPst2. Genomic DNA was digested with *Ban* II and probed with a 695 bp fragment.

3.2.2 Measurement of growth and absorption spectra

Synechocystis sp. PCC 6803 wild-type, ΔPst1 and ΔPst2 strains were grown in either BG-11 or phosphate-limiting BG-11 containing suitable antibiotics and measured growth, pigment contents, alkaline phosphatase and phosphate uptake. Figure 24 shows that the absence of Pst1 or Pst2 system did not affect growth rate. The whole cells spectra corresponding to pigment contents also were not altered when Pst1 or Pst2 system was absent (Fig. 25). The cell spectra of 3 day-old cultures were severely decreased, however, the absorption maxima at 440 nm and 680 nm, due to chlorophyll *a*, and a peak at 620 nm, due to phycobillins, still could be seen (Fig. 25B).

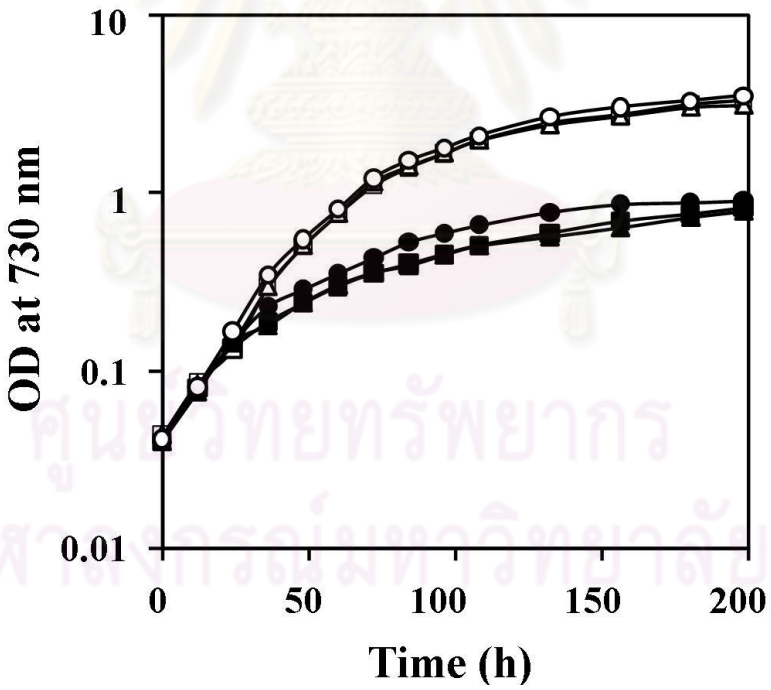

Figure 24 Photoautotrophic growth of the ΔPst1 and ΔPst2 strains. Photoautotrophic growth measured by the optical density at 730 nm of ΔPst1 (triangles), ΔPst2 (squares) and wild type (circles). Cells were grown in BG-11 (white symbols) and phosphate-limiting BG-11 (black symbols).

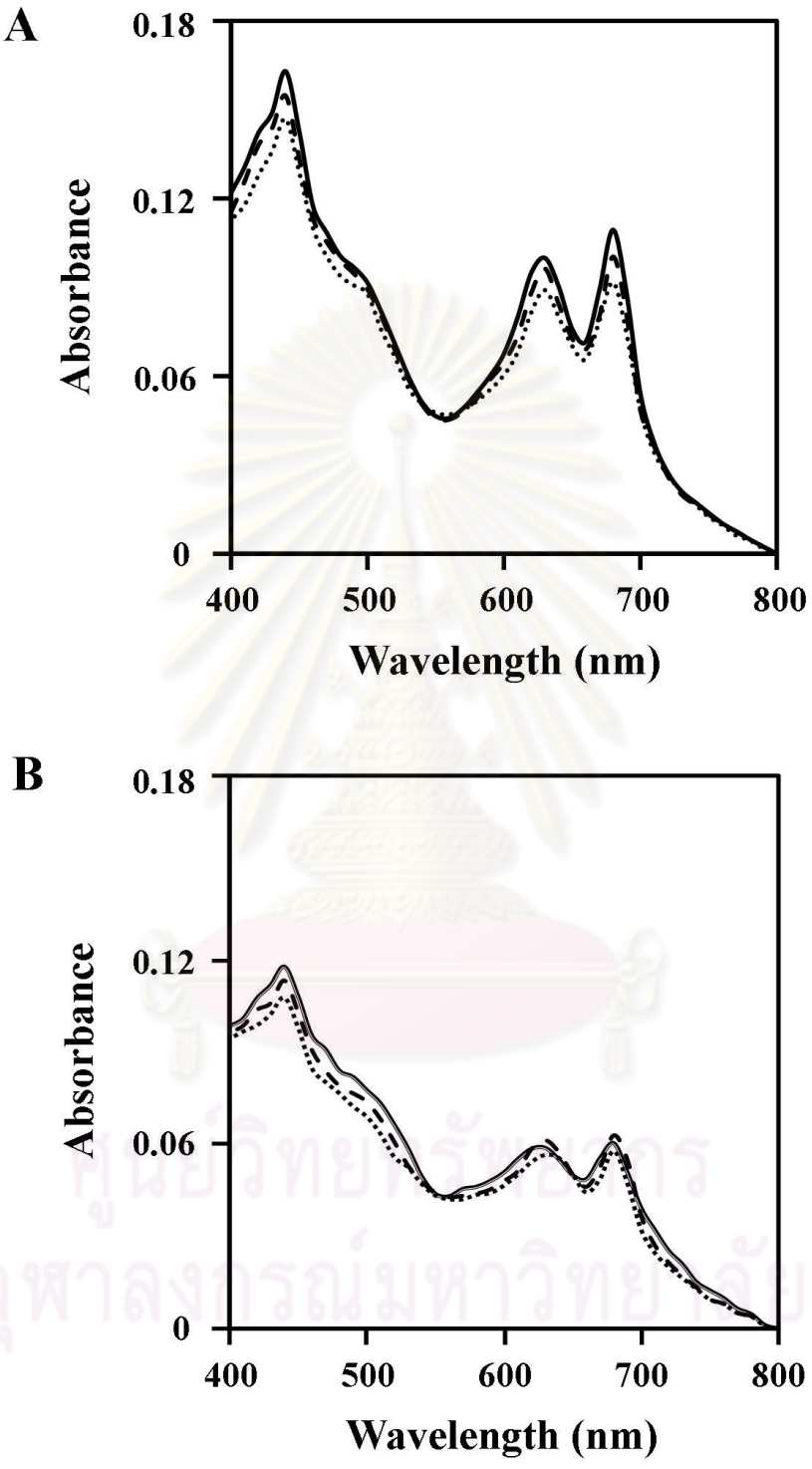

Figure 25 Absorption spectra of whole cells. Cells of wild type (solid lines), ΔPst1 (dot lines) and ΔPst2 (dash lines) grown in (A) BG-11 and (B) phosphate-limiting BG-11 for 3 days.

3.2.3 Measurement of alkaline phosphatase activity

As mentioned above, *E. coli* needs Pst system to form inhibition complex with a negative regulator, PhoU, and a histidine kinase, PhoR, while *Synechocystis* sp. PCC 6803 possesses two Pst systems. The alkaline phosphatase assay was carried out in each deletion strains to identify which system is required for the Pho regulon control. Figure 26 shows the alkaline phosphatase activity in ΔPst1 and ΔPst2 strains, compared with wild type. The ΔPst1 constitutively expressed alkaline phosphatase even grown in phosphate-sufficient conditions and increased in response to phosphate-limiting conditions. By contrast, the ΔPst2 had alkaline phosphatase activity similar to that observed in wild type, suggesting Pst2 system is not required for control of the Pho regulon. The levels of alkaline phosphatase in ΔPst1 were ~70% under phosphate-sufficient conditions and shifted up to ~100% under phosphate-limiting conditions, compared to that observed in wild type under phosphate-limiting conditions. These results showed that only Pst1 system is required for inhibition of Pho regulon expression under phosphate-sufficient conditions and Pst2 system is not involved in regulation of Pho regulon.

3.2.4 Construction of ΔPst1: ΔSphU and ΔPst2: ΔSphU double mutation strains

Both ΔPst1 and ΔPst2 strains were further transformed with pΔslr0741-cam^R to inactivate *sphU*. Transformants were plated on BG-11 agar containing 25 μg/ml of spectinomycin and 15 μg/ml of chloramphenicol for ΔPst1: ΔSphU strain while BG-11 agar containing 25 μg/ml of kanamycin and 15 μg/ml of chloramphenicol for ΔPst2: ΔSphU strain. Verification of the complete segregation of the chloramphenicol-

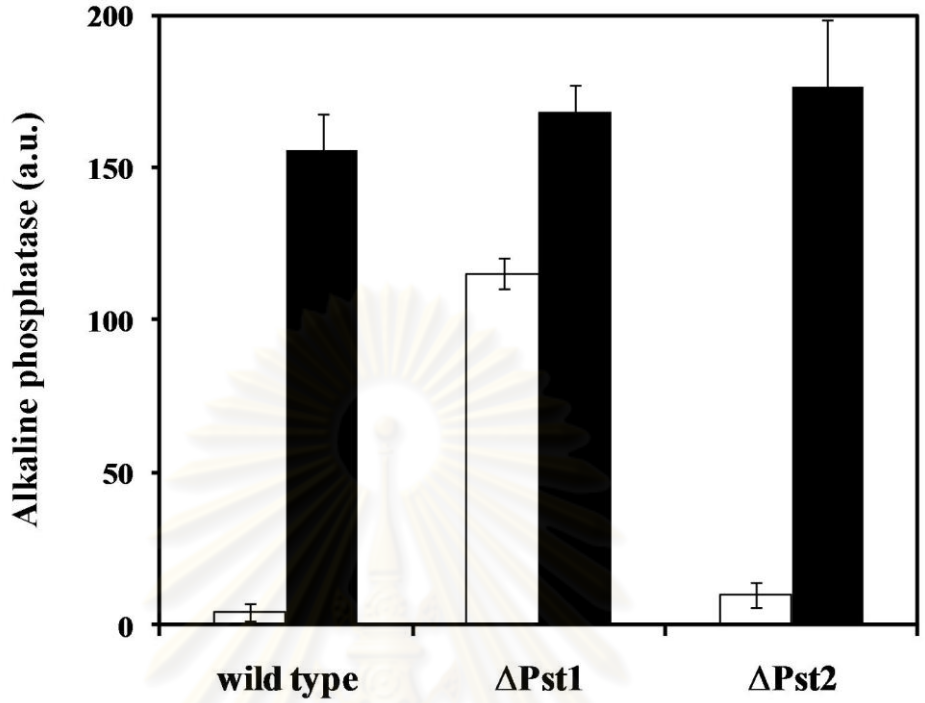

Figure 26 Alkaline phosphatase activity in ΔPst1 and ΔPst2 strains. Cells were grown in BG-11 (white bars) and in phosphate-limiting BG-11 (black bars). Data are the average ± the standard error of three independent experiments.

resistance cassette inserted *sphU* in each strain was performed by colony PCR. The result in Figure 27 demonstrates that *sphU* gene in each mutant was completely segregated showing a 3.9 kb band while a 1.8 kb band was obtained from wild type.

3.2.5 Measurement of alkaline phosphatase activity

Figure 28 shows the alkaline phosphatase activity of ΔPst1: ΔSphU and ΔPst2: ΔSphU strains under phosphate-sufficient and phosphate-limiting conditions, compared with wild type and ΔSphU. All three mutated strains had a similar alkaline phosphatase pattern, the activity under phosphate-sufficient conditions was higher than under phosphate-limiting conditions.

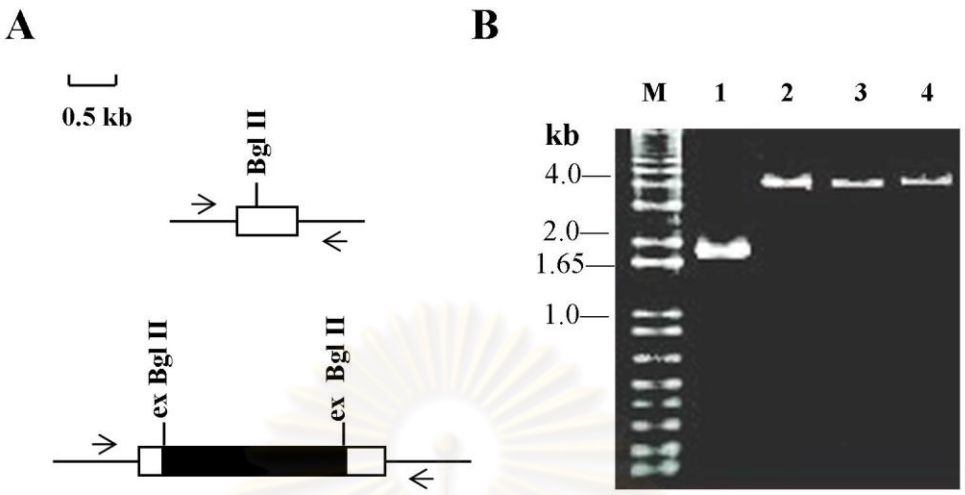

Figure 27 PCR demonstrating complete segregation of the gene encoding chloramphenicol-resistance cassette in the ΔPst1: ΔSphU and ΔPst2: ΔSphU strains. (A) Diagram showing genomic map indicates *sphU* (white box) interrupted by chloramphenicol-resistance cassette (black box) at *Bgl* II site. Short arrows indicate the position of the PCR primers. (B) Agarose gel electrophoresis with 1 kb Plus DNA marker (lane M), wild type (lane 1), ΔSphU (lane 2), ΔPst1: ΔSphU (lane 3) and ΔPst2: ΔSphU (lane 4).

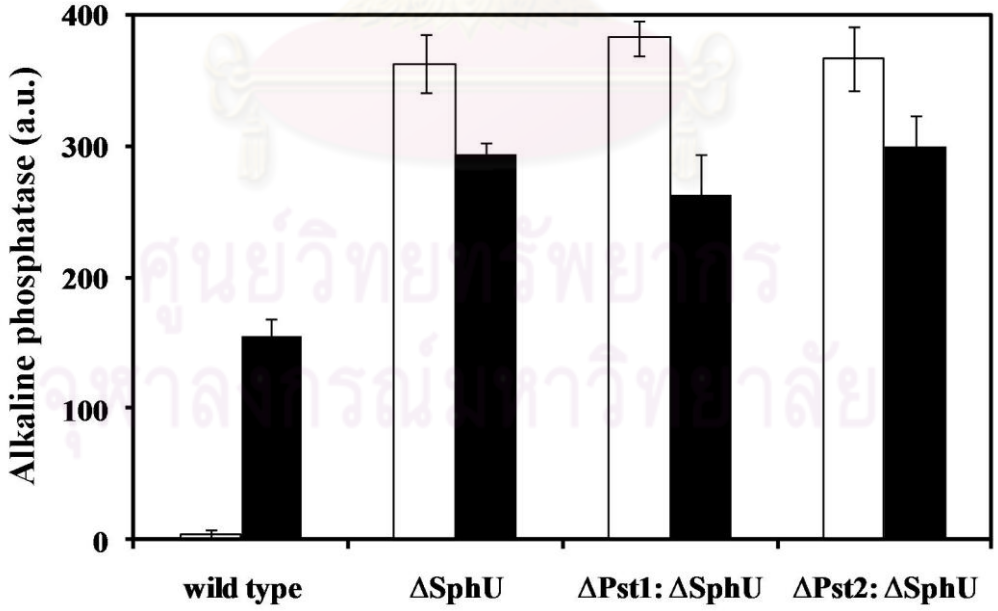

Figure 28 Alkaline phosphatase activity in ΔPst1: ΔSphU and ΔPst2: ΔSphU double mutation strains. Cells were grown in BG-11 (white bars) and in phosphate-limiting BG-11 (black bars). Data are the average ± the standard error of three independent experiments.

3.2.6 Construction of SphS deletion: ΔPst1 strains

The results above showed that the Δ(I8-G15) SphS and ΔPst1 strains constitutively expressed alkaline phosphatase ~66% and ~70% when cells grown under phosphate-sufficient conditions, respectively, compared to that observed in wild type under phosphate-limiting conditions (Fig. 14, 26). Double mutation at both regions was created by transforming pΔpst1-spec^R into Δ(I8-G15) SphS strain, designated Δ(I8-G15): ΔPst1 strain. The mutant carrying a mutation at the second low-complexity region of SphS, Δ(V41-S46) SphS, and the mutant carrying a deletion of the whole putative transmembrane region, Δ(I3-R23), were also transformed with pΔpst1-spec^R, creating Δ(V41-S46): ΔPst1 and Δ(I3-R23): ΔPst1 strains, respectively. The multiplex PCR was carried out to illustrate the homozygosity of the spectinomycin-resistance cassette inserted *pst1* in each strain. A single band of 2.0 kb showing complete segregation of spectinomycin-resistance cassette either Δ(I8-G15): ΔPst1, Δ(V41-S46): ΔPst1 or Δ(I3-R23): ΔPst1 strains while the wild type and mutants carrying a native *pst1* operon showed two bands of 0.86 and 1.0 kb (Fig. 29).

3.2.7 Measurement of alkaline phosphatase activity

Alkaline phosphatase activity of Δ(I8-G15): ΔPst1 double mutation strains was not significantly different from that obtained from both single mutation strains (Fig. 14, 26, 30). The Δ(I8-G15): ΔPst1 mutant exhibited alkaline phosphatase~ 50% under phosphate-sufficient conditions and increased to ~100% under phosphate-limiting conditions. Mutation at Pst1 system in Δ(V41-S46): ΔPst1 mutant elevated level of alkaline phosphatase to ~60 % under phosphate-sufficient conditions but not under phosphate-limiting conditions, compared to that observed in wild type under

phosphate-limiting conditions. However, no alkaline phosphatase was observed in Δ(I3-R23): ΔPst1 under both conditions (Fig. 30).

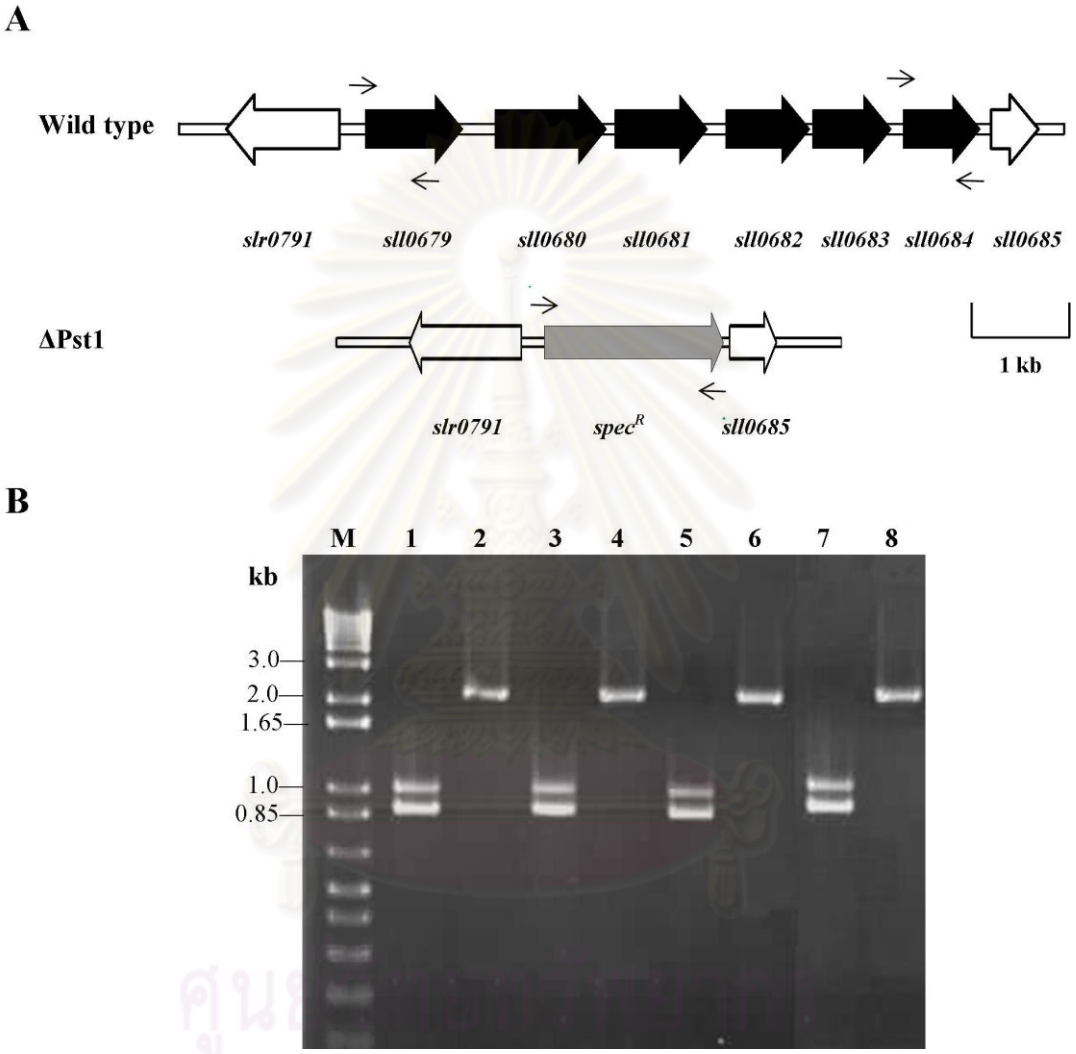

Figure 29 PCR demonstrating complete segregation of the gene encoding spectinomycin-resistance cassette in the Δ(I3-R23): ΔPst1, Δ(I8-G15): ΔPst1 and Δ(V41-S46): ΔPst1 double mutation strains. (A) Diagram showing genomic DNA maps indicates *pst1* operon (top) and spectinomycin-resistance cassette replacement (bottom). The open reading frames of genes in *pst1* operons are demonstrated in black arrows and the genes located upstream and downstream of *pst1* operons are indicated in white arrows. The gray arrow represents spectinomycin-resistance cassette. Short arrows indicate the position of the PCR primers. (B) Agarose gel electrophoresis with 1 kb Plus DNA marker (lane M), wild type (lane 1), ΔPst1 (lane 2), Δ(I8-G15) (lane 3), Δ(I8-G15): ΔPst1 (lane 4), Δ(V41-S46) (lane 5), Δ(V41-S46): ΔPst1 (lane 6), Δ(I3-R23) (lane 7) and Δ(I3-R23): ΔPst1 (lane 8).

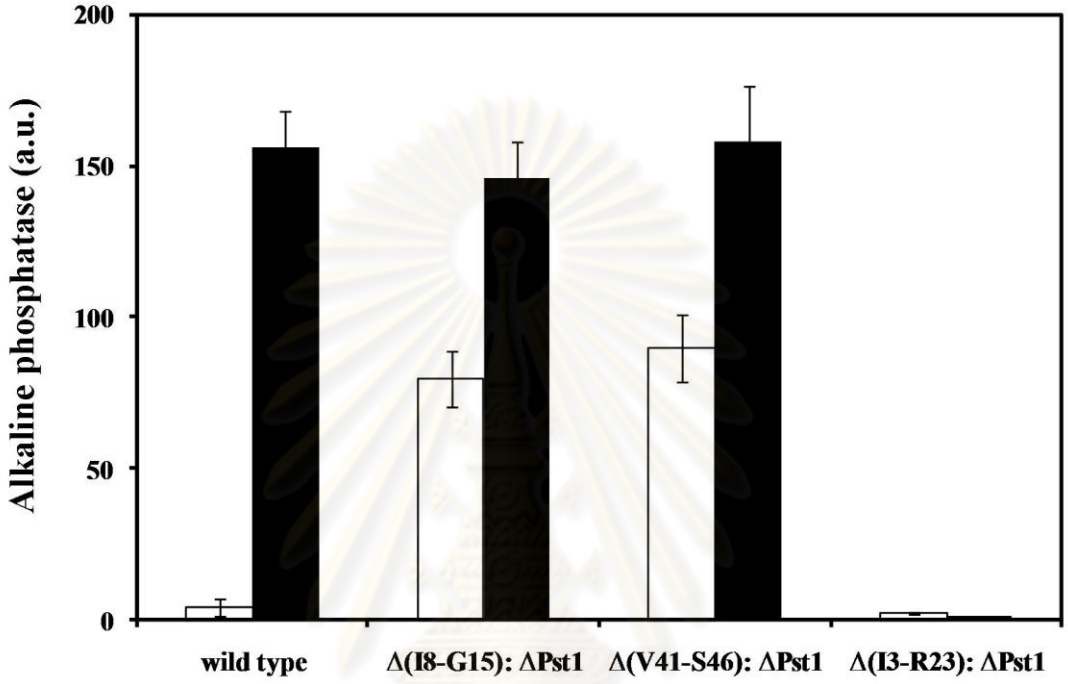

Figure 30 Alkaline phosphatase activity in Δ(I8-G15): ΔPst1, Δ(V41-S46): ΔPst1 and Δ(I3-R23): ΔPst1 double mutation strains. Cells were grown in BG-11 (white bars) and in phosphate-limiting BG-11 (black bars). Data are the average ± the standard error of three independent experiments

3.3 Phosphate uptake

The presence of two Pst systems but Pit system is absent in *Synechocystis* sp. PCC 6803. Therefore, in this study the ΔPst1 was used to study the phosphate uptake kinetics of Pst2 system and in the same manner, the Pst1 system was kinetically studied in the ΔPst2. Both of the Pst1 and Pst2 systems are members of ABC (ATP-binding cassette) transport superfamily, consisting of periplasmic phosphate-binding protein(s), transmembrane or permease proteins and ATP-binding protein(s). Amino acid sequence alignments between Pst1 and Pst2 systems showed that the phosphate-binding proteins, SphX and PstS1 in Pst1 system and PstS2 in Pst 2 system, had low identity and similarity while the others, permease and ATP-binding proteins, had higher ~50% identity and ~70% similarity in both of them (Fig. 31 and Table 4).

3.3.1 Kinetics of phosphate transport in wild type

Synechocystis sp. PCC 6803 wild-type cells were grown in either BG-11 or phosphate-limiting BG-11 for 1 day. Cells were collected and resuspended in phosphate-free HEPES-KOH buffer pH 7.5. The K_2HPO_4 solution was added to be 150 μM in the cell suspension to initiate phosphate uptake. The cells grown in phosphate-sufficient conditions (BG-11) showed no apparent phosphate uptake activity while cells grown in phosphate-limiting conditions exhibited a linear increase in phosphate uptake during 30 min (Fig. 32). The phosphate uptake activity depended on concentrations of phosphate which showed saturation kinetics. Under phosphate-limiting conditions, double-reciprocal plots yielded a K_m of 80.67 μM and maximum velocity (V_{max}) of 3.12 μmol/ min/ mg chlorophyll *a* for wild type (Fig. 33).

A

```
PstS1   MTTFKQIKKLSKHLVPTASILALTVGLAACGGGGGGGDTAQTGGGDATTTTAADAFASKV 60
PstS2   -----MLSSLQK--VATFSVVSVIVGFGGIG-------QAIAG----------------- 29
SphX    ------MFDLSRLSRGIVPMALLLLGISACT-------PSQTS----------------Q 31
              : .*.:      .:  : :*:..          : :.

PstS1   SLTGAGASFPAPLYQGWFVALNQAVPNLEVNYQSVGSGAGVEQFMSKTVDFGASDVAMDD 120
PstS2   TLNGAGASFPAPLYQRYFAEYKKATGN-TVNYNSVGSGAGIRQFIGETVDFGATDAVPTS 88
SphX    SIAINGSSTVYPITEAIVADFSGGKKGVDIDVEFSGTGGGFKLFCEGKTDIADASRPINK 91
        ::   *:*   *: :  ..  . .  .  :: :  *:*.*.. *   ..*:. :.    .

PstS1   EEIAKVNG---EVVMLPMTAGSIVMAYNLPGVEGLKLSQEALAGIMLG----NITKWNDP 173
PstS2   AQRQQMKR---GVVMVPTAGGAVAVVYNLPGKK-VQLSRIALGKIFTG----ELKTWN-- 138
SphX    QEMKLCNDNQVRYVELPIAFDAITVVSNPKNDWLKSLTVEELKRIWEPAAEKTLTRWN-- 149
         :    :      * :* : .::.:. *   .    .*:   *  *        :. **

PstS1   KLVADNPDLTLPDRPITVVHRSDGSGTTAVFTMNLAAMSPEFKETIGDGKTVEWPTSKGK 233
PstS2   -----QVDSKLPNTPIRVVVRADGSGTTDIFTSHLSAISSTFRSKIGASQDPNWG---FQ 190
SphX    -----QVRPEFPDQPINLYSPGEDSGTFDYFTEAIVGQAGASRLDT-------------- 190
             :    :*: ** :   .:.***   **  : . :   :

PstS1   FIGGKGNEGVTAGIQQNEGAIGYVEYGYATNN---NLTMASLQNKDGQFVVPTDENASAT 290
PstS2   VLKGPKNDGVAATVKQTPGAIGYVQDTFARRNEGPNLQTAKVQNKAGQYVEPSLAEANKA 250
SphX    -LKSEDDEILVQGVVQDLYSLGYFGFAYYEGR-IADLKAIGVDNGRG-PVLPSRETVEKS 247
         : .  :: :.  : *   ::**.   :   .   :*    ::*  *  * *:   .. :

PstS1   LAAVELPENLREFITNPAGADSYPIVTYTWMLLYPQYADAEKAKGIEAMVEFGLNEGQTM 350
PstS2   ISGAKFDANFVAEISDPASG--YPIVGLTWLLVYQNNKNANVAKDVKALVRWILTTGQNH 308
SphX    EYQPLSRPLFIYVNATKAQDNPALREFVDFYLANASATATKVGYIPLPEEAYNLGKISFN 307
                :    :  *          : *   .   :: .    .   : *   .

PstS1   APTLGYVPLPQNVREKVAAAADKISPDYTITLK 383
PstS2   NTQLEYTKIPPAVAQRVIAAVNKIK-------- 333
SphX    KGEVGTVFGGESVMDLTIGELLKKQASFE---- 336
           :  .     * : . .   * .
```

B

```
PstC1    MTTAPYSRTKPLASR-------SDLEKNLEKGFKYLTLAFAVSIGLILLAIALLILSQSV 53
PstC2    MVEGFSRRSEFTLARGGDITQGNSLTNGLDWGFKQLTRLCSLGVVVILGWIAWVVFTDAR 60
         *. .   *::   :*       ..* :.*: *** **   ::.: :**  ** ::::::

PstC1    PAIKAFGLGFITNNTWNPVTSQYGILAIMVGTLVNSGLALLLAIPLGIGTALFLSEDFIP 113
PstC2    PAIAKFGWEFIVSQQWDSSGQLFGGLPYIFGSVVSSFIALIFALPLGLAVAVMTSENLLP 120
         ***  **  **..: *:.  . :* *. :.*::*.* :**::*:***:..*:: **:::*

PstC1    SKIRTVLTFMVELLAAIPSVVYGLWGIFVIIPLIKPVGMWLNEYFGWIPLFSTPPAGPGM 173
PstC2    APVRVPIAFLVELIASIPSVIIGLWGIFVFIPVLMPVQGALFKYLGWLPIFGTEPFGPSM 180
         : :*. ::*:***:*:****: *******:**:: **   * :*:**:*:*.* * **.*

PstC1    LPASIVLAIMILPIITAIARDSLASLPPELRQASLGLGATRWETIFRVLIPAAFSGIVGG 233
PstC2    LVAGLVLTVMIIPTIASISRDILLSVSPSLRSASMALGATRWETICSVILPSASSGIIGA 240
         * *.:**::**:* *::*:** * *:.*.**.**:.*********  *::*:* ***:*.

PstC1    IMLALGRAMGETMAVTMIIGNSNRLSWSLLNPANTIASLLANQFAEAS-GMQVSALMYAG 292
PstC2    TILALGRALGETMAVTMVIGNSNIISASLLAPGYTIPSVLANQFAEAVDELHIGALMYLA 300
          :******:********:***** :* *** *. **.*:********   :::.**** .

PstC1    FVLIVLTFIVNILAELIVNKVKAKY--- 317
PstC2    LILFVITLGINSLAVLMVATIRRQGESN 328
         ::*:*:*: :* ** *:* .:: :
```

C

```
PstA2    MKSSAPSSLLAPLSFFRNGFAWVMGGLSFTLTLVALLPLLAILAAIIQRGLPTLSWEVFI 60
PstA1    ---MTAVNLQKKKSDLRAIFGYSMTAVSAACLLATVIPLFAVLIFVAIQGFRSLNLNLFL 57
             :. .*    * :*  *.: * .:* :  *.:::**:*:*  :  :*: :*. ::*:

PstA2    HLPAPVGVEGEPNGFANAIVGTLTMVGLGALFSVPLGVMTGVFLAEFAAGSAIANGVRFV 120
PstA1    KLPPAPGLAG--GGVGNAIIGTFIVVAIATVIAVPIGVLSAVYLSEFSGDNQVARAVRFA 115
         :**.. *: *  .*..***:**: :*.:.::::**:**::.*:*:**:... :*..***.

PstA2    TVILSSVPSVIVGVFAYGVLVIT-TKQFSAYAGGLALGVIMTPIIALTTEEALKLVPLHY 179
PstA1    TNLLSGIPSIIAGVFAYGALVSSGLFGFSAIAGGVALAVLMLPTIIRTTDEALQIVPQDI 175
         * :**.:**:*.******.** :   *** ***:**.*:* * *  **:***::** .

PstA2    RLGSAALGASKWETTVKTVIPCAIPAITTGVLLAVARAAGETAPLMFTALFSQFWQEGLM 239
PstA1    RWAALGVGAYKYQTVLFVVLPAALSSIITGVTLAIARAAGETAPLIFTALYSNFWPRGLK 235
         * .: .:** *::*.: .*:*.*:.:* *** **:**********:****:*:** .**

PstA2    APTPSLPVLIYNYASSPFEEQNAIAWTASLVLLMLVLTINLSSRLLIRRRF- 290
PstA1    EPIATLAVLVYNFASVPYKSQQELAWAASLLLVFLVLITNITARFFTRKKAY 287
          * .:*.**:**:** *::.*: :**:***:*::***  *:::*:: *::
```

D

```
PstB1     MN----ESPAQPLTETIPVFTTQNLDIYYGSHRAVRDVSLTIPKNKITAFIGPSGCGKST 56
PstB1'    MV----VSNG---VATKGVLEAQGVNVYYGSHLAVKDCNISIPERRVVAFIGPSGCGKST 53
PstB2     MTNLSGSMPSSTAADLQPALRVEGLGFYYGTKKVLEGVTMAIPVGKVTAMIGPSGCGKST 60
          *        .   .    .: .:.:..***:: .:.. .::**  ::.*:**********

PstB1     ILRCFNRLNDLIESFRLEGKVLYHSQDLYSPNIDVTAVRKYIGMVFQKPNPFPKTIFDNV 116
PstB1'    LLRCFNRMNDLVSIARVEGRITYHGSDIYAPSVDPVGLRCSIGMVFQKANPFPKSIYENI 113
PstB2     LLKAFNRIAELEGRVKVTGKIEFFGQNIYDQKVNINSLRREIGMVFQRPNPFPTSIYDNI 120
          :*:.***: :*    :: *:: :...::*  .::  .:*  ******:.****.:*::*:

PstB1     VYGARVNG--YKGNLEELAEDSLRRAALWDEVKDKLKASGFSLSGGQQQRLCIARAIAMQ 174
PstB1'    AWGAKLNN--FQGDMDELVETSLRRAALWDEVKDKLKASGFSLSGGQQQRLCIARAIAVQ 171
PstB2     VYGVKLCCNVSRAELDEIVERSLTRAVLWDEVKDSLKKSALGLSGGQQQRLCIARALAVN 180
          .:*.::     :.::::*:.* ** **.*******.** *.:.**************:*::

PstB1     PEVLLMDEPCSALDPISTLKVEELMNELKENYTIIIVTHNMQQATRVADYTAFYNAEATD 234
PstB1'    PEVILMDEPCSALDPISTLKIEGLMHELKEQFTIVIVTHNMQQASRVSDYTAFFNVESVD 231
PstB2     PKVLLMDEPCSALDPISTLKIEELINSLRENVTITIVTHNMQQALRVSDYTAFFNTDES- 239
          *:*:*****************:* *:::*:*: ** ********* **:*****:*.:

PstB1     KGNKVGYLVEFDRTGKVFGDPQEQETKDYVSGRFG 269
PstB1'    RGAKVGSLVEYGPTEEIFQNPLKESTRDYVSGRFG 266
PstB2     ---RIGQLVEFDTTQNIFSSPQETQTRDYVAGRFG 271
             ::* ***:. * ::* .* : .*:***:****
```

Figure 31 Alignment of amino acid sequences between protein homologs of Pst1 and Pst2 system. (A) Alignment of periplasmic phosphate-binding proteins, SphX, PstS1 and PstS2. (B) Alignment of permease proteins, PstC1 and PstC2. (C) Alignment of permease proteins, PstA1 and PstA2. (D) Alignment of ATP-binding proteins, PstB1, PstB1' and PstB2. Alignment was done with CLUSTAL W 2.0.12 using default parameters.

Table 4 Comparison of amino acid sequences between protein homologs of the Pst1 and Pst2 systems[a].

	% Identity	% Similarity
Pi-binding protein (Periplasm)		
Sll0679 (SphX) : Sll0680 (PstS1)	20	37
Sll0679 (SphX) : Slr1247 (PstS2)	27	41
Sll0680 (PstS1) : Slr1247 (PstS2)	41	57
Permease (Transmembrane)		
Sll0681 (PstC1) : Slr1248 (PstC2)	47	67
Sll0682 (PstA1) : Slr1249 (PstA2)	47	68
ATP-binding protein (Cytosol)		
Sll0683 (PstB1) : Sll0684 (PstB1')	65	84
Sll0683 (PstB1) : Slr1250 (PstB2)	54	73
Sll0684 (PstB1') : Slr1250 (PstB2)	55	70

[a]The deduced amino acid sequences of the subunits were analyzed using BLASTP (Altshul et al., 1997)

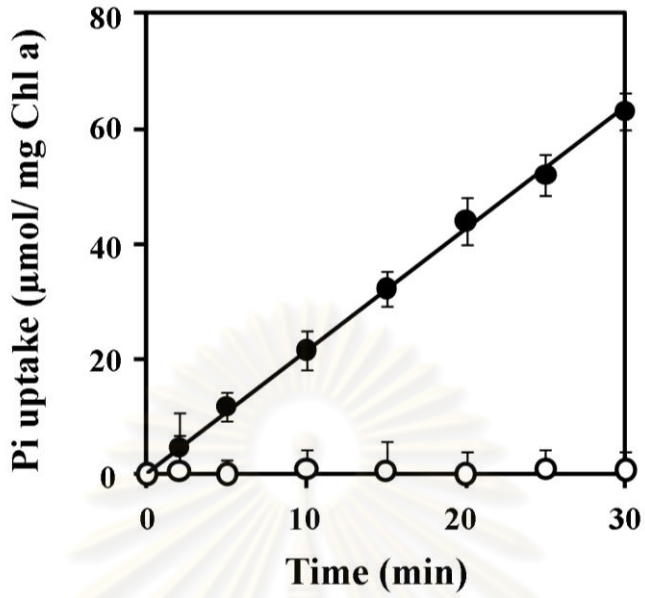

Figure 32 Phosphate uptake in *Synechocystis* sp. PCC 6803 wild-type cells. Cells grown in BG-11 (white circles) or phosphate-limiting BG-11 (black circles). Phosphate uptake was measured at 150 µM. Data are the average ± the standard error of three independent experiments.

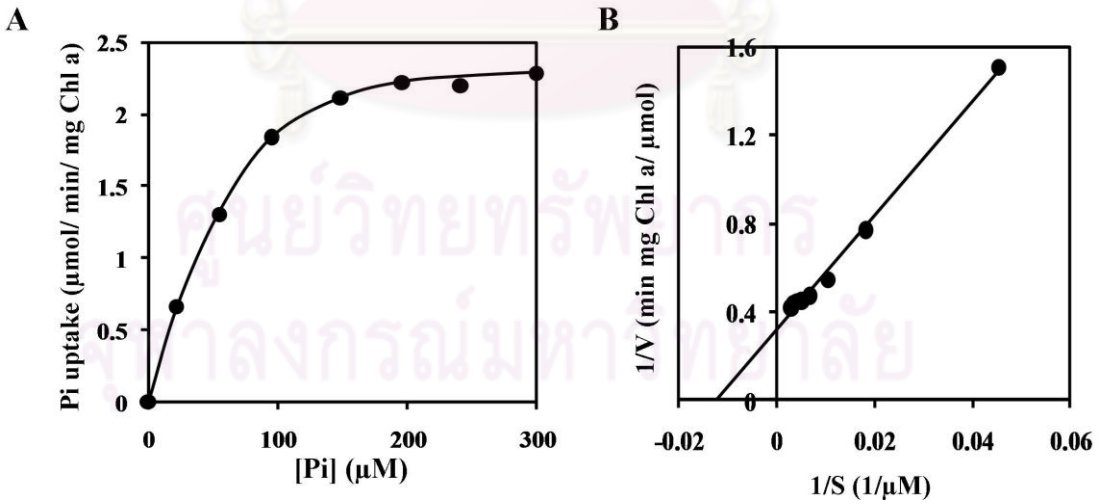

Figure 33 Kinetics of phosphate uptake in *Synechocystis* sp. PCC 6803 wild-type strain. (A) Saturation curve of phosphate uptake into wild-type cells. (B) Double-reciprocal plot of phosphate uptake into wild-type cells. Cells grown in phosphate-limiting BG-11.

3.3.2 Effect of metabolic inhibitors and phosphate analogs on phosphate transport

Bioinformatics analysis suggested both Pst systems are members of ABC transport superfamily which use energy directly from hydrolysis of ATP to drive substrate transport through membrane. The photosynthetic *Synechocystis* sp. PCC 6803 obtains energy from light and produces ATP, therefore, the phosphate uptake of *Synechocystis* sp. PCC 6803 was half reduced under dark conditions (Table 5). Similar results were found when cells were incubated with a specific photosynthesis inhibitor, DCMU, or KCN, as CN^- known to inhibit both respiration and photosynthesis. The presence of various ion-gradient dissipating agents slightly affected phosphate uptake which reduced 10-20% of phosphate uptake, compared to that observed in the absence of inhibitor. The uptake of phosphate was extremely reduced in the presence of ATP-synthetic inhibitor, CCCP, remaining activity ~25%, as well as the presence of N-ethylmaleimide strongly reduced activity to ~30%. Phosphate analogs, Na_2AsO_4 and $NaVO_3$, were selected as phosphate competitors for phosphate uptake. The phosphate uptake was significantly reduced ~30% when either Na_2AsO_4 or $NaVO_3$ was present. The inhibition of both phosphate analogs was not concentration dependent as increasing the concentrations of both analogs did not increase the inhibition of phosphate uptake activity (data not shown).

Table 5 Effect of metabolic inhibitors, incubation in the dark and phosphate analogs on phosphate uptake in *Synechocystis* sp. PCC 6803[a].

Treatment	Phosphate uptake (%)
Control	100 ± 2
Dark	48 ± 5
DCMU 20 µM[b]	51 ± 6
KCN 5 mM	54 ± 3
Na ionophore 10 µM	91 ± 4
Gramicidin10 µM	80 ± 3
Valinomycin 20 µM	77 ± 4
Amiloride 20 µM	77 ± 5
Monensin 20 µM	69 ± 4
DCCD 40 µM[b]	91 ± 6
NaF 1 mM	93 ± 5
CCCP 40 µM[b]	23 ± 6
N-ethylmaleimide 1 mM	31 ± 6
Na_2AsO_4 20 µM	72 ± 4
$NaVO_3$ 20 µM	74 ± 6

[a]Cells were preincubated with inhibitors for 30 min before the addition of K_2HPO_4 to initiate uptake at 70 µM. Data are the mean of three experiments ± SD. [b]Cells were preincubated with inhibitors for 2 min before assays.

3.3.3 Effect of external pH on phosphate transport

Phosphate transport in a cyanobacterium *Synechococcus* sp. PCC 9742 has been reported that the kinetic parameters at either pH 7.5 or pH 10 were not significantly different (Ritchie et al., 1997). In this study phosphate uptake was performed at different pH values from pH 5 to 11 using 25 mM each of MES-KOH (pH 5.0-6.0), HEPES-KOH (pH 7.0-8.5) and ethanolamine-KOH (pH 10.0-11.0). Figure 34 shows a broad activity of phosphate uptake under alkaline conditions ranging from pH 7 to 10. The phosphate uptake activity was demolished at acid conditions and strong alkaline conditions. In addition, phosphate uptake activity in either HEPES-KOH or Tris-HCl was similar, suggesting buffer species had no effect on phosphate uptake.

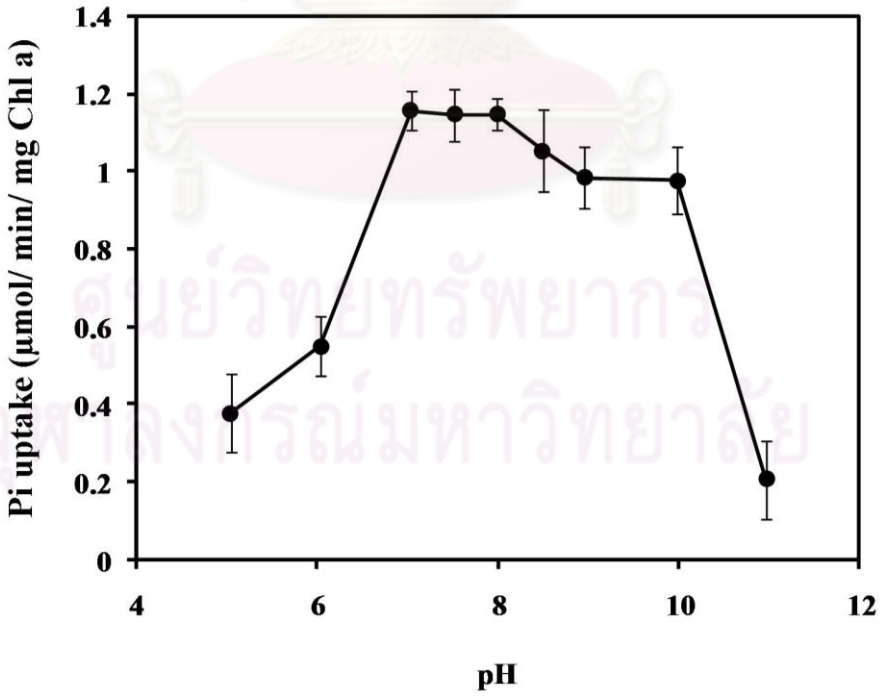

Figure 34 Effect of external pH on phosphate uptake in *Synechocystis* sp. PCC 6803. Cells were preincubated in MES-KOH (pH 5.0-6.0), HEPES-KOH (pH 7.0-8.5) and ethanolamine-KOH (pH 10.0-11.0). Phosphate uptake was measured at 70 µM. Data are the average ± the standard error of three independent experiments.

3.3.4 Effect of divalent cations on phosphate transport

Phosphate uptake in cyanobacteria showed a specific cation requirement, such as Ca^{2+}, Mg^{2+} and Sr^{2+} (Rigby et al., 1980; Ritchie et al., 1997). The effect of such divalent cations on phosphate uptake was tested by adding of $CaCl_2$, $CaSO_4$, $MgCl_2$ or $MgSO_4$ 0.5mM into uptake sample. However, the phosphate uptake activity was not different when the $CaCl_2$ or $CaSO_4$ was present (data not shown). In the presence of $MgCl_2$ or $MgSO_4$, phosphate uptake was significantly increased ~30% after 20 min and shown to be decreased to the same as control when the sample was added with ion chelator, EDTA (Fig. 35). These results suggested that the anions, Cl^- and SO_4^{2-}, had no effect on phosphate uptake in *Synechocystis* sp. PCC 6803.

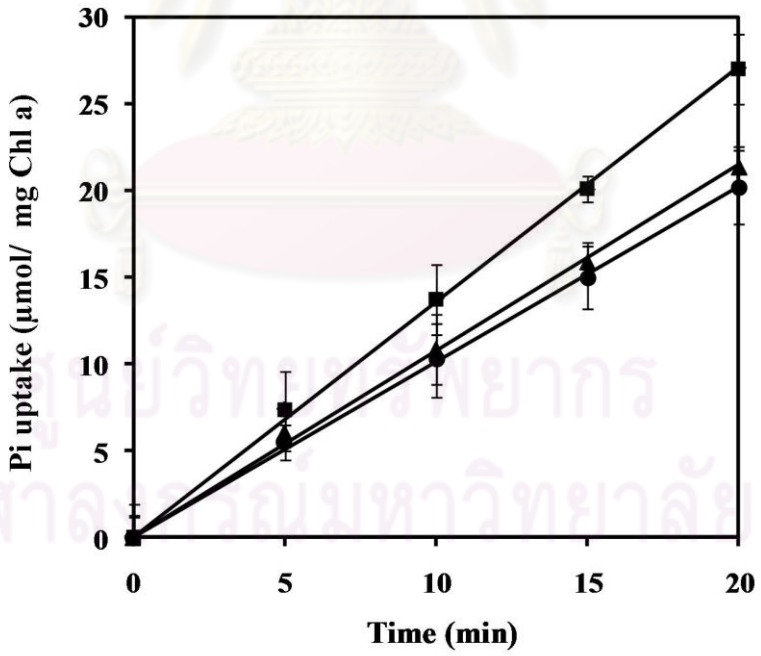

Figure 35 Effect of Mg^{2+} on phosphate uptake in *Synechocystis* sp. PCC 6803. Cells were preincubated in HEPES-KOH buffer pH 7.5 (circles), HEPES-KOH buffer pH 7.5 containing 0.5 mM $MgSO_4$ (squares) and 0.5 mM of each $MgSO_4$ and EDTA (triangles). Phosphate uptake was measured at 70 µM. Data are the average ± the standard error of three independent experiments.

3.3.5 Effect of osmolality on phosphate transport

The presence of NaCl could generate ionic stress and osmotic stress. To test whether ionic stress or osmotic stress affected phosphate uptake, experiments were performed by varying the concentrations of NaCl, sorbitol, and the combination of NaCl and sorbitol with a fixed osmolality equivalent to 100 mOsmol/ kg. Figure 36 shows that ionic stress imposed by NaCl stimulated phosphate uptake whereas osmotic stress imposed by sorbitol reduced phosphate uptake. The osmolality of 100 mOsmol/ kg contributed solely by sorbitol caused ~50% reduction in phosphate uptake. However, increasing the concentration of NaCl while keeping the osmolality at 100 mOsmol/ kg led to a progressive increase of phosphate uptake.

3.3.6 Kinetics of phosphate transport in ΔPst1 strain

Alkaline phosphatase gene (*phoA*), *pst1* and *pst2* operons were reported to be involved in Pho regulon (Suzuki et al., 2004). As mentioned above, *Synechocystis* sp. PCC 6803 ΔPst1 strain constitutively expressed alkaline phosphatase (Fig. 26). This strain also had phosphate uptake activity constitutively. Similar to alkaline phosphatase activity, cells grown under both conditions exhibited a linear increase in phosphate uptake during 30 min in which cells under phosphate-limiting conditions took phosphate up more than cells under phosphate-sufficient conditions (Fig. 37), however, the uptake rates under both conditions were very lower than wild type (Fig. 32). These also showed saturation kinetics under either phosphate-sufficient or phosphate-limiting conditions. Double- reciprocal plots yielded a K_m of 0.13 and 0.18 μM and a V_{max} of 0.22 and 0.18 μmol/ min/ mg chlorophyll *a* under phosphate -limiting and phosphate-sufficient conditions, respectively (Fig. 38).

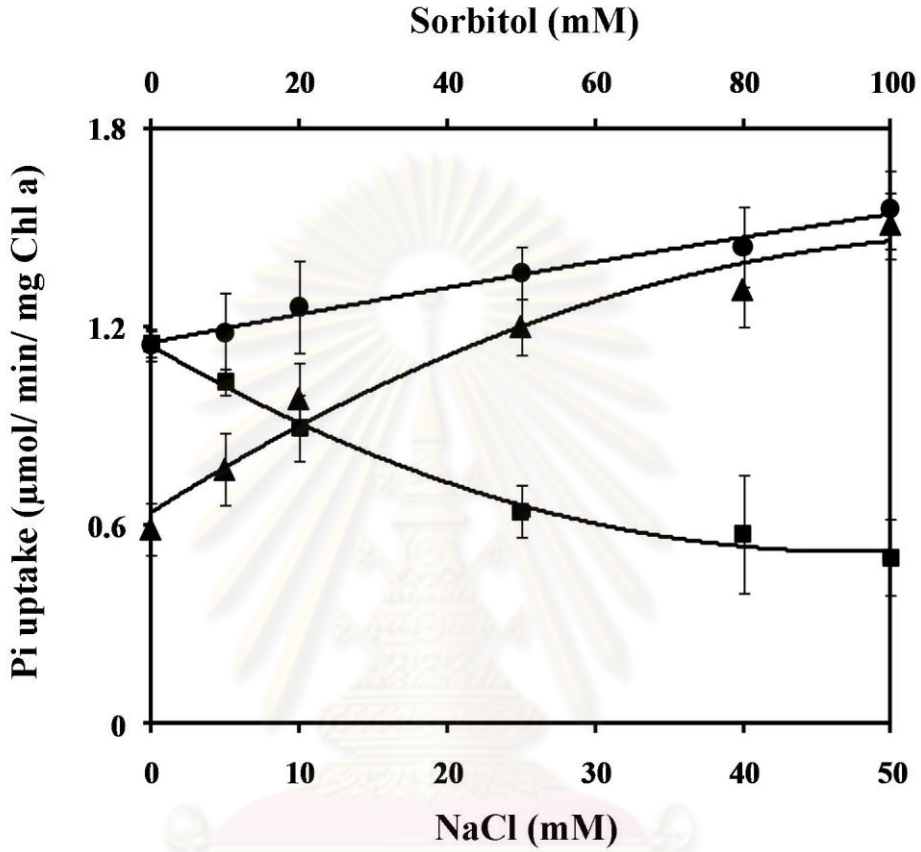

Figure 36 Effect of salt stress and osmolality stress on phosphate uptake in *Synechocystis* sp. PCC 6803. Phosphate uptake were done in 25 mM HEPES-KOH buffer pH 7.5 containing NaCl (circles), NaCl and sorbitol to keep osmolality equivalent to 100 mOsm/ kg (triangles), and sorbitol (squares). Phosphate uptake was measured at 70 µM. Data are the average ± the standard error of three independent experiments.

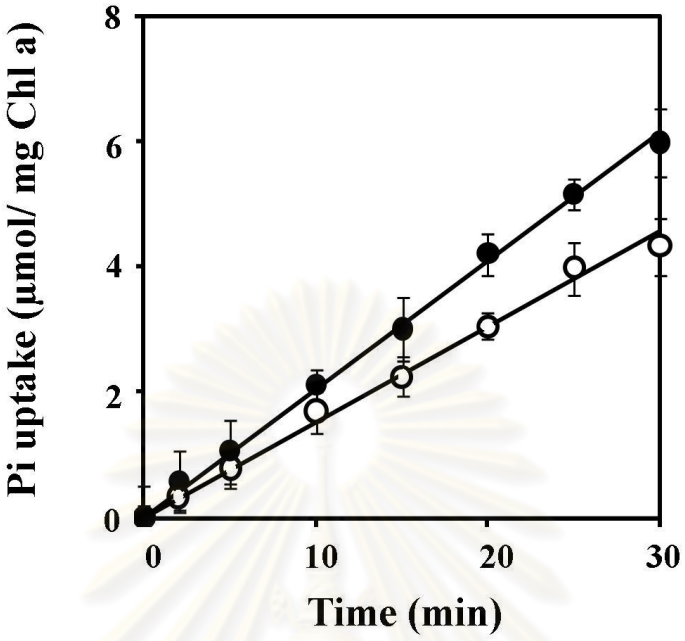

Figure 37 Phosphate uptake in *Synechocystis* sp. PCC 6803 ΔPst1 cells. Cells grown in BG-11 (white circles) or phosphate-limiting BG-11 (black circles). Phosphate uptake was measured at 50 µM. Data are the average ± the standard error of three independent experiments.

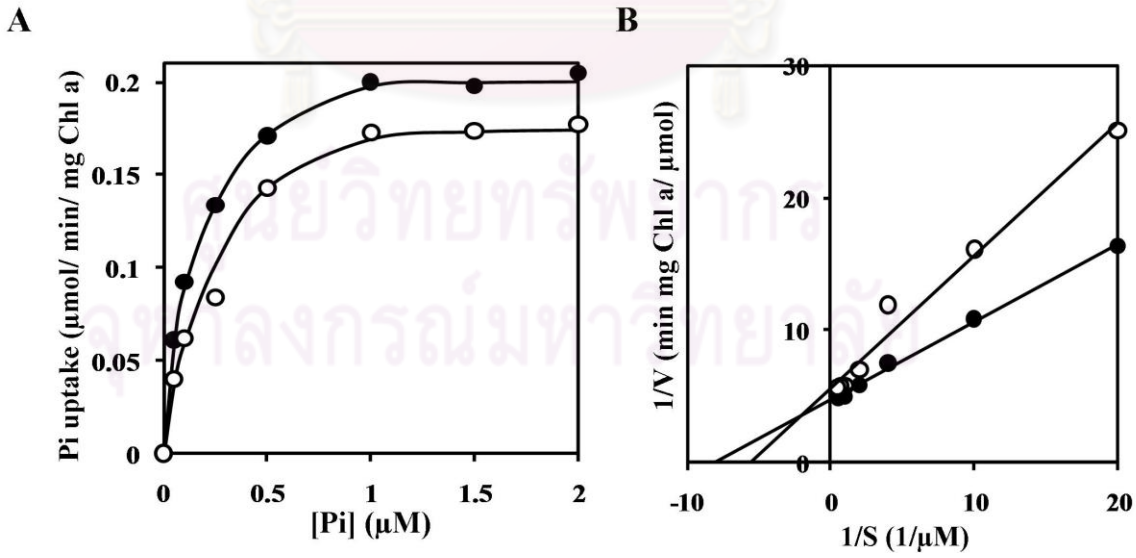

Figure 38 Kinetics of phosphate uptake in *Synechocystis* sp. PCC 6803 ΔPst1 strain. (A) Saturation curve of phosphate uptake into ΔPst1 cells. (B) Double-reciprocal plot of phosphate uptake into ΔPst1 cells. Cells grown in BG-11 (white circles) or phosphate-limiting BG-11 (black circles).

3.3.7 Kinetics of phosphate transport in ΔPst2 strain

Synechocystis sp. PCC 6803 ΔPst2 strain did not lose the control of Pho regulon as found in ΔPst1 strain. Therefore, the phosphate uptake activity under phosphate-sufficient conditions was not observed while cells under phosphate-limiting conditions showed a linear increase in phosphate uptake during 30 (Fig. 39). Similarly, phosphate uptake in ΔPst2 strain also showed saturation kinetics under phosphate-limiting conditions (Fig. 40). Under phosphate-limiting conditions, double-reciprocal plots yielded a K_m of 5.16 μM and maximum velocity (V_{max}) of 2.17 μmol/ min/ mg chlorophyll *a* for ΔPst2.

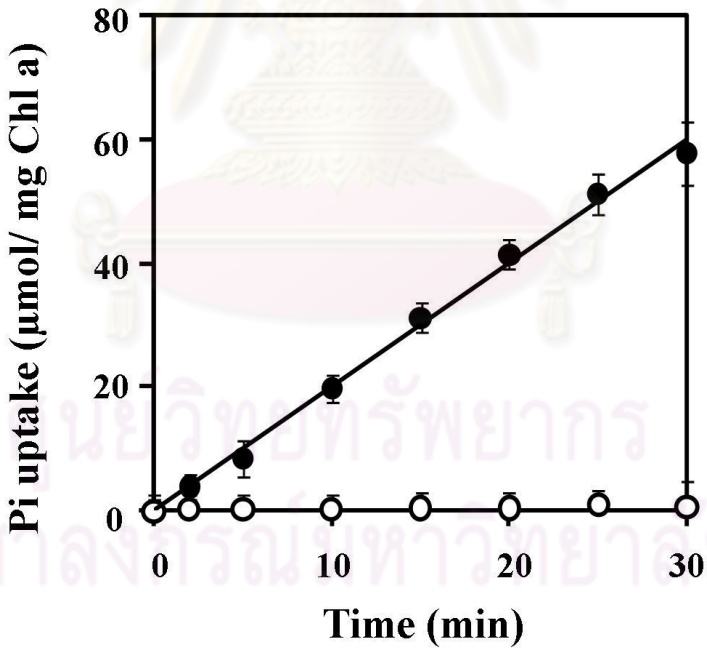

Figure 39 Phosphate uptake in *Synechocystis* sp. PCC 6803 ΔPst2 cells. Cells grown in BG-11 (white circles) or phosphate-limiting BG-11 (black circles). Phosphate uptake was measured at 50 μM. Data are the average ± the standard error of three independent experiments

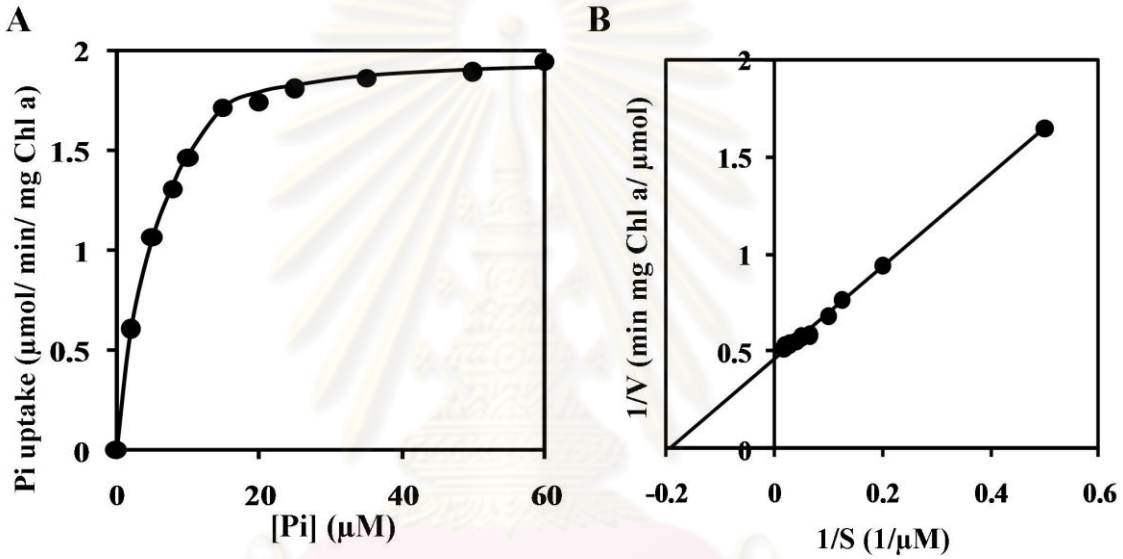

Figure 40 Kinetics of phosphate uptake in *Synechocystis* sp. PCC 6803 ΔPst2 strain. (A) Saturation curve of phosphate uptake into ΔPst2 cells. (B) Double-reciprocal plot of phosphate uptake into ΔPst2 cells. Cells grown in phosphate-limiting BG 11.

CHAPTER IV

DISCUSSION

Bioinformatics analysis of SphS revealed a putative transmembrane region between amino acids Ile-4 and Ile-19 (Fig. 9) and mutants lacking this region completely lost a positive function of histidine kinase, increasing the Pho regulon expression after phosphate limitations exposure (Fig. 14). Deletion of 8 amino acids within the putative membrane-spanning region (Δ(I8-G15) mutant) resulted in the loss of a negative function of histidine kinase in which the Pho regulon was constitutively derepressed. However, other mutants lacking 4, 6 and 9 amino acids at second low-complexity region (amino acids 41-51) retained both positive and negative functions which repressed the Pho regulon expression under phosphate-sufficient conditions and activated the expression of the Pho regulon under phosphate-limiting conditions (Fig. 14). These mutants still contained the intact membrane-associated region, suggesting the important role of this region while amino acids between Val-41 and Ser-49 were not necessary for either both positive or negative functions of SphS-SphR system. The membrane-associated region (amino acids 4-19) requirement, however, amino acids at 8, 9, 10, 15 and 16 of SphS were not essential residues as alanine-scanning mutagenesis at these amino acids of SphS showed nothing in response to phosphate-limiting conditions was different to wild type significantly (Fig. 14). Hence, the role of the membrane-associated region was probably guidance on SphS localization into membrane. Furthermore, it has been reported recently that the PAS domain (amino acids 70-137) of SphS is required for suppression of alkaline

phosphatase and heterologous expression of SphS in *E. coli* indicates SphS is membrane protein (Kimura et al., 2009). In addition, Kimura et al. (2009) also showed the mutant carrying chimeric SphS had similar phosphate limitation response as wild type. This fusion SphS contained N-terminal hydrophobic 222 amino acids of NrsS, Nickel-sensing histidine kinase, and C-terminal SphS kinase core (amino acids 51-430) including a PAS domain. The result from such protein emphasized that the SphS is membrane-anchoring protein and neither sequence specificity at transmembrane region nor amino acids at second low-complexity is required for SphS-SphR system control. Disruption of membrane-associated region in Δ(I8-G15)SphS, ΔPst1 and Δ(I8-G15): ΔPst1 strains constitutively expressed alkaline phosphatase at similar levels suggesting membrane-associated domain of SphS and Pst1 system both target the same control mechanism probably via hydrophobic interaction. In addition, transmembrane region of SphS might form dimer as found in almost histidine kinases using Leu-Gly interface. Figure 41 shows the predicted amino acids lied in N-terminal α-helix of SphS indicating a long hydrophobic residue of Ile interface and a short residue of Gly interface in which possibly form dimer interface as found in glycophorin A (Fig. 42), a membrane protein of human erythrocyte (MacKenzie et al., 1997). Together with gene expression studies that the expression of *sphS* and *sphR* are not up-regulated whereas the *phoB-phoR* transcript is increased in response to phosphate-limiting conditions (Hirani et al., 2001; Suzuki et al., 2004), these suggested the different mechanisms in regulation of phosphate-sensing systems between *E. coli* and *Synechocystis* sp. PCC 6803.

The deleted SphSs lacking membrane-spanning region were likely cytosolic protein, however, it was hardly detected since the expression levels of *sphS* was too

low both RNA and protein levels, as they could not be detected by Northern and Western blots (Hirani et al., 2001; Juntarajumnong et al., 2007b, c; Kimura et al., 2009). Mutants carrying these deleted SphS still showed no alkaline phosphatase activity when a negative regulator SphU was interrupted (Fig. 18), these were similar to those observed in ΔSphU: ΔSphS and ΔSphU: SphS-H207Q (formerly called ΔSphU: SphS-H160Q, number changed as a result of the new start codon of *sphS* was identified) (Juntarajumnong et al., 2007b). It could be concluded that SphS lacking membrane-spanning region fully lost histidine kinase activity.

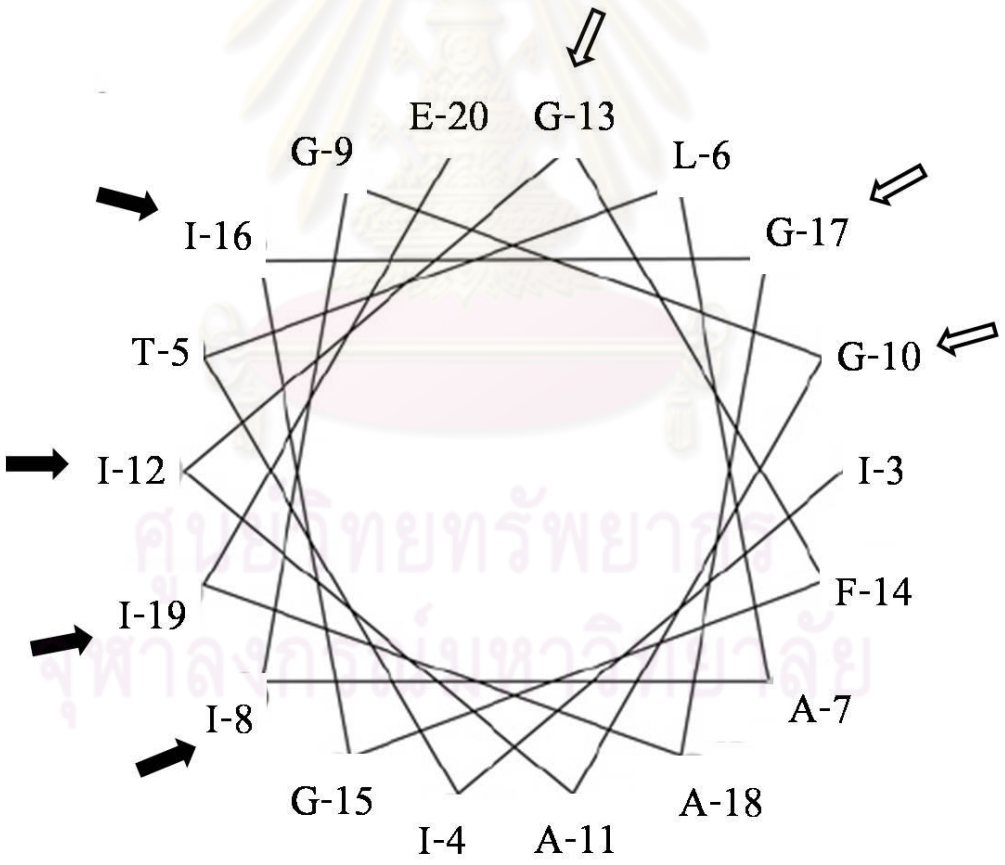

Figure 41 Helical wheel representation of the predicted N-terminal α-helix of SphS. Hydrophobic Ile and Gly residues are indicated with black and white arrows, respectively.

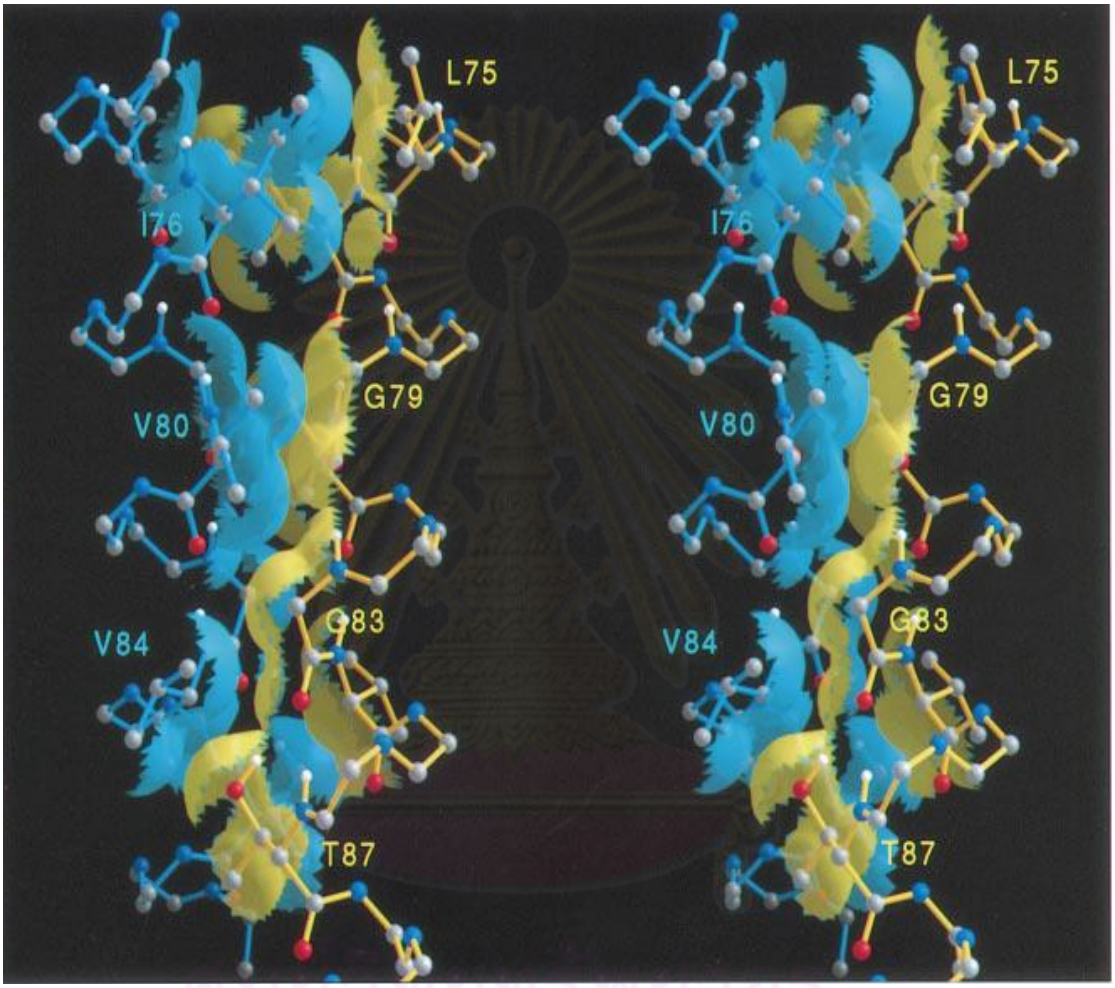

Figure 42 Stero view of the transmembrane domain of glycophorin A. Molecular surfaces of each monomer were drawn at radii corresponding to the van der Waals hard sphere. The backbone and molecular surface of each monomer is distinguished by blue and yellow colors (PDB accession number: 1AFO) (MacKenzie et al., 1997).

In *E. coli*, a low-affinity Pit and a high-affinity Pst phosphate transport systems are present. The Pst system and negative regulator PhoU, belonging to Pho regulon, play crucial roles in control of PhoR-PhoB phosphate-sensing system which regulate the Pho regulon expression in *E. coli*. In contrast to *Synechocystis* sp. PCC 6803, the *pit* gene is absent while two operons encoding Pst system are present, the *pst1* and *pst2* operons belong to the Pho regulon and both are up-regulated when grown under phosphate-limiting conditions but not for a negative regulator SphU whose expression is independent of phosphate (Suzuki et al., 2004). The influx of phosphate into *Synechocystis* sp. PCC 6803 grown in phosphate-sufficient medium was not observed under experimental conditions either at a low (0.1 µM) (Hirani et al., 2001) or high (150 µM) concentration of phosphate in the assay. These also supported the absence of the constitutive Pit transport system and the very low expression of the Pho regulon under phosphate-limiting conditions.

As mentioned above, the absence of Pit low-affinity phosphate transport system in *Synechocystis* sp. PCC 6803 is not surprising as found in many marine cyanobacteria. Typically marine cyanobacteria that are exposed to oligotrophic conditions where phosphate is limiting also lack Pit phosphate uptake systems (Moore et al., 2005; Martiny et al., 2006). In addition, the genomes of these cyanobacteria usually contain genes encoding multiple phosphate-binding proteins, but not all such genes involved in the Pho regulon. The expression study showed that some genes encoding phosphate-binding proteins were not up-regulated in phosphate limitation response (Moore et al., 2005; Martiny et al., 2006). However, it seems that only *Synechocystis* sp. PCC 6803 genome contains two Pst systems while other cyanobacteria have only one Pst system. The presence of two Pst systems which share

high homology (~70-80% similarities in permease and ATP-binding proteins) (Table 4) together with the monophasic phosphate uptake observed in wild type (Fig. 32) suggested a possible heterologous combination of both Pst systems.

We have identified the Pst1 system is necessary for negative regulation of the SphS-SphR phosphate-sensing system controlling the Pho regulon expression (Fig. 26). Hence, the Pst1 system should be present possibly at basal level in the inactive form since no noticed phosphate uptake activity in both wild-type and ΔPst2 strains (Fig. 33, 40).

Kinetics study of phosphate uptake found that the affinity of Pst2 system was higher than Pst1 system, K_m of 0.13 and 5.16 μM, respectively, while the wild type containing both systems had a very low affinity toward phosphate with a K_m of ~80 μM. The V_{max} values were also calculated of 0.18, 2.17 and 3.12μmol/ min/ mg chlorophyll *a*, for ΔPst1, ΔPst2 and wild type, respectively (Fig.33, 38, 40). The very low kinetic parameters in ΔPst1, however, growth and pigment content of this strain were not defective, compared to wild type either under phosphate-sufficient or phosphate-limiting conditions (Fig. 24, 25). These indicated each strain had stored phosphate sufficiently as wild type over the course of the measurements despite lacking the Pst1 or Pst2 system (Rao et al., 2009). The very high K_m that observed in wild type could be explained that *Synechocystis* sp. PCC 6803 adapted to external phosphate concentration as reported in its neighbor *Synechococcus* sp PCC 7942 Wagner et al. (1995) revealed that the kinetics properties for phosphate uptake by cyanobacteria adapts to the external phosphate concentration. Therefore, the K_m of ~80 μM for phosphate in wild type likely reflected acclimation of the phosphate

uptake apparatus to the high level of phosphate in BG-11 in which practical concentration of phosphate is 175 µM.

It could be concluded that the phosphate uptake in *Synechocystis* sp. PCC 6803 was energy-dependent from the results of amino acid sequence analysis together with phosphate uptake study in the presence of various metabolic inhibitors (Table 5). The uptake of phosphate was able to transport phosphate in $H_2PO_4^-$ and HPO_4^{2-} forms since the activities at pH 7 and pH 10 were not significantly different (Fig. 34).

The stimulation of phosphate uptake by various cations in cyanobacteria has been reported (Rigby et al., 1980; Fernandez Valiente & Avendano, 1993; Avendano & Fernandez Valiente, 1997; Ritchie et al., 1997). However, only Mg^{2+} and Na^+ slightly activated phosphate uptake in *Synechocystis* sp. PCC 6803. The different results might be explained that those cyanobacteria posses both Pit and Pst system while the Pit system is absent in *Synechocystis* sp. PCC 6803.

The phosphate-sensing system in *Synechocystis* sp. PCC 6803 could be simplified as shown in Figure 43. The Pst1 phosphate transport system and negative regulator SphU were required to repress the expression of the Pho regulon under phosphate-sufficient conditions which are thought to form inhibition complex as reported in *E. coli* (Fig. 5). Even though the Pst2 system had an affinity toward phosphate higher than the Pst1 system, the Pst2 system was not involved in the regulation of the phosphate-sensing system (Fig. 26). In addition, the response regulator SphR has been shown to bind specifically at regulatory elements upstream of the Pho regulon genes, called Pho boxes (Suzuki et al., 2004).

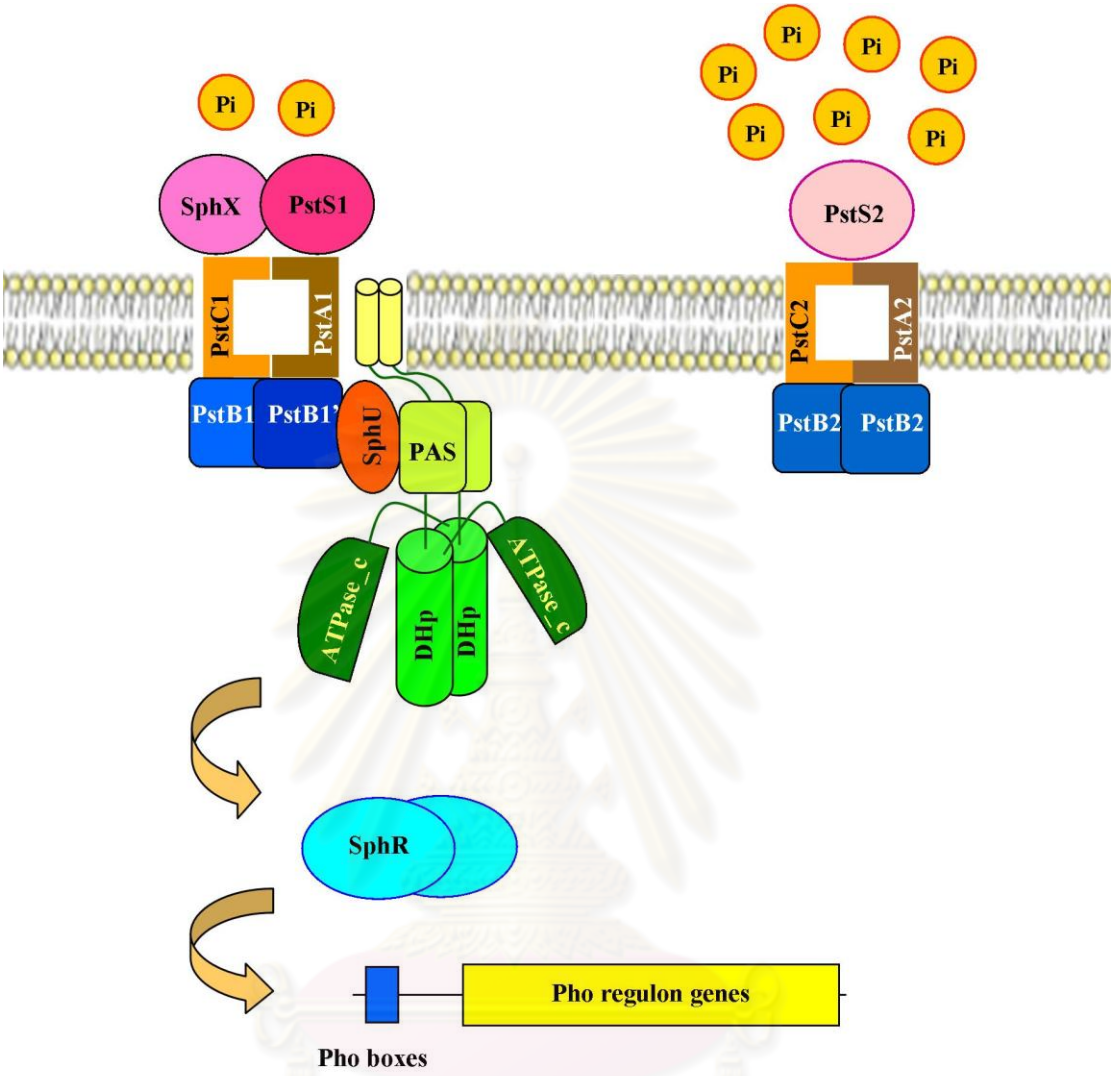

Figure 43 The proposed model of phosphate-sensing system in *Synechocystis* sp. PCC 6803. The Pst1, SphU and SphS form inhibition complex. The Pst2 system had an affinity toward phosphate higher than Pst1 system, the former was not involved in regulation of the phosphate-sensing system. The SphS is shown in cartoon model with a transmembrane domain (yellow), a PAS domain (light green), a dimerization domain (green) and a catalytic ATP-binding domain (dark green). The signal is transduced across membrane to SphR and SphR binds at Pho boxes to regulate the expression of the Pho regulon genes.

CHAPTER V

CONCLUSION

The present study using *Synechocystis* sp. PCC 6803 has revealed the following findings:

1. The membrane-associated region of the SphS between amino acids Ile-4 and Ile-19 was essential for regulation of the SphS-SphR phosphate-sensing system, deletion of this region (Δ(I3-R23), Δ(I3-S44) and Δ(I3-S49)) resulted in the loss of the induction of alkaline phosphatase activity, whereas internal deletion of this region (Δ(I8-G15)) resulted in constitutive expression of the alkaline phosphatase activity
2. Amino acids Ile-8, Gly-9, Gly-10, Gly-15 and Ile-16 of the membrane-associated region and amino acids between Val-41 and Ser-49 were not important amino acids for SphS-SphR system regulation.
3. The SphS lacking the membrane-spanning region completely lost the positive function to up-regulate the alkaline phosphatase expression even the SphU or Pst1 system was inactivated.
4. The Pst1 system, but not the Pst2 system, was required for regulation of the SphS-SphR phosphate-sensing system. In addition, the absence of Pst1 or Pst2 had no effect on growth and pigment content, suggesting only one system took up phosphate sufficiently for cell utilization.
5. Deletion of the Pst1 did not alter alkaline phosphatase activity in the strains carrying mutation at membrane-associated region of the SphS.

6. The ΔPst1 strain showed constitutive activity of alkaline phosphatase as well as phosphate uptake. The kinetics study revealed the K_m values of 0.13 and 0.18 μM and the V_{max} values of 0.22 and 0.18 μmol/ min/ mg chlorophyll *a* were observed in the ΔPst1 mutant under phosphate-limiting and phosphate-sufficient conditions, respectively.
7. Phosphate uptake was not observed in wild-type and ΔPst2 strains grown in phosphate-sufficient medium and genomic information suggested no pit gene. Hence, the constitutive phosphate transport (Pit) system is absent in *Synechocystis* sp. PCC 6803.
8. The phosphate uptake in wild type had a K_m of 80.67 μM and a V_{max} of 3.12 μmol/ min/ mg chlorophyll *a*.
9. The ΔPst2 strain had a K_m of 5.16 μM and a V_{max} of 2.17 μmol/ min/ mg chlorophyll *a* for phosphate transport.
10. The phosphate uptake was energy and pH-dependent which could be significantly stimulated in the presence of Mg^{2+} and Na^{+} while the osmolality generated by sorbitol decreased the phosphate uptake.

REFERENCES

Aiba HM, Nagaya M & Mizuno T. (1993). Sensor and regulator proteins from the cyanobacterium *Synechococcus* species PCC 7942 that belong to the bacterial signal-transduction protein families: implication in the adaptive response to phosphate limitation. *Mol Microbiol* 8: 81–91.

Altschul SF, Madden TL, Schäffer AA, Zhang J, Zhang Z, Miller W & Lipman DJ. (1997). Gapped BLAST and PSI-BLAST: a new generation of protein database search programs. *Nucleic Acids Res* 25: 3389-3402.

Avendano MC & Valiente EF. (1994). Effect of sodium on phosphate uptake in unicellular and filamentous cyanobacteria. *Plant Cell Physiol* 35: 1097-1011.

Baek JH & Lee SY. (2006). Novel gene members in the Pho regulon of *Escherichia coli*. *FEMS Microbiol Lett* 264: 104–109.

Cai SJ, Khorchid A, Ikura M & Inouye M. (2003). Probing catalytically essential domain orientation in histidine kinase EnvZ by targeted disulfide crossinking. *J Mol Biol* 328: 409-418.

Carmany DO, Holingsworth K & McCleary WR. (2003). Genetic and biochemical studies of phosphatase activity of PhoR. *J Bacteriol* 185: 112-115.

Cox GB, Webb D, Godovac-Zimmermann J & Rosenberg H. (1988). Arg-220 of the PstA protein is required for phosphate transport through the phosphate-specific transport system in *Escherichia coli* but not for alkaline phosphatase repression. *J Bacteriol* 170: 2283-2286.

Daigle F, Fairbrother JM & Harel J. (1995). Identification of a mutation in the *pst-phoU* operon that reduces pathogenicity of an *Escherichia coli* strain causing septicemia in pigs. *Infect Immun* 63: 4924–4927.

Dutta R, Qin L & Inouye M. (1999). Histidine kinases: diversity of domain organization. *Mol Microbiol* 34:633-640.

Dyhrman ST & Haley ST. (2006). Phosphorus scanvenging in the unicellular marine diazotroph *Crocosphaera watsonii*. *Appl Environ Microbiol* 72: 1452-1458.

Eaton-Rye JJ & Vermaas WFJ. (1991). Oligonucleotide-directed mutagenesis of *psb*B, the gene encoding CP47, employing a deletion mutant strain of the cyanobacterium *Synechocystis* sp. PCC 6803. *Plant Mol Biol* 17: 1165-1177.

Falkner R, Wagner F, Aiba H & Falkner G. (1998). Phosphate-uptake behaviour of a mutant of *Synechococcus* sp. PCC 7942 lacking one protein of the high-affinity phosphate-uptake system. *Planta* 206: 461-465.

Fernandez Valiente E & Avendano MC. (1993). Sodium-stimulation of phosphate uptake in the cyanobacterium *Anabaena* PCC 7119. *Plant Cell Physiol* 34: 201-207.

Gomi M, Sonoyama M & Mitaku S. (2004). High performance system for signal peptide prediction: SOSUIsignal. *Chem-Bio Info* J 4: 142-147

Haralalka S, Nandi S & Bhadra RK. (2003). Mutation in the *relA* gene of *Vibrio cholerae* affects in vitro and in vivo expression of virulence factors. *J Bacteriol* 185: 4672–4682.

Hirani TA, Suzuki I, Hayashi H, Murata N & Eaton-Rye JJ. (2001). Characterization of a two-component signal transduction system involved in the induction of

alkaline phosphatase under phosphate-limiting conditions in *Synechocystis* sp. PCC 6803. *Plant Mol Biol* 45: 133–144.

Hudson JJ, Taylao WD & Schindler DW. (2000). Phosphate concentrations in lakes. *Nature* 406: 54-56.

Hulko M, Berndt F, Gruber M, Linder JU, Truffault, Schultz A, Martin J, Schultz JA, Lupas AN & Coles M. (2006). The HAMP domain structure implies helix rotation in transmembrane signaling. *Cell* 126: 929-940.

Ikeuchi M & Tabata S. (2001). *Synechocystis* sp. PCC 6803 – a useful tool in the study of the genetics of cyanobacteria. *Photosynth Res* 70: 73-83.

Inouye M. (2006). Signalling by transmembrane proteins shift gears. *Cell* 126: 829-831.

Juntarajumnong W. (2004). Effect of phosphate on two-component signal transduction system in the cyanobacterium *Synechocystis* sp. PCC 6803. Ph.D. Thesis.Department of Biochemistry, Chulalongkorn University.

Juntarajumnong W, Eaton-Rye JJ & Incharoensakdi A. (2007a). Two-component signal transduction in *Synechocystis* sp. PCC 6803 under phosphate limitation: Role of acetyl phosphate. *J Biochem Mol Biol* 40: 708-714.

Juntarajumnong W, Hirani TA, Simpson JM, Incharoensakdi A & Eaton-Rye JJ. (2007b). Phosphate sensing in *Synechocystis* sp. PCC 6803: SphU and the SphS-SphR two-component regulatory system. *Arch Microbiol* 188: 389-402.

Juntarajumnong W, Incharoensakdi A & Eaton-Rye JJ. (2007c). Identification of the start codon for *sphS* encoding the phosphate-sensing histidine kinase in *Synechocystis* sp. PCC 6803. *Curr Microbiol* 55:142-146.

Kamberov ES, Atkinson MR, Feng J, Chandran P & Ninfa AJ. (1994). Sensory components controlling bacterial nitrogen assimilation. *Cell Mol Biol Res* 40: 175-191.

Kaneko T, Sato S, Kotani H, Tanaka A, Asamizu E, Nakamura Y, Miyajima N, Hirosawa M, Sugiura M, Sasamoto S, Kimura T, Hosouchi T, Matsuno A, Muraki A, Nakazaki N, Naruo K, Okumura S, Shimpo S, Takeuchi C, Wada T, Watanabe A, Yamada M, Yasuda M & Tabata S. (1996). Sequence analysis of the genome of the unicellular cyanobacterium *Synechocystis* sp. strain PCC 6803. Sequence determination of the entire genome and assignment of potential protein-coding regions. *DNA Res* 3: 109-136.

Katewa SD & Katyare SS. (2003). A simplified method for inorganic phosphate determination analysis in enzyme assays. *Anal Biochem* 323: 180-187.

Khorchid A & Ikura M. (2006). Bacterial histidine kinase as signal sensor and transducer. *Int J Biochem Cell Biol* 38: 307-312.

Kimura S, Shiraiwa Y & Suzuki I. (2009). Function of the N-terminal region of the phosphate-sensing histidine kinase, SphS, in *Synechocystis* sp. PCC 6803. *Microbiol* 155: 2256-264.

Kohanski MA & Collins JJ. (2008). Rewiring bacteria, two components at a time. *Cell* 133: 947-948.

Lamarche MG, Dozois CM, Daigle F, Caza M, Curtiss R III, Dubreuil JD & Harel J. (2005). Inactivation of the pst system reduces the virulence of an avian pathogenic *Escherichia coli* O78 strain. *Infect Immun* 73: 4138–4145.

Lamarche MG, Wanner BL, Crepin S & Harel J. (2008). The phosphate regulon and bacterial virulence: a regulatory network connecting phosphate homeostasis and pathogenesis. *FEMS Microbiol Rev* 32: 461-473.

Laub MT & Goulain M. (2007). Specificity in two-component signal transduction pathways. *Annu Rev Gent* 41: 121-145.

Letunic I, Copley RR, Pils B, Pinkert S, Schultz J & Bork P. (2006). SMART 5: domains in the context of genomes and networks. *Nucleic Acids Res* 34: D257-D260.

MacKenzie KR, Prestegard JH & Engleman DM. (1997). A transmembrane helix dimer: structure and implications. *Science* 267: 131-133.

MacKinney G. (1941). Absorption of light by chlorophyll solutions. *J Biol Chem* 140: 315-322.

Martiny AC, Coleman ML & Chisholm SW. (2006). Phosphate acquisition genes in *Prochlorococcus* ecotypes: Evidence for genome-wide adaptation. *Proc Natl Acad Sci USA* 103: 12552-12557.

Mary I & Vaulot D. (2003). Two-component systems in *Prochlorococcus* MED4: Genomic analysis and differential expression under stress. *FEMS Microbiol Lett* 226: 135-144.

Mascher T, Helmann JD & Unden G. (2006). Stimulus perception in bacterial signal-transducing histidine kinases. *Microbiol Mol Biol Rev* 70: 910-938.

Mayes SR, Cook KM, Self SJ, Zhang Z & Barber J. (1991). Deletion of the gene encoding the photosystem II 33 kDa protein from *Synechocystis* sp. PCC 6803 does not inactivate water-spitting but increases vulnerability to photoinhibition. *Biochim Biophys Acta* 1060: 1-12.

Medveszky N & Rosenberg H. (1971). Phosphate transport in *Escherichia coli*. *Biochim Biophys Acta* 373: 369-382.

Moore LR, Ostrowski M, Scanlan DJ, Feren K & Sweetsir T. (2005). Ecotypic variation in phosphorus-acquisition mechanisms within marine picocyanobacteria. *Aquat Microb Ecol* 39: 257-269.

Qi Y, Kobayashi Y, Hullet FM. (1997). The *pst* operon of *Bacillus subtilus* has a phosphate-regulated promoter and is involved in phosphate transport but not in regulation of the Pho regulon. *J Bacteriol* 179: 2534-2539.

Rao NN, Gomez-Garcia MR & Kornberg A. (2009). Inorganic polyphosphate: Essential for growth and survival. *Annu Rev Biochem* 78: 605-647.

Rigby CH, Craig SR & Budd K. (1980). Phosphate uptake by *Synechococcus leopoliensis* (Cyanophyceae): enhancement by calcium ion. *J Phycol* 16: 389-393.

Ritchie RJ, Trautman DA & Larkum AWD. (1997). Phosphate uptake in the cyanobacterium *Synechococcus R-2* PCC 7942. *Plant Physiol* 38: 1232-1241.

Rosenber H. (1987). Phosphate transport in prokaryotes, In: B.P. Rosen, S. Silver (Eds), *Ion Transport in Prokaryotes*. pp. 205-248. New York: Academic Press.

Rost B, Fariselli P & Casadio R. (1996). Topology prediction for helical transmembrane proteins at 86% accuracy. *Protein Sci* 5: 1704-1718.

Schachtman DP, Reid RJ & Ayling SM. (1998). Phosphorus uptake by plants: from soil to cell. *Plant Physiol* 116: 447-453.

Schindler DW. (1977). Evolution of phosphorus limitation in lakes. *Science* 195: 260-262.

Scholten M & Tommassen J. (1993). Topology of the PhoR protein of *Escherichia coli* and functional analysis of internal deletion mutants. Mol Microbiol 8: 269-275.

Shi L & Hulett FM. (1999). The cytoplasmic kinase domain of PhoR is sufficient for the low phosphate-inducible expression of pho regulon genes in *Bacillus subtilis*. *Mol Microbiol* 31: 211-222.

Skerker JM, Perchuk BS, Siryaporn A, Lubin EA, Ashenberg O, Goulian M & Laub MT. (2008). Rewiring the Specificity of Two-Component Signal Transduction Systems. *Cell* 133: 1043-1054.

Stock AM, Robinson VL & Goudreau PN. (2000). Two-component signal transduction. *Annu Rev Biochem* 69: 183-215.

Sun G, Birkey SM & Hulett. (1996). Three two-component signal-transduction systems interact for Pho regulation in *Bacillus subtilis*. *Mol Microbiol* 19: 941-948.

Sundareshwar PV, Morris JT, Koepfler EK & Fornwalt B. (2003). Phosphorus limitation of coastal ecosystem processes. *Science* 299: 563-565.

Suzuki S, Ferjani A, Suzuki I & Murata N. (2004). The SphS-SphR two component system is the exclusive sensor for the induction of gene expression in response to phosphate limitation in *Synechocystis*. *J Biol Chem* 279: 13234-13240.

Szurmant H, Bu L, Brooks III C L & Hoch JA. (2008). An essential sensor histidine kinase controlled by transmembrane helix interactions with its auxiliary proteins. *Proc Natl Acad Sci USA* 105:5891-5896

Tusnady GE, Kalmar L, Hegyi H, Tompa P & Simon I. (2008). TOPDOM: database of domains and motifs with conservative location in transmembrane proteins. *Bioinfomatics* 24: 1469-1470.

Ubersax JA & Ferrell JE. Jr. (2007). Mechanisms of specificity in protein phosphorylation. *Nat Rev Mol Cell Biol* 8: 530-541.

Van Veen HW. (1997). Phosphate transport in prokaryotes: molecules, mediators and mechanisms. *Antonie van Leeuwenhoek* 72: 299-315.

Wagner F, Falkner R & Falkner G. (1995). Information about previous phosphate fluctuations is stored via an adaptive response of the high-affinity phosphate uptake system of the cyanobacterium *Anacystis nidulans*. *Planta* 197: 147-155.

Wang L, Sun YP, Chen WL, Li JH & Zhang CC. (2002). Genomic analysis of protein kinases, protein phosphatases and two-component regulatory systems of the cyanobacterium *Anabaena* sp. Strain PCC 7120. *FEMS Microbiol Lett* 217: 155-165.

Wanner BL. (1993). Gene regulation by phosphate in enteric bacteria. *J Cell Biochem* 51: 47-54.

Wanner BL. (1996). Phosphorus assimilation and control of the phosphate regulon. In: Neidhardt FC, Curtiss III R, Ingraham JL, et al. (eds), *Escherichia coli and Salmonella: Cellular and Molecular Biology*, 2nd ed., Vol. 1. pp 1357-1381. American Society for Microbiology: Washington, DC.

West AH & Stock AM. (2001). Histidine kinases and response regulator proteins in two-component signaling systems. *Trends Biochem Sci* 26: 369-376.

Williams JKG. (1988). Construction of specific mutations in PSII photosynthetic reaction center by genetic engineering. *Methods Enzymol* 167: 766-778.

Willsky GR & Malamy MH. (1980). Characterization of two genetically separable inorganic phosphate transport systems in *Escherichia coli*. *J Bacteriol* 144: 356-365.

Wu J, Sunda W, Boyle EA & Karl DM. (2000). Phosphate depletion in the Western North Atlantic Ocean. *Science* 289: 759–762.

Wu P, Ma L, Hou X, Wang M, Wu Y, Liu F & Deng XW. (2003). Phosphate starvation triggers distinct alterations of genome expression in Arabidopsis roots and leaves. *Plant Physiol* 132: 1260–1271.

Yamada M, Makino K, Shinagawa H & Nakata A. (1990). Regulation of the phosphate regulon of *Escherichia coli*: Properties of *phoR* deletion mutants and subcellular localization of PhoR protein. *Mol Gen Genet* 220: 366-372.

APPENDICES

APPENDIX A

BG-11 medium (1,000 ml)

	Solid medium	**Liquid medium**
H_2O	947 ml	967 ml
Bacto-agar	15 g	-
100x BG-FPC*	10 ml	10 ml
189 mM Na_2CO_3	1 ml	1 ml
175 mM K_2HPO_4	1 ml	1 ml
6 mg/ml Ammonium ferric citrate	1 ml	1 ml
1 M TES	10 ml	-
30% $Na_2S_2O_3$ $5H_2O$	10 ml	-
1 M HEPES-NaOH, pH 7.5	20 ml	-

100x BG-FPC*

(100 ml)

$NaNO_3$	14.96 g
$MgSO_4.7H_2O$	0.75 g
$CaCl_2.2H_2O$	0.36 g
Citric acid	0.065 g
0.5 M Na-EDTA	55.4 µl

After autoclaved, add 10 ml of 1,000x Trace metal mix**

1,000x Trace metal mix**

(1,000 ml)

H_3BO_3	2.86 g
$MnCl_2.4H_2O$	1.81 g
$ZnSO_4.7H_2O$	0.221 g
$Na_2MoO_4.2H_2O$	0.390 g
$CuSO_4.5H_2O$	0.080 g
$Co(NO_3)_2.6H_2O$	0.049 g

Sterile filtrate, store at 4 ^oC

APPENDIX B

Medium for *Escherichia coli*

LB medium (1 liter)

	Liquid medium	Solid medium
Bacto tryptone	10 g	10 g
Yeast extract	5 g	5 g
NaCl	10 g	10 g
Agar	-	15 g

2x YT media (1 liter)

	Liquid medium	Solid medium
Bacto tryptone	16 g	16 g
Yeast extract	10 g	10 g
NaCl	5 g	5 g
Agar	-	15 g

All compositions were dissolved together with 1liter of distilled water. The medium was sterilized by autoclaving at 15 Ib/in^2 for 15 minute.

APPENDIX C

Reagents for heat-shock transformation

ψB media (500 ml)

yeast extract	2.5 g
bactotryptone	10 g
KCl	0.38 g

Adjust the pH to 7.6 with KOH then autoclave. After autoclaving, cool down and add 17 ml of sterile 1 M $MgSO_4$

TfBI Solution (500 ml)

potassium acetate	1.47 g
$MnCl_2$	4.95 g
RbCl	6.05 g
$CaCl_2$	0.74 g
Glycerol	75 ml

Adjust the pH to 5.8 with 0.2 M acetic acid then autoclave. Store at 4˚C

TfBII Solution (100 ml)

100 mM MOPS (pH 7.0)	10 ml
$CaCl_2$	1.10 g
RbCl	0.12 g
Glycerol	15 ml

Autoclave and store at 4˚C in the dark

APPENDIX D

Reagents for alkaline lysis

Solution I (100 ml)

5.0 ml 1.0 M Glucose

2.5 ml 1.0 M Tris-HCl, pH 8.0

2.0 ml 0.5 M EDTA, pH 8.0

After autoclave 20 μg/ml of RNase was added and stored at 4^{o}C

Solution II (25 ml)

0.5 ml 10 M NaOH

1.25 ml 20% SDS

Solution III (500 ml)

147 g potassium acetate

57.5 ml glacial acetic acid

Autoclave and store at 4^{o}C

TE buffer (500 ml)

5 ml 1 M Tris-HCl, pH 8.0

1 ml 0.5 M EDTA

Autoclave and store at room temperature

APPENDIX E

Reagents for DNA electrophoresis

5x TBE buffer (1 liter)

Tris base	54 g
Boric acid, anhydrous	27.5 g
0.5 M EDTA pH 8.0	20 ml

20 x SB buffer (50 ml)

Na_2B4O_7 $10H_2O$	1.9 g
H_3BO_3	1.2 g

Loading dye (20 ml)

Bromophenol blue	0.05 g
Xylelne cyanol FF	0.05 g
Glycerol	6 ml

APPENDIX F

Reagents for Southern blot

20x SSC (1 liter)

175.3 g	NaCl
88.2 g	Na_3 citrate • $2H_2O$
800 ml	H_2O

Adjust the pH to 7.0 with 1 M HCl and make to 1 liter with milli-q water

100x Denhardts solution (50 ml)

1 g	Ficoll 400
1 g	polyvinylpyrrolidone
1 g	BSA (Fraction V)

Make up to 50 ml with milli-q water. Filter-sterilize, store at –20ºC

Denhardts Pre-hyb solution

5x Denhardts solution

1% SDS

5x SSC

50% formamide

APPENDIX G

Reagents for making probe of Southern blot

Solution O (20 ml)

1.25 M Tris-HCl pH 8.0

0.125 M $MgCl_2$

Solution A (Store at -20°C)

5 µl dGTP, 5 µl dATP, 5 µl dTTP

18 µl 2-mercaptoethanol (14.4 M)

1 ml Solution O

Solution B (Store at 4°C)

2 M HEPES-NaOH pH 6.6

Solution C

Random Primer

BSA Solution

10 mg/ml (make 5 ml or less)

Stop Solution

20 mM Tris-HCl pH 7.8

20 mM NaCl

2 mM EDTA

0.25% (w/v) SDS

OLB Solution (make fresh)

2 µl Solution A

5 µl Solution B

3 µl Solution C

APPENDIX H

Reagents for RNA gel electrophoresis

DEPC-Water

1 ml DEPC

1l milli-Q water

Stir for a couple of hours. Incubate overnight at 37ºC Autoclave at 15 psi, for 15 minutes, to inactivate the DEPC.

10x MOPS buffer (1 liter)

0.2 M MOPS (41.86 g)

0.05 M NaAc (16.65 ml from 3 M stock, pH 5.0)

0.01 M EDTA (40 ml from 0.25 M stock, pH 8.0)

Adjust to pH 7.0 with NaOH. Wrap in tin foil.

2x RNA Loading buffer (1 ml)

500 µl formamide

160 µl formaldehyde

100 µl 10x MOPS

100 µl glycerol

105 µl sterile DEPC-water

25 µl bromophenol blue (make stock of 10 mg/ml in ethanol)

10 µl ethidium bromide (stock of 10 mg/ml)

APPENDIX I

Reagents for pTZ19U mutagenesis

High salt buffer

300 mM NaCl

100 mM Tris-Hcl, pH 8.0

1 mM EDTA

DTT Solution

0.1 M DTT in 0.01 M Sodium acetate, pH 5.2

Neutralized ATP

0.1 M ATP, pH 7.0 (adjust pH with 0.1 M NaOH)

Make up to 1 ml with water and dilute to 1 mM ATP

10x Annealing buffer

200 mM Tris-Hcl, pH 7.4

20 mM $MgCl_2$

500 mM NaCl

TE stop buffer

10 mM EDTA

10 mM Tris-Hcl, pH 8.0

10x Synthesis buffer

100 mM Tris-Hcl, pH 7.9

5 mM each dNTPs

10 mM ATP

50 mM $MgCl_2$

15 mM DTT

APPENDIX J

Standard curve of phosphate

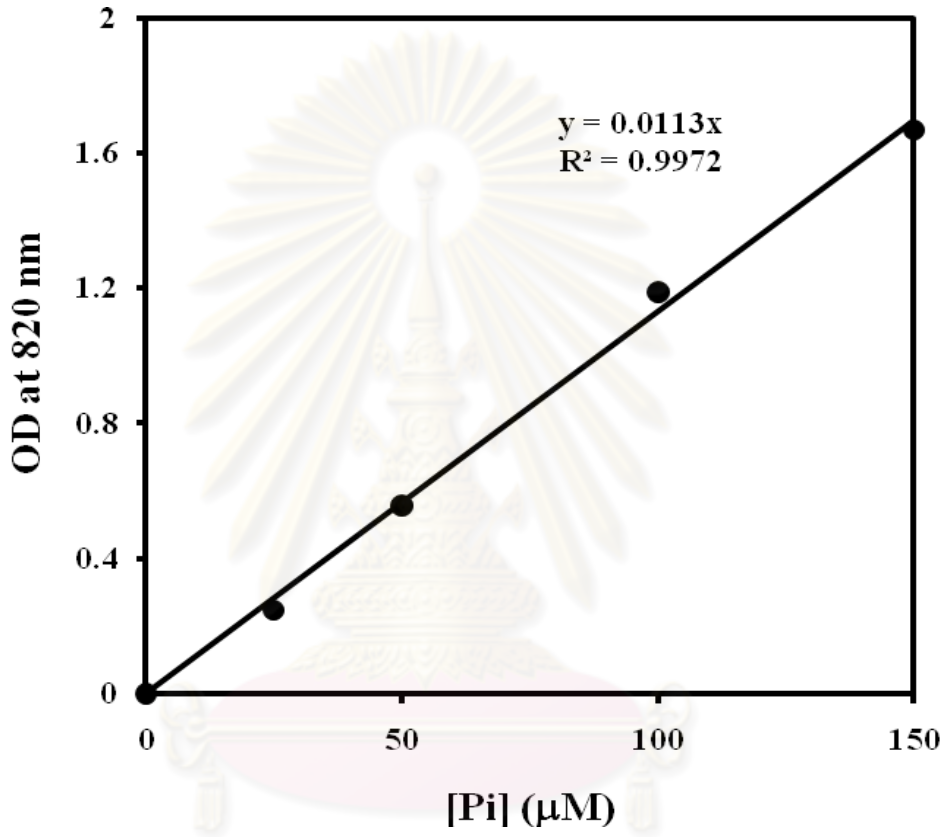

BIOGRAPHY

Mr. Surachet Burut-Archanai was born on December 16, 1983 in Bangkok, Thailand. He graduated with a Bachelor of Science degree (1st class honor) in Biochemistry from Chulalongkorn University in 2005. He has further studied for the Doctor of Philosophy degree in Biochemistry Department, Chulalongkorn University since 2005.